Aus dem Department für Diagnostische Labormedizin der

Universität Tübingen

Institut für Medizinische Mikrobiologie und Hygiene

Establishment and evaluation of *Staphylococcus aureus* strains with integrative reporter-plasmids for detection of *cap* and *agr* promoter activity and establishment of a 3D collagen model

Inaugural-Dissertation
zur Erlangung des Doktorgrades
der Medizin

der Medizinischen Fakultät
der Eberhard Karls Universität
zu Tübingen

vorgelegt von

Nguyen, Thien Ngoc Tran

2018

Dekan: Professor Dr. I. B. Autenrieth

1. Berichterstatter: Prof. Dr. C. Wolz
2. Berichterstatter: Prof. Dr. M. Schindler

Tag der Disputation: 27.06.2018

Table of contents

List of abbreviations

Ab	Antibody
Agr	Accessory gene regulator
AIP	Autoinducing peptide
B. fragilis	*Bacteroides fragilis*
BM	Basal medium
bp	Base pair
BSA	Bovine serum albumin
Clf	Clumping factor
Coa	coagulase
CP	Capsular polysaccharide
E. coli	*Escherichia coli*
emp	Extracellular matrix binding protein
geh	Glycerol ester hydrolase
Hla	α-hemolysin
LB	Luria-Bertani
MAM	Microcolony associated meshwork
mRNA	Messenger RNA
MSCRAMM	Microbial surface components recognizing adhesive matrix molecules
P. aeruginosa	*Pseudomonas aeruginosa*
PBS	phosphate-buffered saline
PGFE	Pulsed-field gel electrophoresis

PIA/PNAG	polysaccharide intercellular adhesion/poly-β(1-6)-N-acetyglucosamine
PMN	Polymorphonuclear leukocyte
ROS	Reactive oxygen species
RT	Room temperature
S. aureus	*Staphylococcus aureus*
SAC	Staphylococcal abscess community
SaPI	S. aureus pathogenicity island
Sar	Staphylococcal accessory regulator
SpA	Protein A
SSTI	Skin and soft tissue infections
TAE	Tris-acetat-EDTA
TSA	Tryptone soy broth agar
TSB	Tryptone soy broth
vWbp	Von Willebrand factor binding protein
vWF	Von Willebrand factor
WTA	Wall teichoic acid

1 Introduction

1.1 The role of *Staphylococcus aureus* as a human pathogen

1.1.1 *Staphylococcus aureus* as a pathogen

Staphylococcus aureus (S. aureus) is a bacterium with a split personality. It is a part of the normal skin and nasal flora, and commonly colonises the anterior nares without causing symptoms. However, *S. aureus* is also a pathogen responsible for superficial skin and wound infection, and infections of internal organs such as endocarditis, pneumonia and osteomyelitis, often following bacteremia.

1.1.2 Nasal carriage as a risk factor for infection

Approximately 20% of the population are persistent carriers of *S. aureus*. A further 20% of the population are almost never colonized and the majority, 60% or so of the population, are intermittent carriers (J. A. N. Kluytmans, 1997). Nasal colonization increases the risk of infection by a factor of 2-12 (Botelho-Nevers et al., 2016). Analysis of *S. aureus* isolates of infected patients who are also carriers reveals that, in a majority of cases, infection is endogenous (Weidenmaier, Goerke, & Wolz, 2012). However, circumstances that lead to the transition from colonization to invasion have not been fully explored. There is a strong link with skin defects acting as an entryway, and immunosuppression functioning as a promoting factor. For example, asymptomatic carriers of *S. aureus* undergoing surgical procedures are prone to infection. In an intervention trial Kluytmans *et al.* (1998) administered mupirocin nasal ointment to eradicate colonisation and found a significant reduction in surgical site infection.

So far, a variety of factors in both the pathogen and the host contributing to nasal colonisation have been identified. Colonisation predominantly takes place in the anterior nasal cavity, which is a habitat posing several challenges. It is lined with

squamous epithelium of which the upper layer is constantly shed and coated with mucus which contributes to trapping and clearing pathogens. Antimicrobial substances present include lysozyme, bactericidal fatty acids such as palmitic acid and cis-6-hexadecanoic acid, immunoglobulins, defensins and the host's complement system. *S. aureus* produces an arsenal of factors to counteract those habitat challenges. It is noteworthy that the order in which different factors are up- or downregulated also plays an important role in successful colonisation. They are orchestrated in a precise manner of which most mechanisms are at best only partially understood. Adhesion factors such as wall teichoic acids (WTA) and microbial surface components recognizing adhesive matrix molecules (MSCRAMM) play a major role in initiation of *Staphylococcus* adherence (Speziale et al., 2009) whereas clumping factor B, which binds to cytokeratin 10 (O'Brien, Walsh, Massey, Peacock, & Foster, 2002, Foster, 2009) along with iron-regulated surface determinant A, are major contributors to persistence of *S. aureus* in nares (Steven & Steinert, 1994, Clarke *et al.*, 2009). On the host side, carrying *S. aureus* seems to be associated with genetic predisposition (van den Akker *et al.*, 2006, Emonts *et al.*, 2008, Ruimy *et al.*, 2010).

1.1.3 Overview of *S. aureus* virulence gene regulation systems

1.1.3.1 *S. aureus* toxinoses

S. aureus pathogenicity emanates from a complex system of regulators and not all mechanisms are fully understood. There are only few cases in which cause and effect can be directly linked. In those cases, so-called toxinoses, disease is caused by a single toxin. They include the toxic shock syndrome caused by toxic shock syndrome toxin-1, the staphylococcal scalded skin syndrome caused by the exfoilative toxins A and B and staphylococcal food poisoning caused by staphylococcal enterotoxins.

1.1.3.2 Virulence gene regulators

Pathogenicity beyond toxinoses is considered multifactorial and a range of different cell surface proteins, secreted toxins and enzymes are responsible. Many different extracellular and cell-envelope-associated proteins have been described. Virulence factors can be classified according to their function during different stages of infection (Plata, Rosato, & Węgrzyn, 2009). The fact that soluble extracellular proteins are produced mainly during the post-exponential growth phase suggests a common underlying regulation mechanism. There are numerous regulators involved in controlling virulence gene expression to ensure that gene products acting as an interface between the bacterium and the host reflect the biologcal needs of the organism. These include two-component regulatory systems, which are commonly found across bacterial species. Two well-characterised two-component systems are the accessory gene regulator (Agr) system and SaeR/S system. Furthermore, transcription control factors such as CodY and Sar-family regulators and sigma factors also act as gene regulators. These regulatory systems are highly interactive, as can be seen with the Agr system, which is influenced by CodY, SarA and sigma factor B (σ^B). These complex interactions ensure that appropriate adaptive or virulence factors are made on demand during the different stages of colonization and infection.

1.2 *S. aureus* abscess formation

1.2.1 Clinical burden of *S. aureus* blood stream, skin and soft tissue infections

According to the SENTRY survey (Dryden, 2010), *S. aureus* is the most frequent pathogen causing blood stream infections, skin and soft tissue infection (SSTI) and lower respiratory tract infections combined across all geographic areas that have been surveyed (US, Canada, Latin America, Europe and the Western Pacific region). Most community-acquired *S. aureus* infections manifest as SSTIs (DeLeo, Otto, Kreiswirth, & Chambers, 2010; Fridkin et al., 2005; Talan et al.,

2011) with abscess formation and cellulitis being the most frequent clinical presentation of an SSTI (Ray, Suaya, & Baxter, 2013).

1.2.2 General physiological reaction to tissue lesions

An abscess is defined as an inflammatory lesion releasing purulent material and it is a standard immune response for many biological, chemical or physical insults to tissue (Lowy, 1998). Abscesses can be superficial and self-limiting, but can also occur in deeper sites, such as muscle tissue, and any other organ system. Clinically, the most common type of abscess occurs in the abdominal cavity with *Bacteroides fragilis* (*B. fragilis*) being the most commonly associated pathogen. Even though the understanding of cellular and molecular mechanisms has grown in the past, the high complexity of the nonlinear inflammation response makes it difficult to predict the impact of each component.

1.2.3 Stages and features of *S. aureus* abscess formation

In a murine infection model, injection of heat-killed staphylococci does not induce abscess formation (Cheng et al., 2009). This contrasts with injections of other biological material, such as purified capsular polysaccharide of *B. fragilis* which by itself can activate abscess formation (Onderdonk, Shapiro, Finberg, Zaleznik, & Kasper, n.d.; Tzianabos, Kasper, Cisneros, Smith, & Onderdonk, 1995). These findings suggest distinctive features of *S. aureus* abscess formation exclusive to interaction between the live pathogen and the host. In the following section, stages of a bloodstream infection with subsequent abscess formation are described.

1.2.3.1 *S. aureus* in the blood stream

Following entryways such as breaches in the skin barrier or intravascular medical devices, *S. aureus* enters the bloodstream and survives by bypassing the host's innate immune system. The most important components of the innate immune system are polymorphonuclear leukocytes (PMN) and the complement system.

PMNs have the ability to phagocytose pathogens. This process is most efficient when the bacterium is opsonized with antibody and complement. Pathogens express surface molecules such as lipopolysaccharides, lipoproteins and lipoteichoic acids, which can be recognized by specific antibodies in the bloodstream. Antibody binding enables deposition of complement. Complement and antibody Fc region is recognized by various PMN surface receptors (e.g. ClqR, CD35 and CR3 for complement and e.g. CD64, CD32 and CD89 for Fc fragment). After engulfment into the PMN, the vesicle containing the bacterium fuses with specific vesicles containing bactericidal agents (Kobayashi, Malachowa, & DeLeo, 2015). Bactericidal agents include reactive oxygen species (ROS), multiple other oxygen metabolites (e.g. hydrogen peroxide, superoxide anion and hypochlorus acid) and oxygen-independent agents (e.g. α-defensins, cathepsins and lysozyme) (Borregaard, Sørensen, & Theilgaard-Mönch, 2007). Staphylococci deploy several mechanisms to survive in a phagosome for several days. These mechanisms include protective factors against ROS, such as catalase, superoxide dismutase and staphyloxanthin. Clumping factor (Clf) A and B play a role in escape from opsonophagocytosis, by depositing fibrinogen on the bacterial surface. The antiphagocytotic effect was demonstrated as *ClfA*-defective strains were not able to survive in murine blood (Cheng, unpublished observation).

S. aureus protein A (SpA) has an important role in manipulating the immune response. It can bind the Fc component of immunoglobulins (Uhlén *et al.*, 1984, Jensen, K., 1958), therefore inhibiting opsonisation. Furthermore, SpA can activate platelet aggregation (Rg Hartleib *et al.*, 2000), it can function as a B-cell superantigen (Roben *et al.*, 1995) and it can induce staphylococcal pneumonia (Gómez et al., 2004).

1.2.3.2 Exiting vasculature

Having escaped innate immune defences in blood, *S. aureus* leaves the bloodstream and disseminates to organ tissues to form abscess lesions. Baba *et*

al. have demonstrated in a murine model that, within six hours of intravenous inoculation of 1 x 10^7 CFU, 99.9% of staphylococci have disappeared from the bloodstream (Cheng et al., 2011). There are several routes by which staphylococci exit vasculature, but molecular mechanisms have only been partially elucidated. Endothelial adhesion is the first step, mediated by adhesion factors of the MSCRAMM family (Foster, Geoghegan, Ganesh, & Höök, 2014; Weidenmaier et al., 2005) and WTA. Both MSCRAMMS and WTAs also play a major role in adherence and colonization of the nasal cavity as mentioned above. Most prominent members of the MSCRAMMS family are fibronectin-binding proteins FnBPA and FnBPB, which are recognized by receptors on the endothelial surface. This in turn, triggers bacterial uptake (Sinha et al., 1999).

Another exit model involves von Willebrand factor (vWF), a glycoprotein released by endothelial cells during vascular injury (Sadler, 1998). *Staphylococcus* von Willebrand factor binding protein (vWbp) is secreted into the bloodstream and interacts with vWF. Since both proteins are secreted into the blood stream, it remains unclear, how this interaction leads to adhesion and promotes uptake of *S. aureus* into the tissue. Claes *et al.* (Claes et al., 2014) have found that vWbp interacts with fibrin fibers and endothelial adhesion is mediated via induction of microthrombi that form around staphylococci Another exit possibility is provided by professional phagocytes. As mentioned above, staphylococci are able to survive in phagosomes. Studies on mice have shown that staphylococci can exit vasculature and disseminate in tissue using PMNs as their Trojan horse (Gresham et al., 2000).

Disruption of the endothelial barrier is mediated by α-hemolysin (Hla). Hla displays metalloprotease activity and is able to cleave endothelial cadherin, a transmembrane protein of adherens junctions (Powers, Kim, Wang, & Bubeck Wardenburg, 2012). Hla also targets other cell types such as epithelial cells, blood cells and platelets (Berube & Wardenburg, 2013).

1.2.3.3 Early lesion: *S. aureus* induces a large immune response

Following invasion of host tissue, lesions are visible in a hematoxylin-eosin stained thin-section of the tissue two days post infection. At this stage, the lesion does not show discernible organization (Cheng et al., 2009). A distinct feature of *S. aureus* lesion is the induction of a large immune response. *In vitro* and murine infection experiments have revealed that *S. aureus* elicits expression of a variety of proinflammatory factors including interleukins 1α (Olaru & Jensen, 2010), 1ß (Cho et al., 2012), 6 (Puel et al., 2008), 8 (König, Prévost, Piémont, & König, 1995) and interleukin 17 (Cho et al., 2010) as well as tumour necrosis factor α (Prabhakara et al., 2013). These factors contribute to PMN recruitment to the site of infection. Production of chemotaxins by keratinocytes, T-cells, macrophages and PMNs further increases extravasation of immune cells (Abtin et al., 2014; Cho et al., 2010; McLoughlin et al., 2006; Minegishi et al., 2009). Some experiments have shown contradictory results, whereby secreted staphylococcal superantigen-like protein-5 and protein-11 block PMN rolling in the vessel, leading to reduced extravasation of PMNs (Bestebroer et al., 2007; Durr et al., 2006). *S. aureus* can also deploy chemotaxis inhibitory protein and staphylococcal complement inhibitory protein to block chemotaxis (de Haas et al., 2004; M Rooijakkers et al., n.d.; Prat, Bestebroer, de Haas, van Strijp, & van Kessel, 2006; Rooijakkers et al., 2006).

1.2.3.4 Interaction with PMNs

During infection, *S. aureus* directly alters physiological functions of PMNs. PMN phagocytosis is inhibited by SpA, which binds the antibody Fc region and therefore blocks opsonization. As mentioned above, ClfA contributes to protection from phagocytosis. *S. aureus* can induce programmed necrosis in PMNs, a process similar to apoptosis, leading to cell death (Greenlee-Wacker et al., 2014). Direct PMN lysis can be induced by *S. aureus* leukotoxins Panton-Valentine leukocidin, leukocidin GH, leukocidin DE and *S. aureus* phenol-soluble modulins, γ-hemolysin and δ-toxin (Alonzo III et al., 2012; Cooney, Kienle, Foster, & O 'toole2t, 1993; Graves et al., 2010; Gravet et al., 1998; Kreger, Kim, Zaboretzky, & Bernheimer, 1971; Malachowa et al., n.d.; Panton & Valentine, 1932; Prévost et al., 1995; Ventura et al., 2010; Wang et al., 2007).

1.2.3.5 Mature lesion: Organised Abscess

In the animal model of Cheng *et al.*, the characteristic morphology of an *S. aureus* abscess is formed within 48-72 hours post infection (Cheng et al., 2009; Thammavongsa, Missiakas, & Schneewind, 2013). A staphylococcal abscess community (SAC) can be found at the centre of the lesion, surrounded by a layer of eosinophilic fibrin deposits. At the periphery of the lesion, immune cells accumulate in concentric layers with the inner layer being necrotic PMNs and the outer layer consisting of healthy PMNs (Cheng et al., 2009; Thammavongsa et al., 2013). Bordering the abscess, a rim of necrotic PMNs can be found. They are surrounded by an eosinophilic, amorphous mass that separates healthy tissue from the nidus of infection. The SAC itself contains staphylococci, some erythrocytes, but no immune cells (see Figure 1).

1.2.3.6 Abscess rupture and staphylococci dissemination

Abscesses mature over weeks and can eventually rupture. In the case of the mouse model by Cheng *et al.*, ruptured abscesses in the kidneys resulted in dissemination of staphylococci in the peritoneal cavity and led to new sites of infection.

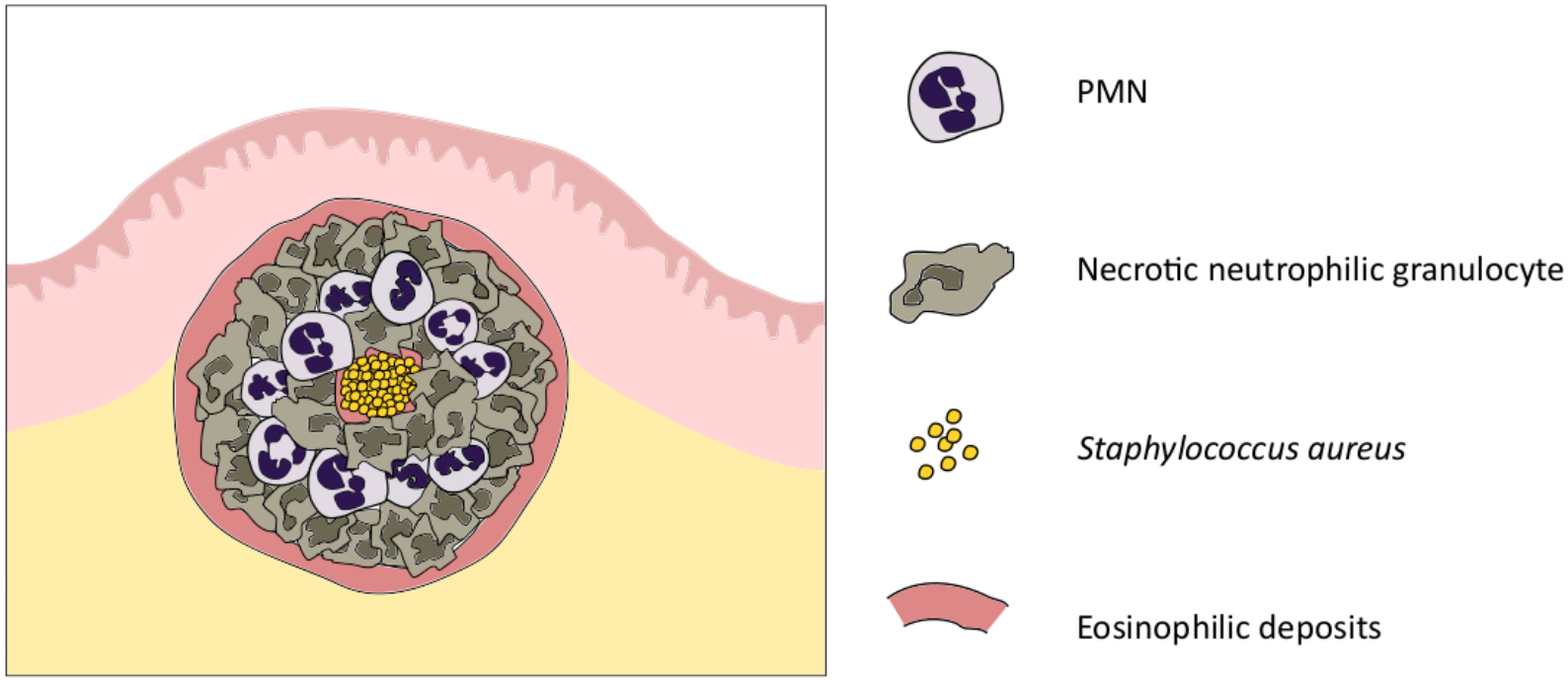

Figure 1. Characteristic morphology of an *S. aureus* abscess. Depicted is a subcutaneous abscess, staphylococci are in the centre of the lesion, surrounded by a wall of eosinophilic deposits, constituting the SAC. The SAC is surrounded by a wall of necrotic PMNs, a wall of vital PMNs and a wall of necrotic PMNs. The lesion is demarcated from healthy tissue by an eosinophilic capsule. Modified after Thomer *et al.* 2016.

1.2.4 Experimental abscess models

Guggenberger *et al.* have established an *in vitro* infection model by embedding staphylococci in bovine collagen type I. The collagen forms a rigid matrix for the growth of *S. aureus* colonies. Staphylococci do no interact with or degrade matrix structures throughout the course of the infection model. This makes this model suitable for growth assays. In their study, *S. aureus* strain Newman has been embedded into the collagen matrix. The colonies, when staphylococci were grown with RPMI 1640 medium, are irregularly formed, whereas colonies are more distinct and discrete when RPMI 1640 was supplemented with fibrinogen. Supplementation of fibrinogen results in the formation of two concentric structures form around the colonies, the pseudocapsule, which directly encloses a staphylococcus conglomeration resembling the SAC, and the microcolony associated meshwork (MAM), which forms a broad halo around the colony. These structures only form in the presence of fibrinogen and rapidly degrade upon addition of plasmin, which is suggestive of these structures being made up of fibrin. In a neutrophil challenge assay, the MAM acts as a mechanical barrier, keeping PMNs away from the microcolony. A Newman *vWbp* and extracellular matrix binding protein (*emp*) mutant is not able to form a MAM, but forms a pseudocapsule. The pseudocapsule also keeps staphylococci mechanically sheltered from PMNs, however, this barrier is invaded by PMNs within a matter of a few hours, suggesting it only acts as a weaker second barrier. Genes that enable MAM formation include vWbp, as a vWbp mutant is unable to form an MAM during growth. For pseudocapsule formation, the coagulase (coa) gene is required. A coa mutant forms irregularly shapes pseudocapsules (Guggenberger et al., 2012a).

1.3 The quorum sensing controlled Agr-system in *S. aureus*

1.3.1 Quorum sensing

One of the main global gene regulating systems is the Agr system. The *agr locus* encodes a circuit that allows control of gene expression mainly by sensing bacterial density. In general, these circuits consist of a low-molecular-weight signaling molecule known as the autoinducer and response systems to this molecule. The mechanism is based on the fact that as a population grows and continuously secrets the autoinducer, the local concentration increases as a function of population density. At a certain level, the autoinducer can then trigger very rapid population-wide responses, an effect termed quorum sensing (Greenberg, 1994).

1.3.2 The Agr circuit in *S. aureus*

Like many other bacterial species, *S. aureus* utilizes a quorum sensing circuit to regulate virulence gene expression. The *agr locus* consists of two transcriptional units expressed from two promoters P2 and P3. The P2 transcript contains four genes in a unit known as an operon, consisting of AgrA, B, C and D. AgrA and AgrC code for the classical two-component signaling module consisting of a membrane-bound receptor-histidine kinase AgrC and the cytoplasmic response regulator AgrA. AgrD codes for the active ligand Autoinducing Peptide (AIP) and AgrB acts as an integral membrane endopeptidase and SpsB signal peptidase to process the peptide precursor AgrD into its final structure. The P3 promoter induces expression of an RNA molecule, RNAIII, which acts as the effector molecule. Figure 2 gives a schematic overview of the Agr locus (Novick & Geisinger, 2008). The autoinduction circuit is formed by AgrA-D. Upon activation by extracellular AgrD, the signal is transmitted from the receptor AgrC to an intracellular AgrA via phosphorylation. AgrA then drives both the P_2 promoter of the autoinducing circuit, as well as the P_3 promoter to transcribe the effector molecule RNAIII.

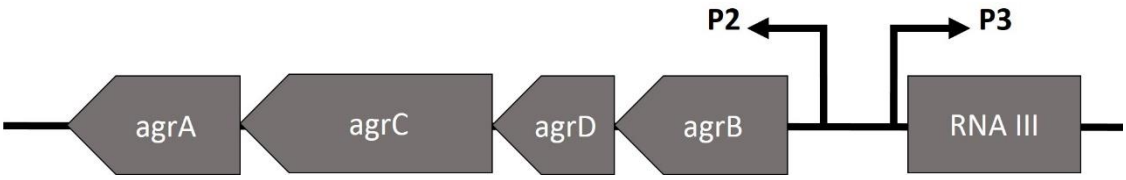

Figure 2. The *agr* locus. There are two transcriptional units expressed from promoters P_2 and P_3. *agrA* and *agrC* constitute the two-component signaling module, *agrD* forms the autoinducer AIP and *agrB* acts as an endopeptidase, processing the AIP into its final structure. Autoinduction occurs when extracellular AIP binds to AgrC, inducing the transcription of the two *agr* promoters via AgrA. The P_2 promoter activates the autoactivation circuit, the P_3 promoter activates the transcription of RNAIII, which is the effector molecule of the Agr system. Modified after Novick *et al.* 2008.

In staphylococci, there are allelic variations in the Agr B, D and C region and this has resulted in at least four Agr specificity groups and four different groups of AIPs. Heterologous AIP-receptor-pairing results in cross-inhibition which causes the Agr-regulated virulon to be blocked. This is depicted in Figure 3 below. Cross inhibition occurs between all AIP molecules except from group I and IV which can be attributed to its structural resemblance. AIP molecules are seven to nine amino acids in length and its cyclic structure proved to be crucial for Agr activation or inhibition (Lyon, Mayville, Muir, & Novick, 2000; Mayville et al., 1999; MDowell et al., 2001) and for AIP II the tail region is also critical for activation (Mayville et al., 1999).

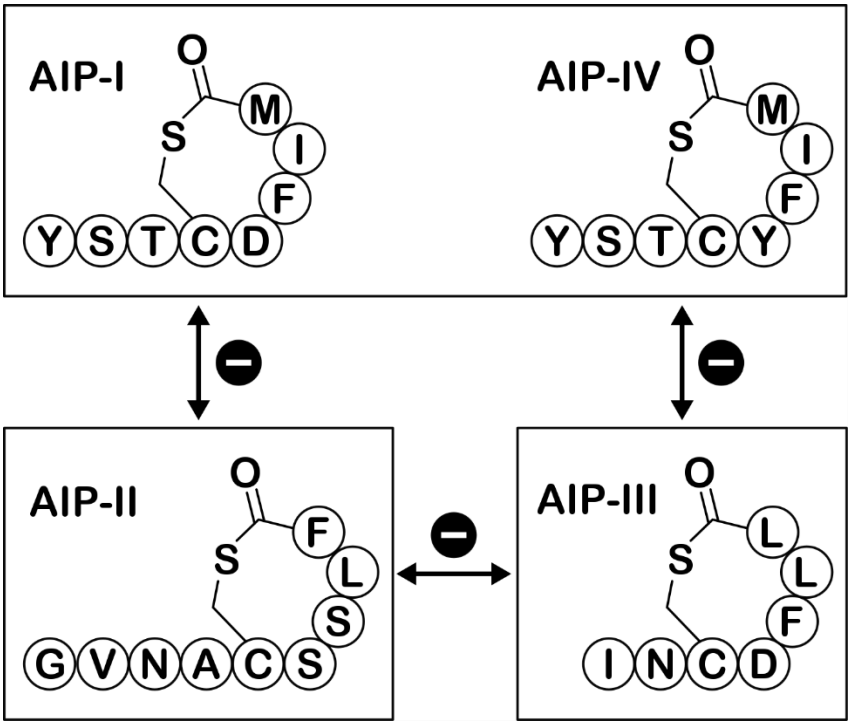

Figure 3. AIP groups and their cross-inhibition. The four different AIP groups arising from allelic variations show cross-inhibition of heterologous receptors. Cross-inhibition occurs between all AIP groups except for between AIP-I and AIP-IV. Modified after Novick *et al.* 2008.

RNAIII is a 514-nt RNA with a complex secondary structure. As the effector molecule of the Agr circuit, it is stable and highly abundant RNA with a variety of regulatory effects. The main function of RNAIII is regulation of translation of individual exoproteins and pleiotropic regulators. It directly upregulates translation of Hla by adversing a translation-inhibiting structure in the *Hla* messenger ribonucleic acid (mRNA) leader (Morfeldt, Taylor1, Von Gabain2, & Arvidson3, 1995) and it directly downregulates the translation of Protein A and of Fibrinogen-binding protein by pairing with the translation-initiation regions (Novick et al., 1993). RNAIII also interacts with a global virulence gene regulator Rot. Effects driven by Rot include the upregulation of translation of surface protein genes and the downregulation of translation of secreted proteins (Saïd-Salim et al., 2003). RNA III inhibits ribosome binding to rot mRNA and thus counteracts the effects brought about by Rot (Boisset et al., 2007).

1.3.3 Agr in the network of other virulence gene regulators

The interaction between gene regulators and transcription factors is highly complex. The Agr system shows interactions with several other gene regulators, including the pleiotropic regulator Staphylococcal accessory regulator (SarA), a winged helix-turn-helix DNA-binding protein, which binds both P2 and P3 promoters and is necessary for transcription of RNAIII (Cheung, Bayer, & Heinrichs, 1997; Chien & Cheung, 1998; Heinrichs, Bayer, & Cheung, 1996; Rechtin et al., 1999). Another regulator modulating the Agr quorum sensing circuit is the transcription factor σ^B (Saïd-Salim et al., 2003; Ziebandt et al., 2004), which also influences the expression of SarA (Tuchscherr et al., 2015). Figure 4 summarises the interactions in a simplified manner. Most interactions have been analysed in *in vitro* experiments. In vivo gene regulation is likely to be much more complex.

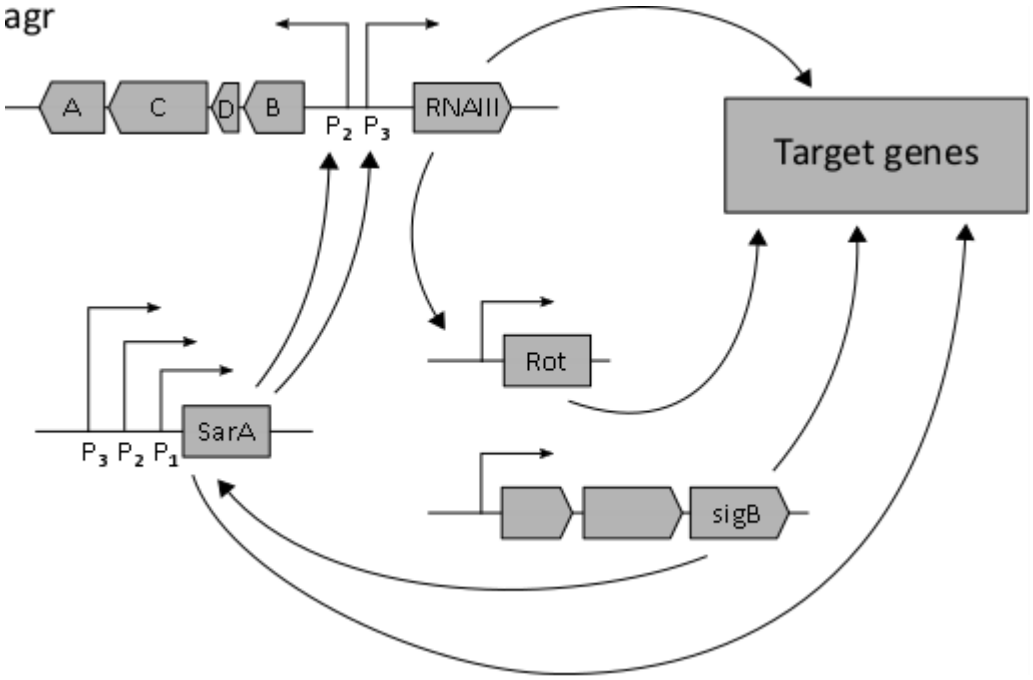

Figure 4. Network of virulence gene regulators Agr, SarA, Rot and σ^B. Both Agr promoters are modulated by the pleiotropic regulator SarA, which is in turn regulated by transcription factor σ^B. The effector molecule of the Agr circuit, RNAIII, inhibits Rot, which acts as an inhibitor of virulence genes. RNAIII also has effects on a multitude of target genes. Modified after Pragman *et al.* 2004 and Gonser *et al.* 2009.

1.4 Capsular polysaccharide in *S. aureus*

1.4.1 The role of *S. aureus* cell envelope in pathogenesis

The bacterial cell envelope is the collective term for the plasma membrane and cell wall. All proteins that are exposed on the cell surface are referred to together as the surfactome. The surfactome itself represents an interface between host and pathogen but also a potential target for drugs and antibodies.

Major *S. aureus* surface polysaccharides are capsular polysaccharide (CP), WTAs and polysaccharide intercellular adhesin/poly-β(1-6)-N-acetyl glucosamin (PIA/PNAG) (Weidenmaier & Lee, 2015). Several different CP serotypes have been described in the past and serotype 5 and 8 have been found to be most prevalent, accounting for 25% and 50% of all isolates of clinical and commensal origin (Arbeit, Karakawa, Vann, & Robbins, 1984; Hochkeppel et al., 1987; J. C. Lee, Liu, Parsonnet, & Arbeit2, 1990; Sompolinsky et al., 1985). Heavily encapsulated strains CP1 and CP2 are very rare (Grunert et al., 2013). *S. aureus* laboratory strain Newman, which was used in this study, is a capsular serotype 5 producer.

1.4.2 Determinants of CP5 expression

The expression of *S. aureus* CP5 is highly susceptible to a number of environmental factors when grown *in vitro*. Iron limitation, solid medium broth, growth in milk and medium with up to 5% NaCl supplementation has been found to enhance CP5 expression (J. C. Lee, Takeda, Livolsi, & Paoletti, 1993; Pöhlmann-dietze et al., 2000; Sutra, Rainard, & Poutrel, 1990) whereas yeast extract, alkaline growth conditions, anaerobiosis, and elevated levels of CO_2 of 1-5% (B. Dassy, Stringfellow, Lieb, & Fournier, 1991; S Herbert et al., 1997; Silvia Herbert et al., 2001) were shown to influence capsule formation negatively. Expression of CP5 is also highly dependent on growth phase. During logarithmic phase, there is limited CP5 expression, whereas during stationary phase, maximal CP5 expression has been found (Cunnion, Lee, & Frank, 2001; Bruno

Dassy & Fournier, 1996; Pöhlmann-dietze et al., 2000; B Poutrel, Gilbert, & Lebrun, 1995). This is thought to be an adaptive measure of staphylococci. Adhesion assays suggest that expression of CP5 correlates with reduced adherence (Pöhlmann-dietze et al., 2000), therefore expression of CP5 is thought to be reserved for post-exponential phase when adhesion to tissue is secondary and host immune invasion is paramount.

As discussed in the previous two sections, Agr acts as a global gene regulator with a number of pleiotrophic effects regarding expression of virulence genes. Capsular polysaccharide is hypothesized to be among these virulence factors. This thought arises from the observation that *agr* mutants are diminished in CP production (Fischer *et al.* 2014. Luong *et al.* (2002) have carried out examinations of members of each of the four Agr groups (RN 8465, group III; RN4850, group IV; RN9130, group II and RN6734, group I). In each case they found a drastic reduction or abrogation in CP5 or CP8 specific mRNA levels in Agr mutant strains.

Early flow cytometry experiments performed by Poutrel *et al.* (B Poutrel, Rainard, & Sarradin, 1997) reported a high level of heterogeneity in CP5 expression within a population. In their study, they analysed thirty isolates from human and animal sources. The results showed wide intra-isolate heterogeneous distribution of CP expression. This phenomenon has since been observed in multiple different studies *in vitro* and *in vivo*. Pöhlmann-Dietze *et al.* (Pöhlmann-dietze et al., 2000) analysed Newman strain staphylococci in stationary growth phase and detected CP5 expression in 39% of the bacteria. Leading up to our experiments, we sampled single bacterial clusters in three *S. aureus* nasal carriers and stained them with immunofluorescence to assess for CP expression. The result is consistent with previous *in vitro* observations, that is that only a subpopulation of staphylococci within a single cluster expressed CP (George et al., 2015). This heterogeneity is sometimes referred to as non-genetic individuality and thought to arise as an adaptive feature of a bacterial population. Changes of the environment may favour a certain subpopulation and therefore the phenotypic variability would ensure the survival of the well-adapted subpopulation.

1.4.3 Virulence of capsular polysaccharide in vivo

As mentioned above, CP is a major surface polysaccharide in *S. aureus* serving as a virulence factor by protecting the bacterium from opsono-phagocytosis (Riordan & Lee, 2004).

Findings from a murine bacteriaemia infection model show that virulence of wildtype *S. aureus* strains compared to their CP5 mutant is highly dependent on growth conditions, growth phase and site of infection. First experiments with wildtype strain Reynolds and CP mutant strains were performed with inocula of log-phase bacteria. They revealed similar LD_{50} numbers for the wildtype and mutant strain suggesting no difference attributable to CP production. However, when wildtype and mutant strains were grown on solid agar, which provides optimal conditions for CP expression, and subsequently inoculated into mice, the LD_{50} value was 10-fold lower for the wildtype (Thakker, Park, Carey, & Lee, 1998). In addition, level of bacteremia was significantly higher and clearance was less efficient in wildtype strain infection compared to mutant strain infection suggesting higher virulence of the wildtype strain due to CP5 formation (Riordan & Lee, 2004). The same outcome was observed in murine infection models for renal and subcutaneous abscesses and septic arthritis (Nilsson, Lee, Bremell, Rydé N, & Tarkowski, 1997; Portolé, Kiser, Bhasin, Chan, & Lee, 2001). Weight loss and mortality was significantly higher in mice infected with CP potent *S. aureus* strains. On the other hand, it has been shown that CP5 masks adhesins, and it seems that CP5 expression in infection sites, where adherence is crucial, puts the bacterium at disadvantage.

This can be seen in a murine endocarditis model. Endocarditis is an inflammatory disease of heart valves. Since heart valves do not have their own blood supply and due to constant movement of the valves, it is crucial for infecting pathogens to be able to attach themselves firmly to heart valve structures. As discussed above, CP expression hinders staphylococcal adhesion by masking adhesins on the cell surface. This leads to a decrease in virulence (Nemeth & Lee, 1995). In

a murine endocarditis model, it was observed that the LD_{50} of the loss-of-function mutant strain was 10-fold lower than that of their parent strain (Baddour et al., 1992).

Interestingly, this phenomenon can also be observed when evaluating the role of capsular polysaccharide in nasal colonisation. CP deficient strains persist significantly better on endothelial cells compared to its parent strain (J.C. Lee, unpublished observations).

1.5 Fluorescent reporter protein green fluorescent protein (GFP)

1.5.1 Properties of GFP

GFPs were discovered in jellyfish *Aequorea victoria* several decades ago (Merzlyak et al., 2007; Shcherbo et al., 2007) and have since come to be the most popular reporter protein in cell biology. The major advantage offered by this protein is its ability to form an internal chromophore without requiring accessory cofactors, enzymes or substrates other than molecular oxygen (Campbell et al., 2002; Labas et al., 2002; Zacharias, Baird, & Tsien, 2000). This opens up the possibility of chromophore formation in live organisms, tissues and cells (Cubitt et al., 1995).

1.5.2 GFP mutants

Since its isolation, GFP has been modified in a number of ways to enhance and alter its properties. For example, variants have been created with different absorption and emission wavelengths, allowing multiple reporters to be used simultaneously. Variants in our study were Cerulean (Rizzo, Springer, Granada, & Piston, 2004) and Venus (Nagai *et al.*, 2002). The excitation and emission spectrum of Cerulean and Venus are depicted below (modified after Sarkar *et al.* 2009) .

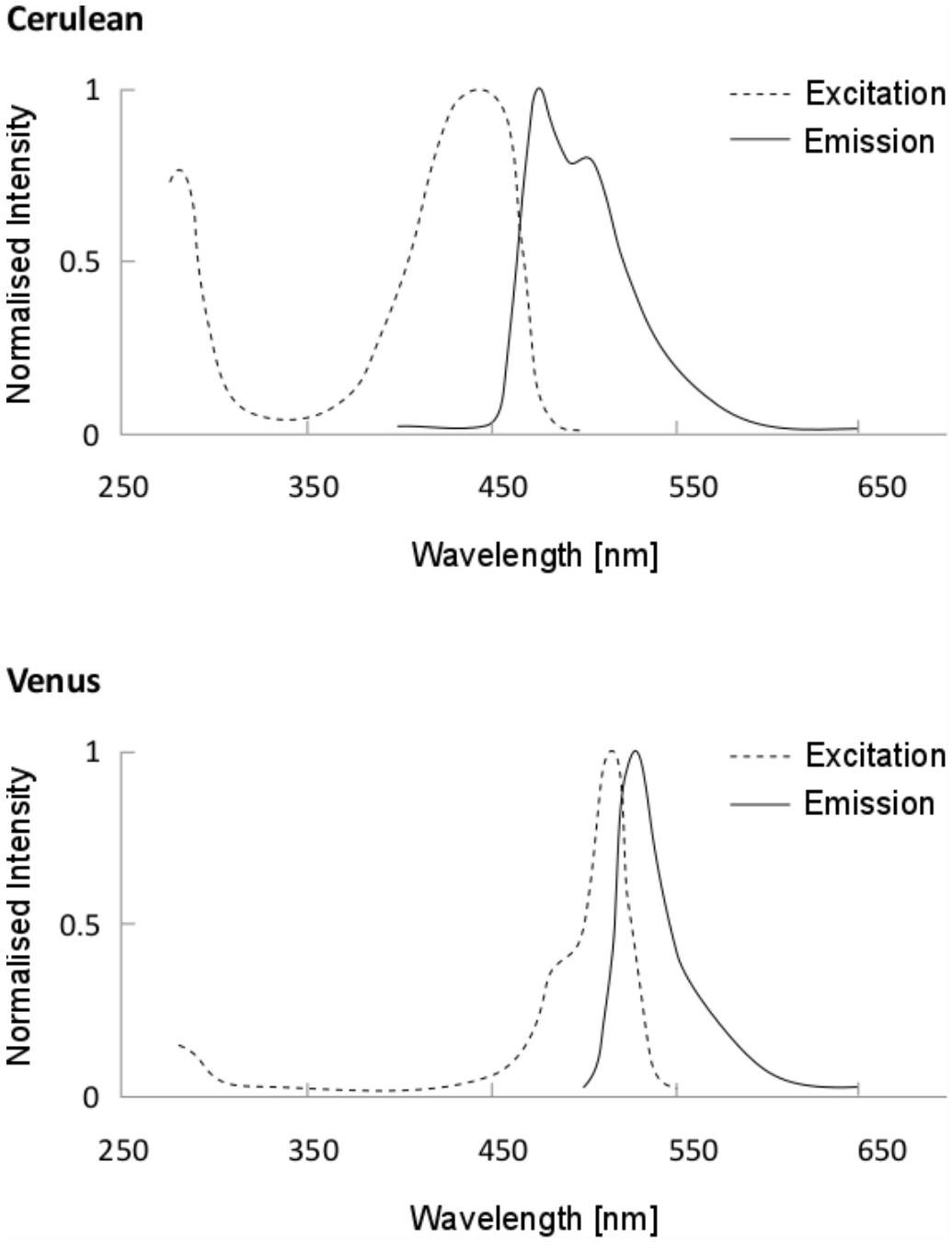

Figure 5. Emission and excitation spectra of GFP derivatives Cerulean and Venus, after Sarkar *et al.* 2009.

1.6 Molecular cloning constructs in *Escherichia Coli* and *S. aureus*

1.6.1 Principles of reporter strain construction

In order to assess promoter activity in *S. aureus*, plasmids have to be obtained containing (i) the promoter of interest, (ii) an *S. aureus* replicon, (iii) selection genes in *Escherichia coli* (*E. coli)* and *S. aureus*, (iv) reporter genes and (v) a multiple cloning site. Charpentier *et al.* (2004) have developed *E. coli*-staphylococcal shuttle vectors to facilitate exchange of *S. aureus* gene cassettes for replicons, selection genes and reporter genes. This vector shuttle system provides the ability to manipulate *S. aureus* strains. The gene cassettes were created by PCR amplification using primers flanking specific restriction enzyme sites. Products where then digested with restriction enzymes recognizing the flanking sites and vectors constructed by assembly of cassettes along their flanking restriction sites. Figure 6 (modified after Charpentier *et al.*, 2004) depicts the cassette. In this system, cassettes can be replaced or interchanged using the same restriction enzymes, thus providing a versatile tool. Plasmids containing cassettes of choice are created by cloning in *E. coli* strain DH5α or Top 10 and subsequently transformed into *S. aureus* strain RN4220.

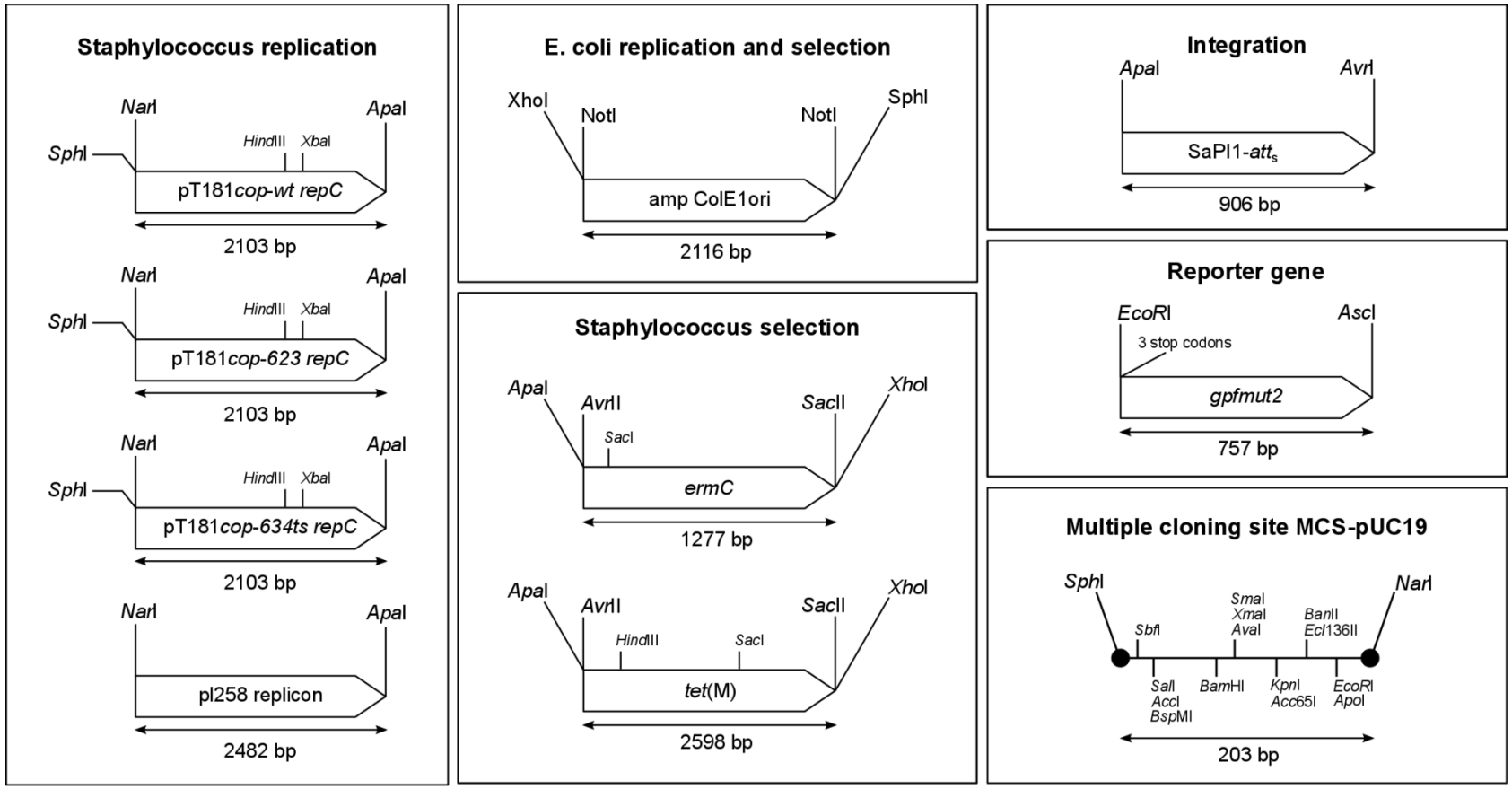

Figure 6. Vector shuttle system cassettes. The vector shuttle system utilizes four different *S. aureus* replicons, one *E. coli* replicon with a selection marker for Ampicillin, two *S. aureus* selection markers for Erythromycin and Tetracycline, one integration cassette into the SaPI1 site and one reporter gene. The cassettes can be cloned into a vector plasmid with the multiple cloning site MCS-pUC19. After Charpentier *et al.* 2004.

Assessing gene expression where the promoter of interest is on a plasmid, creates the issue of varying plasmid copy number between individual bacteria. It is therefore difficult to predict the exact gene dosage. To avoid this issue, chromosomal integration is preferred to obtain single-copy integration vectors. Integration requires an attachment site on the bacterial chromosome, the attB site, and an attachment site on the plasmid, the attP site. Once integrated, the segment is flanked by the attL and attR site. In the vector shuttle system of Charpentier, *S. aureus* replicon cassettes can be replaced with the *S. aureus* pathogenicity island 1 (SaPI1) integration cassette. This allows integration of the plasmid into the SaPI1 site of *S. aureus* chromosome. *S. aureus* strain RN9011, which was used in our study, represents strain RN4220 containing plasmid pRN7023 expressing SaPI1 integrase.

Another effective site-specific integration system is the integration site on the *S. aureus* glycerol ester hydrolase gene (*geh*), also known as lipase (Lee, Buranen, &ah c Ye, 1991). Luong and Lee *et al.* (T. T. Luong & Lee, 2007) have developed an integration plasmid vector that allows cloning into the L54a attB site located within the *geh* locus. *S. aureus* strain CYL316 was used in our study for site specific integration and represents RN4220 with plasmid pYL119Δ19 expressing the *L54a int* gene.

1.7 Aims

Many preexisting fluorescent reporter strains of *S. aureus* rely on multicopy plasmids, meaning that it is not possible to determine whether expression differences are a result of differential promoter activity or just copy number variation between bacteria.

The first aim of this study was therefore to establish single- and double-fluorescent reporter strains in *S. aureus* strain Newman with chromosomally integrated reporter genes, allowing for more precise quantification of gene expression on a single-cell level. We analysed the activity of two different promoters -– agr and cap – upstream of the fluorophore gene using these reporter strains.

In a second part, the aim was to create an *in vitro* abscess model, in which growth and promoter activity can be observed over time in three-dimensional space. The final goal is the establishment of an *in vitro* abscess model, in which bacteria and surrounding abscess structures can be studied.

2 Materials and Methods

2.1 Materials

2.1.1 Chemicals and media components

100bp ladder GeneRuler 100bp Plus	Thermo scientific, Waltham, USA
Agar, Bacto-Agar	Becton Dickinson, Sparks, USA
Agarose	Lonza, Rockland, USA
Ampicillin	Sigma-Aldrich, St. Louis, USA
Ampuwa	Fresenius Kabi, Bad Homburg
Bovine collagen PureCol EZ	Sigma-Aldrich, St. Louis, USA
Bovine Albumin	Sigma-Aldrich, St. Louis, USA
Calcium chloride ($CaCl_2$)	Merck, Darmstadt, Germany
Casaminoacids	BD, Sparks, USA
dNTPs	Quiagen, Hilden, Germany
EDTA Titriplex	Merck, Darmstadt, Germany
EGTA	AppliChem, Darmstadt
Erythromycin	Fluka, Buchs, Switzerland
Ethanol absolute	VWR, Radnor, USA
Formaldehyde	Applichem, Darmstadt, Germany
Glycerol	Applichem, Darmstadt, Germany

Human plasma 0^+	University Hospital Blood Bank, Tübingen, Germany
Mounting medium	Dako, Glostrup, Denmark
NaCl	Merck, Darmstadt
Nuclease-free water	Ambion, Wiesbaden, Germany
Primer	Biospring, MWG-Biotech, Gibco BRL
RPMI 1640	Merck, Darmstadt, Germany
SYBRsafe	Invitrogen, Karlsruhe, Germany
Tetracycline	Serva, Heidelberg/New York
Tris	Applichem, Darmstadt, Germany
Tryptone Soy Broth (TSB)	Oxoid, Basingstoke, England
Tween 20	Sigma, Munich, Germany
Yeast extract	Becton Dickinson, Sparks, USA

2.1.2 Enzymes and Antibodies

DNAse	Roche, Mannheim, Germany
HotStarTaq DNA-Polymerase	Qiagen, Hilden, Germany
Lysostaphin (stock concentration 5mg/ml)	Ambi, Lawrence, USA
Proteinase K (stock concentration 10mg/ml)	Applichem, Darmstadt, Germany

2.1.3 Media and agars

2.1.3.1 Media

Basal medium (BM)	2.5g peptone, 1.25g yeast extract, 0.25g glucose, 1.25g NaCl, 0.25g K_2HPO_4 ad 250ml $H_2O_{deionised}$
Bovine serum albumin (BSA) medium	5g lyophilised powder ad 50ml $H_2O_{deionised}$
CYPG	10g Casaminoacid, 10g yeast extract, 5g NaCl suspended in 935ml $H_2O_{deionised}$. 25ml of 20% glucose solution and 40ml 1.5M glycerophosphate added after autoclavation
Luria-Bertani Broth (LB)	10g Tryptone, 5g yeast extract, 10g NaCl ad 1L $H_2O_{deionised}$ (pH = 7.5)
TSB	30g TSB-powder ad 1L aqua bidest.

2.1.3.2 Agar

Blood agar	Columbia agar with sheep blood plus, Oxoid, Basingstoke, England
$CaCl_2$ agar	15g Bacto-Agar, 500µl 1M $CaCl_2$ ad 1L TSB
Phage Top Agar	3g Casaminoacid, 3g yeast extract, 5.9g NaCl, 7.5g agar ad 1L $H_2O_{deionised}$
Tryptone Soy Broth Agar (TSA)	15g agar ad 1L TSB
TSA-Top Agar	7.5g TSA Agar, 30g TSB ad 1L TSB

2.1.4 Buffers and solutions

10x TE	10mM Tris-HCl, 1mM EDTA, pH = 8
0.5M EDTA	146g EDTA ad 1000ml $H_2O_{deionised}$, pH = 8
10x phosphate-buffered saline (PBS)	28.46 7mM Na_2HPO_4, 2.7g 3mM KH_2PO_4, 170mM NaCl ad 2000ml aqua bidest.
5x Electrophoresis buffer	9.0g Tris, 43.3g glycine, 3.0g SDS ad 600ml aqua bidest.
FIX-MIX	4ml nuclease free water, 0.5ml 10x PBS, 0.5ml 37% formaldehyde
50x Tris-acetate-EDTA (TAE) Buffer	242g 2M Tris-HCl, 57.1ml 1M acetic acid, 100ml 0.5M EDTA ad 1000ml aqua bidest., pH = 8.0
1M Tris/HCl	121.1g Tris, approx. 42ml HCl ad 1000ml aqua bidest.

Bluejuice	5ml glycerine (50%), 200µl 0.5M EDTA, pH = 8.0, 25mg bromine phenole blue ad 10ml Ampuwa
dNTP-Mix	10mM dATP, dCTP, dTTP, dGTP
Glycerol phosphate	846mM, 50% α, 50% β, 92.5g ad 500ml $H_2O_{deionised}$
PBS-Tween 20	250ml PBS, 250µl Tween
Phage buffer	1ml $MgSO_4$ (stock conc. 100mM), 4ml $CaCl_2$ (stock conc. 100mM), 5ml Tris (stock conc. 1M), pH = 7.8, 5.9g NaCl, 1g gelatine ad 1L Ampuwa
Proteolysis buffer	46.5 Na_2EDTA, 3.8g EGTA, 5g N-Laurylsarcosin, pH = 9, ad 500ml Aqua bidest.

2.1.5 Antibiotics solutions

Ampicillin	stock conc. 50mg/ml in $H_2O_{deionized}$
Erythromycin	stock conc. 10mg/ml in 75% Ethanol
Tetracycline	stock conc. 5mg/ml in 75% Ethanol

2.1.6 Laboratory Materials

µ Angiogenesis chamber slides	Ibidi, Planegg/Martinsried, Germany
Coverslips	Thermo scientific, Waltham, USA
Electroporation cuvettes	BTX, Holliston, USA
Reaction tube 1.5ml	Eppendorf AG, Hamburg, Germany
Photometer cuvettes	Sarstedt AG & Co., Nümbrecht

Inoculation loop 10.0µl	Greiner Bio-One, Solingen, Germany
Microscopy slides	R. Langenbrick, Emmendingen, Germany
Microtubes 2ml	Sarstedt AG & Co., Nümbrecht, Germany
Micro reaction tubes	Eppendorf, Hamburg, Germany
Petri dish	Greiner Bio-One, Solingen, Germany
Sterile filter Millex-GS 0.22µm	Merck, Darmstadt, Germany
Stripette 5ml in 10/10ml, 10ml	Corning Incorporated, Corning, USA
Pipette tips	Ratiolab, Dreieich, Germany
Reaction tube 15ml	Greiner Bio-One, Solingen, Germany
Reaction tube 50ml	Falcon, Reynosa, Mexico
Sterile reaction tube 14ml	Greiner Bio-One, Solingen, Germany

2.1.7 Devices

Centrifuges Centrifuge 5417R Mikro 200R Megafuge 16 Minispin	 Eppendorf, Hamburg, Germany Hettich, Tuttlingen, Germany Thermo Scientific, Waltham, USA Eppendorf, Hamburg
Electric pipetting aid Pipetus	Hirschmann Laborgeräte, Eberstadt, Germany
Electroporator	BTX, Holliston, USA
Gel electrophoresis chamber and current source	BioRad, Munich, Germany
Gel documentation system: Fast Gene GP-Fas-V	Nippon genetics, Japan
Incubator 37°C with shaker Minitron	Infors HAT, Bottmingen/Basel, Switzerland

Incubator 37°C	Binder, Tuttlingen, Germany
Microscope NLO 710	Zeiss, Oberkochen, Germany
PCR thermocycler Biometra Trio T3000 Thermocycler	 Analytik Jena, Jena, Germany LabRepCo, Horsham, USA
Pipettes (2.5µl, 10µl,100µl, 1000µl)	Eppendorf, Hamburg, Germany
Spectrometer Ultrospec 2100 pro	Amersham Biosciences, Little Chalfont, UK
Sterile bench Herasafe	Heraeus, Hanau, Germany
Vortexter Vortex Genie	Bender & Hobein AG, Zurich, Switzerland
Water bath GFL 1083	GFL, Burgwedel, Germany

2.1.8 Computer Software

ZEN 2012 SP1 (Black Edition)	Zeiss, Oberkochen, Germany
Vector NTI	Invitrogen, Karlsruhe, Germany

2.1.9 Strains

Strain	Description	Reference
DH5α	Competent *E. coli* for plasmid transformation	
RN4220	Restriction-deficient *S. aureus* strain	Kreiswirth *et al.*, 1983
One Shot TOP10	Competent *E. coli* for plasmid transformation	Invitrogen
CYL316	RN4220 with L54a integrase gene cloned in plasmid vector (pYL112ð19)	C. Y. Lee, Buranen, and Ye 1991
RN9011	RN4220 with SaPI1 integrase gene cloned in plasmid vector (ppRN7023)	Charpentier *et al.* 2004
Newman	Wild-type strain, prototypic isolate	Lorenz and Duthie 1952

Table 1. List of strains used in this study.

2.1.10 Plasmids

Plasmid	Description	Attachment site	Promoter	Marker	Reference
pJL93	$P1_{sar}$-*yfp*, pT181cop-wt repC, *tetM*	-	SarA	tetM	George *et al.* 2015
pCG295	Integration vector, JL93, with replacement of pT181cop-wt repC by attL54 attachment site, *tetM*	geh	SarA	tetM	George *et al.* 2015
pCG302	pCG295 replacement of $P1_{sar}$ with P_{RNAIII}-*gpcer*, attL54-attS	geh	agr	tetM	This study
pCG303	pCG295 replacement of $P1_{sar}$ with P_{RNAIII}-*gpven*, attL54-attS	geh	agr	tetM	This study
pCG317	pCG295 replacement of $P1_{sar}$ with P_{cap}-*gpcer*, attL54-attS	geh	cap	tetM	Alexander, M. sc. student
pCG318	pCG295 replacement of $P1_{sar}$ with P_{cap}-*gpven*, attL54	geh	cap	tetM	George *et al.* 2015
pJL53	Integration vector, P_{RNAIII}-*gpcer*, SaPI1-attS	SaPI-1	agr	ermC	George *et al.* 2015
pJL54	Integration vector, P_{RNAIII}-*gpven*, SaPI1-attS	SaPI-1	agr	ermC	This study

Table 2. Plasmids used in this study.

2.2 Methods

2.2.1 TSA Plates supplemented with respective antibiotics

To prepare TSA plates supplemented with antibiotics, TSA was melted and then cooled down to a temperature of approximately 50°C before antibiotics from stock solutions 10mg/ml erythromycin or/and 3mg/ml tetracycline were added at a dilution of 1:1000 to obtain concentrations of 10µg/ml Erm and 3µg/ml Tet. The liquid TSA was then poured into empty sterile petri dishes and allowed to solidify at room temperature RT.

2.2.2 Plasmid Purification

Plasmids with desired gene cassette were purified from *E. Coli* strain DH5α according to the instructions of the NucleoSpin® Plasmid QuickPure commercial plasmid purification kit (Macherey-Nagel). Colonies grown on TSA agar plates were re-suspended in 1ml TE-buffer and centrifuged at 11,000g for 3 minutes. Alternatively, bacteria were obtained from a liquid culture and 5ml centrifuged at 5000g for 5 minutes. The resulting pellet contained harvested bacterial cells and the supernatant was discarded. For cell lysis, 250µl Buffer A1 was added and the pellet was re-suspended by vortexting or pipetting up and down. Prior to using Buffer A2, it was checked for precipitated SDS. If a white precipitate was visible, the buffer was heated up for several minutes at 30°C to 40°C until the precipitation had dissolved completely. After the buffer cooled down to RT, it was ready to use. 250µl of Buffer A2 was added and the tube was inverted 6 to 8 times. After this step, the tube was incubated at RT until lysate appeared clear or for a maximum of 5 minutes. Next, 300µl of Buffer A3 was added and the tube was inverted 6 to 8 times. The tube was then centrifuged for 5 minutes at 11,000 x g at RT to separate DNA from cell debris. DNA was then bound in the supernatant to the silica membrane of the plasmid column. For this, a NucleoSpin Plasmid QuickPure Column was placed in a collection tube and the supernatant from the tube was decanted into the column. The column was centrifuged for 1 minute at 11,000 rpm. The flow-through was discarded and this step was repeated with the remaining supernatant. The silica membrane was washed with

500µl of AW buffer and centrifuged at 11,000 g for 1 minute. The flow-through was discarded. To dry the membrane, the tube was centrifuged again for 2 minutes at 11,000g. The final step was to elute DNA from the silica membrane. The plasmid column was placed into a 1.5ml Eppendorf cup and 50µl if AE buffer was added to the silica membrane followed by incubation for 1 minute at room temperature. The tube was then centrifuged at 11,000g for 1 minute and plasmids were eluted into the Eppendorf cup.

2.2.3 Electroporation of plasmids into *S. aureus*

Plasmid constructs were stored at -20°C and defrosted prior to electroporation. 2µl of plasmid was added to 50µl of electrocompetent cells and incubated for 30 minutes at RT. In the meantime, 1.5ml Eppendorf cups were prepared with 950µl BM Medium and 50µl 10% BSA. After the incubation period, electrocompetent cells and plasmid were filled into an electroporation cuvette. The cuvette was tapped on the table several times for the fluid to completely sink to the bottom of the cuvette. Attention was paid to not touch the metal part of the cuvettes. Then electroporation at 2000V was performed and 1ml of the prepared BM medium was promptly administered to the cells in the cuvette afterwards. Then, electroporated bacteria were transferred from the cuvette back to the 1.5µl Eppendorf cup and incubated for at least 1.5 hours at 37°C with agitation. Afterwards, 100µl of electroporated cells were plated on two TSA plates supplemented with antibiotics. The remainder in the Eppendorf cup was centrifuged, the supernatant was discarded and the cells were re-suspended in 100µl PBS. Of the more concentrated solution of electroporated cells, 100µl were plated on another TSA plate with antibiotics. All plates were incubated for 1 to 3 days at 37°C.

2.2.4 Phage lysate preparation

To obtain lysates from strains RN9011 and CYL316, TSA Top Agar was melted in the microwave and allowed to cool down to 50 to 55°C using a water bath. One loop of bacteria was taken from a TSA plate and re-suspended in 1ml phage

buffer to an optical density of approximately 0.2. The fluid was then split into a control and an experiment tube with 500µl each. 50-100µl of phage Φ11 was added to the experiment tube and vortexted briefly. 4ml TSA Top Agar was then added to each tube and mixed by inverting three times. Each tube was then poured onto a TSA 100mM $CaCl_2$ plate yielding an experiment plate and a control plate. The plates solidified at RT, and were then incubated at 37°C for 5 to 6 hours. After the incubation period, the control plate was turbid due to bacterial growth, whereas the experiment plate with the phage was clear due lysis of bacteria by the phage. 3ml of TSB was added onto the experiment plate and the upper layer of agar was carefully scraped off the surface with a single-use pipette tube. The agar pieces were transferred into a 50ml Falcon tube. In the Falcon tube, the mass was homogenised by soaking through the pipette. The tube was then incubated in a 40 to 50°C water-bath for 10 Minutes and centrifuged for 10 minutes at 5000g. The supernatant containing the phage lysate was sterile filtered with a 0.45µm pore size filter into a 1.5ml Eppendorf cup.

2.2.5 Phage Transduction

For transduction, phage top agar was melted in the microwave and allowed to cool down to 55°C in a water bath. Target strain Newman was taken from an overnight growth culture on a TSA plate and re-suspended in 400µl phage buffer. The suspension was then split into a control tube and an experiment tube with 200µl of suspension each. 100µl of phage lysate generated from the donor strain was added to the experimental tube. The experimental tube was then briefly vortexted before incubating both the experimental and the control tubes for 10 minutes at 37°C. Afterwards, 4ml of phage top agar was added to each tube and the tube was inverted three times before its contents was poured on to a TSA plate supplemented with suitable antibiotics. The plate was allowed to solidify at RT and then incubated for 1 to 2 days at 37°C. Following initial incubation, single colonies were picked from the plate. They were streaked onto fresh TSA plates and incubated overnight. This step was repeated twice in order to minimize remaining phage content.

2.2.6 DNA Isolation

For DNA isolation, 1ml of a TSB overnight culture or 1 loop of bacteria from a TSA plate was re-suspended in 1ml 1x TE buffer in a 1.5ml Eppendorf cup and centrifuged for 3 minutes at 10,000 rpm. The supernatant was discarded and the pellet was re-suspended in 200µl of 1x TE buffer. 3µl of lysostaphin was added and the tubes were incubated for 20 Minutes at 37°C. Then, 400µl of proteolysis buffer and 10µl of proteinase K was added and the tubes were incubated for 1h in a 55°C water bath. Proteinase K was then inactivated by incubation in a 95°C heating block for 10 minutes. For subsequent PCR, an aliquot of the yielded DNA was diluted 1:100 with nuclease free water and stored in a 4°C fridge, the rest of the undiluted DNA was stored at −20°C.

2.2.7 Qia-L-N and Qia K-N PCR

PCR amplification of a fragment reading from the bacterial chromosome into the plasmid was used to verify whether site-specific integration of the plasmid had occurred. Primers flanking integration sites were used. PCR products were prepared according to the commercial Qiagen kit. All steps were performed under a clean bench. PCR reagents were defrosted from −20°C at RT. The Taq polymerase was defrosted using an ice block. dNTP mix was prepared using 10µl ATP, 10µl TTP, 10µl GTP and 10µl CTP from Qiagen NTP stocks and 360µl nuclease free water.

The total amount of required PCR master mix was calculated according to the number of reagents needed for one PCR probe depicted in the Table 3 below. All reagents were pipetted into a 1.5ml Eppendorf cup and the stock was then split into micro reaction tubes with 25µl each. As the last step, the DNA was added outside the clean bench. The PCR was run according to the Qia-L-N programme for primer pair GFP control for and GFP control rev (table 4 below) and the Qia-K-N programme for primer pairs SaPI_int_for and SaPI_int_rev, scv1 and pCG295links and scv2.1 and pCG295rechts (table 5).

	25µl stock
H_2O	13.75 µl
Buffer	2.5 µl
dNTP	2.5 µl
$MgCl_2$	2 µl
Primer 1	1 µl
Primer 2	1 µl
Taq	0.25 µl
DNA	2 µl

Table 3**. PCR master mix**

Cycle step	**temperature**	**Duration**	**Number of cycles**
Initialization	95°C	15 minutes	1
Denaturation	95°C	30 s	
Annealing	46°C	30 s	30
Elongation	72°C	90 s	
Final elongation	72°C	10 minutes	1

Table 4**. Cycles of Qia-L-N for fragments > 1kb with low annealing temperature.**

Cycle step	temperature	Duration	Number of cycles
Initialization	95°C	15 minutes	1
Denaturation	95°C	30 s	
Annealing	46°C	30 s	30
Elongation	72°C	45 s	
Final elongation	72°C	10 minutes	1

Table 5**. Cycles of Qia-K-N for fragments < 1kb with low annealing temperature.**

2.2.8 Agarose gel electrophoresis

Electrophoresis on agarose gel was performed to determine the size of PCR products of integration sites and compare it to the calculated size.

1% agarose gel was prepared by adding 0.1 grams of agarose powder for every 10ml 1x TAE buffer. For our large mould, we used 1.3 grams of agarose powder for 130ml of TAE buffer, for the small one 0.9 grams was used in 90ml of TAE buffer. The mixture was heated in the microwave and periodically swayed until it was boiling and the agarose powder had completely dissolved. The gel was then left to cool to about 40-50°C, then 13µl (9µl for the small mould) of SYBRsafe were added to the cooling gel and swayed until it was well mixed. The gel was then immediately poured into the mould. Once solidified, the gel was placed into an electrophoresis chamber containing 1x TAE. For each PCR product, a drop of 3µl blue juice was prepared on parafilm and 5µl of PCR product was mixed with the blue juice drops. The drop containing blue juice and PCR product was transferred into the pouches of the agarose gel. 5µl of 100bp ladder was pipetted

into the first pouch of each row. The electrophoresis was run for 30 minutes, the small gel was run at 80 to 90V, the large gel at a voltage of 120 to 130V.

2.2.9 Bacterial growth conditions for microscopy

To monitor fluorescent bacteria during growth, bacteria were fixed at certain time points and fluorescence behaviour was observed at those points. They were washed and diluted at three time points and mounted onto cover slips in order to observe them using confocal microscopy. The three time points were (i) overnight culture, (ii) T_0 (marking the time point when bacteria were diluted to an OD_{600} of 0.05 from the overnight culture) after being diluted twice to an optical density of 0.05 and grown to a density of 0.3, and (iii) T_0 +6h.

All bacteria were obtained from a -70°C freezing culture and inoculated into 5ml CY medium supplemented with 5µl erythromycin or tetracycline or both, depending on the resistance cassette. The overnight culture was incubated at 37°C in an incubation shaker. After the overnight growth, bacteria were harvested for the first time point and prepared for microscopy. For the day culture, the OD_{600} of the overnight culture was determined and the culture in CYPG was diluted to an OD_{600} of 0.05 in 10ml CYPG. The day culture was incubated at 37°C with shaking. The optical density of the day culture was monitored regularly, by extracting 700µl of culture into photometer cuvettes and determining the OD_{600}. Upon reaching an OD_{600} = 0.3, bacteria were diluted to an OD_{600} of 0.05 again. This step was repeated one more time. The repeated dilution of the day culture ensured, that any AIP in the growth medium was washed out. After the second dilution, bacteria were grown to an OD_{600} of 0.3 and then harvested and prepared for microscopy. The day culture that was diluted from the overnight culture, was incubated for 6h and bacteria were harvested at T_0 + 6h and prepared for microscopy.

2.2.10 Preparation of microscopy slides

To prepare microscopy slides for fluorescence microscopy, the optical density of the culture was determined using either a 700µl sample directly from the culture flask, or a 1:10 or a 1:100 dilution in CYPG, depending on the density of bacteria. The bacteria were diluted to an OD_{600} of 0.3/ml into an Eppendorf cup with CYPG. The cups were centrifuged at 6000rpm for 10 minutes at 4°C, the supernatant was discarded. The pellet was then resuspended in 1ml of prechilled Fix-Mix and incubated at RT for 15 minutes with gentle mixing, by taping the cups to a rotisserie. After incubation, 500µl was transferred to two coverslip-lined wells in a 24-well plate. The plate was centrifuged at 600g for 6 minutes. In this step, fixed bacteria adhered on the coverslip. The coverslip was then gently removed from the well using pipette tips, excess Fix-Mix was removed with a KimWipe. The coverslips were mounted inverted on 3µl of mounting medium on a microscopy slide and leave to dry for 15 minutes.

2.2.11 Growth and preparation of bacteria for 3D colony growth model experiment

All bacteria were obtained from a −70°C freezing culture and inoculated into 5ml CYPG medium supplemented with 5µl erythromycin or tetracycline or both antibiotics, according to resistance cassette. The overnight culture was incubated at 37°C with shaking. For the day culture, the optical density was determined and the overnight culture was diluted to OD_{600} of 0.05 in 10ml CYPG. The day culture was incubated at 37°C with shaking. The optical density of the day culture was monitored regularly, by extracting 700µl of culture into photometer cuvettes and determining the OD_{600}. Bacteria were harvested at OD_{600} = 0.3 and washed two times. For washing, 1ml of culture was filled into a 1.5ml Eppendorf cup, and centrifuged at 6000rpm for 10 minutes. The supernatant was discarded and the pellet was resuspended in 1ml of 1x PBS, the centrifuged at 6000rpm for 10 minutes. The supernatant was discarded and bacteria were resuspended in 1ml of 1x PBS.

2.2.12 Preparation of collagen gel and embedding bacteria

Collagen gel stored at +4°C was allowed to equilibrate to RT under the sterile bench. For our experiments, we used PureCol® EZ gel solution, which consists of purified Type I bovine collagen at a concentration of approximately 5mg/ml. As the experiments by Guggenberger *et al.* used collagen gel from a different manufacturer at the concentration of 1.78mg/ml, we embedded bacteria in collagen solutions of both concentrations. For the 1.78mg/ml collagen solution, we diluted the stock solution with nuclease free water.

This experiment was performed utilizing ibidi Angiogenesis slides. The bottom of the slides was coated with ibiTreat, a physical modification making the surface hydrophilic and adhesive to a multitude of cell types. Figure 7 depicts the experiment set-up.

We embedded $2x10^3$ bacteria in each well suspended in 10µl collagen. For this, the OD_{600} was measured from bacteria prepared in 1x PBS at a 1:10 dilution in 1x PBS and the amount of bacteria suspension was accordingly extracted and pipetted into a new Eppendorf reaction tube. The tubes were centrifuged for 10 minutes at 6000rpm and the supernatant was discarded. The pellet of bacteria was resuspended in 10ml of collagen solution by pipetting the gel up and down. The bacteria-collagen-mixture was then pipetted into the chamber well and the chamber slide was incubated at 37°C for 45 minutes to allow the collagen gel solution to polymerise.

A

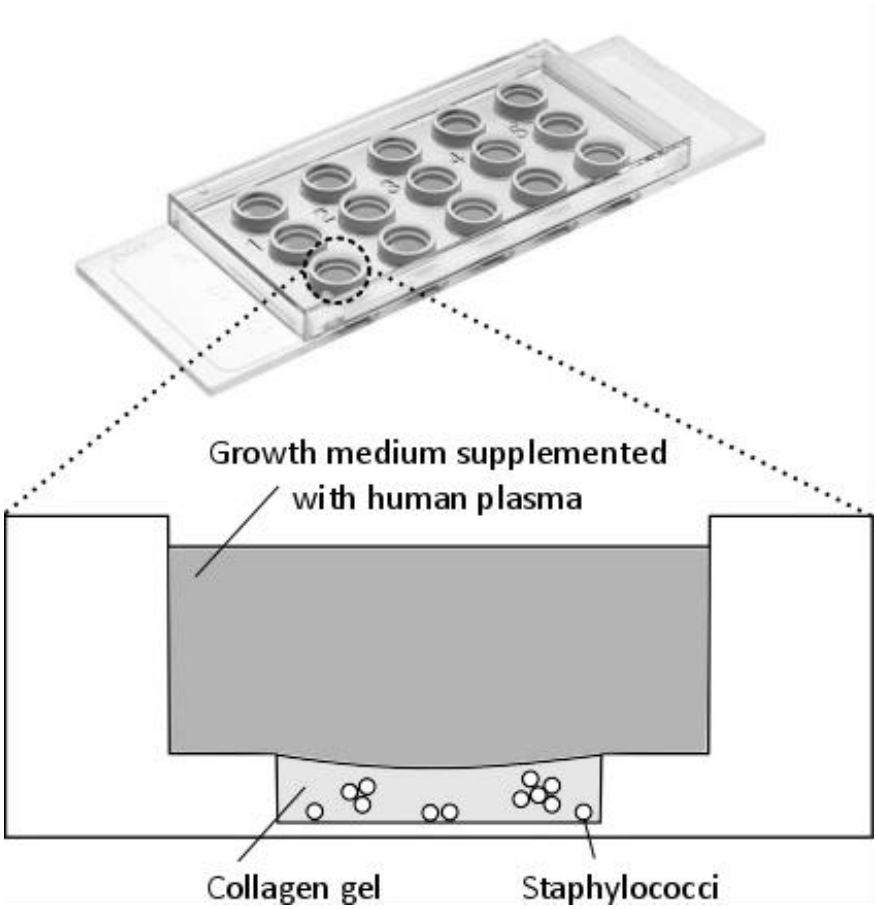

B

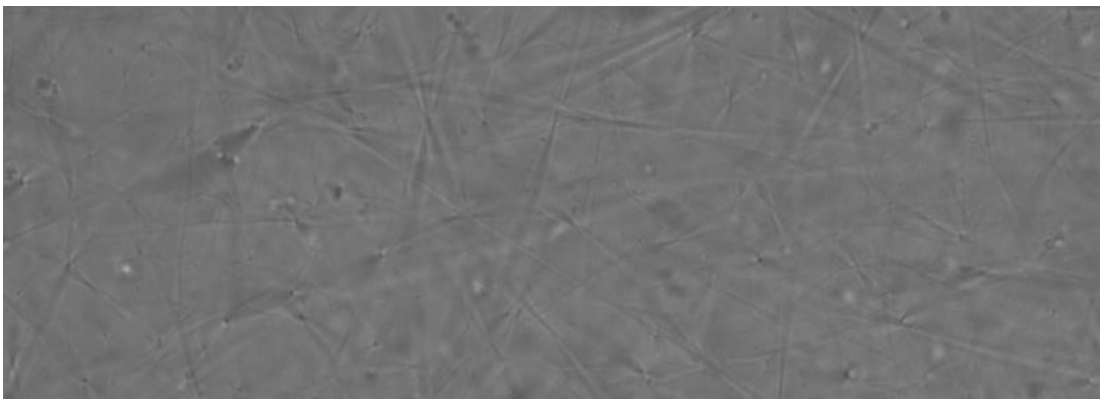

Figure 7. (A) Chambered slide set-up (modified after ibidi website) (B) brightfield image of collagen fibers

2.2.13 Preparation of growth medium supplemented with human plasma

Human plasma was stored at −20°C. Prior to supplementing the plasma to growth medium, it was incubated at 37°C from frozen, then diluted with RPMI 1640 in three different concentrations: 1:10, 1:20 and 1:100.

2.2.14 Confocal microscopy of fluorescent S. aureus strains

Three channels were used, one each for Cerulean (track 1) and Venus (track 2) and the brightfield channel (transmitted light detection). For track 1, the laser excited at 405 nm and detecting from 454 to 516nm, the laser power was set to 1.0 and the gain level was set to 644. For track 2, the laser excited at 514nm and detected from 519 to 621nm, with a set laser power of 1.0 and a gain level of 500. Transmitted light was detected at various gain levels, depending on the thickness of the slide, and adjustments were made for each case. To capture the fluorescence across several planes, z-stacks were made using an interval size of 0.34µm.

2.2.15 Three-dimensional acquisition and time series

To assess growth behaviour over time, live imaging and time series experiments were performed. For this, the angiogenesis chamber slide prepared for the 3D colony growth model, was incubated at 37.5°C in the incubation chamber of the microscope. Z-stacking was used to capture multiple planes. For this, the First/Last setting was chosen and the first and last plane were set, according to observed fluorescence of the microcolonies. The interval was set to 1µm. Several positions were assessed over time to compare growth behavior of two distinct strains, for this the positions were added to the position list. The time series interval was set to 30 minutes. Number of tiles and cycles varied depending on growth behavior. As we were in the process of establishing the collagen model and the time series acquisition, we observed bacteria at various time points and acquired images at time points +13h, +17h, +37h and +39h after incubation.

2.2.16 Image processing

All images were processed using the Zeiss ZEN blue and Zeiss ZEN black software. With the ZEN blue software, all images were cropped to the size of 200x200 pixels. The channels were exported separately to create z-stack images only of the fluorescence channel and brightfield images of a single plane. These z-stack images of the fluorescence channel were processed in the ZEN black software by using the maximum intensity projection, which was then merged with the single-plane brightfield image. For the both fluorescence channels, the digital contrast has been enhanced to a contrast ration of 26,000:1, for the abscess images, the digital contrast has been enhanced for both channels to a white value of 12,000:1. The images were exported as TIFF files using the Zen blue software.

3 Results

3.1 Construction and genetic verification of fluorescent *S. aureus* reporter strains

3.1.1 Construction of single fluorescence-labeled *S. aureus* reporter strains

To generate single fluorescence-labeled *S. aureus* reporter strains, existing plasmids containing the desired promoter-GFP-derivative fusion protein were purified from *E. coli*. These plasmids were constructed using a cassette-based shuttle vector system. Figure 8 depicts the promoter–GFP-derivative fusion protein in a simplified version.

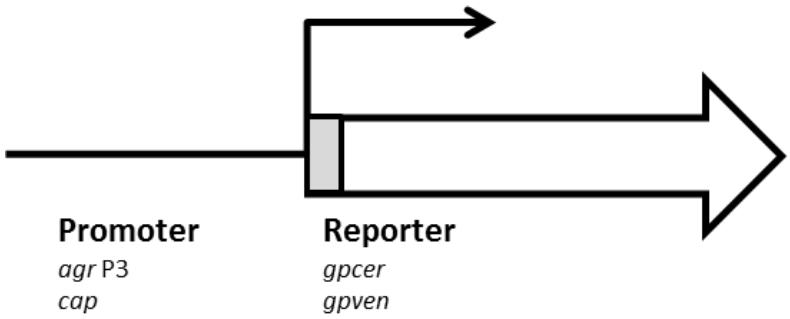

Figure 8. Schematic of the promoter–GFP-derivative fusion constructs

The vector plasmid that integrates into the SaPI1 site is based on pRN7145 (Charpentier *et al.*, 2004) (Figure 9). This plasmid contains the attachment site SaPI1-attP for chromosomal integration into the SaPI1 site with a resistance cassette for Erm. The pT181 replicon was removed and a fragment containing *gpcer* under the control of the *agr* P_3 promoter (see Figure 9) was cloned into the multiple cloning site to generate plasmid pJL53. Plasmid pJL54 was generated in the same manner using a fragment containing *gpven* under the control of the *agr* P_3 promoter.

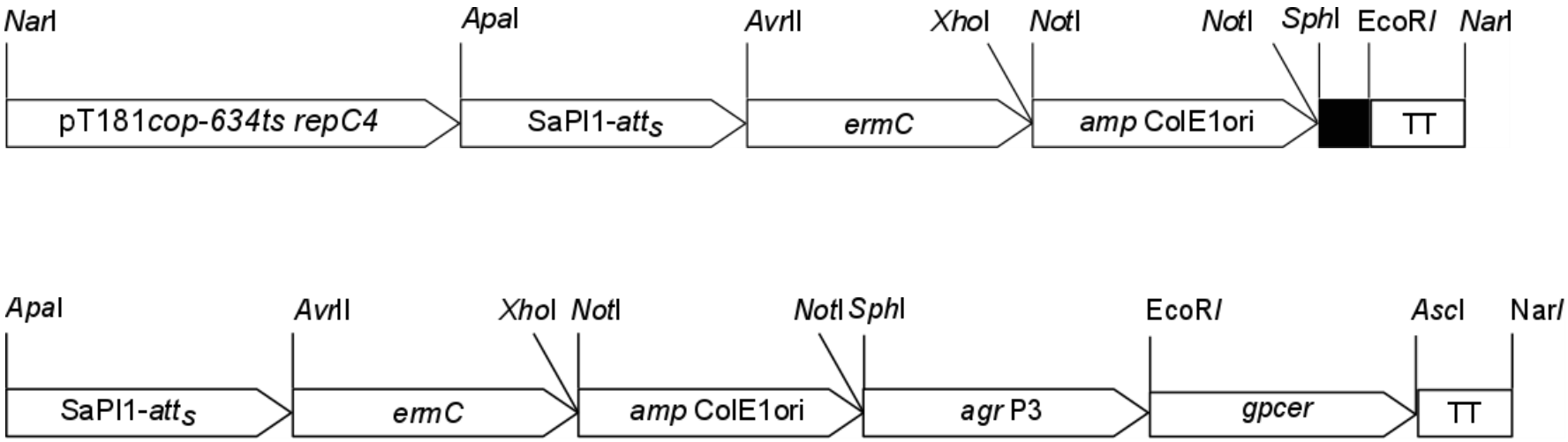

Figure 9. Plasmid pRN7145 (top) and integration vector pJL53 (bottom).

Fluorescent reporter genes *gpcer* and *gpven* both use *gfpmut2* as a template and mutations have been introduced to shift excitation/emission spectra.

The vector plasmid that integrates into the *geh* locus is based on pJL93. Plasmid pJL93 was created based on pJL53, replacing the *erm*C cassette with an *tet*M cassette from pCN36 (Charpentier *et al.*, 2004). The pT181 replicon was replaced by the attL54 site from pCL84 (Lee, 1991). This yielded plasmid pCG295 (Figure 10). A fragment containing *gpven* under the control of the cap promoter was cloned into *Sph*I-*EcoR*I restricted pCG295 plasmid to generate plasmid pCG318 (Figure 10). Plasmid pCG317 uses a fragment containing *gpcer* under the control of the cap promoter. Plasmid pCG302 was generated in a similar manner, using the *agr* P_3 promoter instead of the cap promoter.

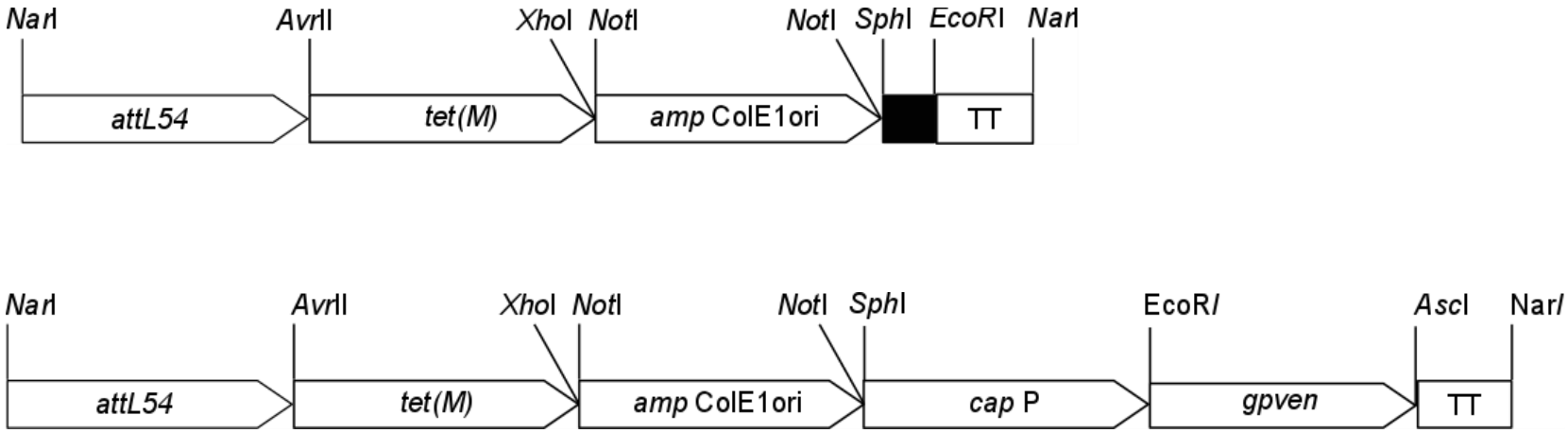

Figure 10. Plasmid pCG295 (top) and integration vector pCG318 (bottom).

The purified plasmids were electroporated into electrocompetent *S. aureus* strains with chromosomally encoded site-specific integrases. For the integration into the *geh* locus, strain Cyl 316 was used. Cyl 316 contains a site-specific integrase for the *geh* locus on its chromosome (Lee, Ye, 1991). For integration into the SaPI1 site, strain RN9011, containing a site-specific integrase for SaPI1 on its chromosome, was used. Electroporation resulted in *S. aureus* strains with single-copy, chromosomally integrated plasmids in specific attachment sites *geh* and SaPI1.

Lysis and transduction into target strain Newman gave rise to *S. aureus* strains Newman with reporter plasmids integrated into the chromosome (Table 6).

Strain	Description	Marker
Newman, pJL53	Agr-P3-gpcer::SaPI1; pJL53	Erm
Newman, pJL54	Agr-P3-*gpver*::SaPI1; pJL54	Erm
Newman, pCG302	Agr-P3-*gpcer*::geh; pCG302	Tet
Newman, pCG317	cap-*gpcer*::geh; pCG317	Tet
Newman, pCG318	cap-*gpven*::geh; pCG318	Tet

Table 6. Constructed strains.

3.1.2 Construction of double fluorescence-labeled *S. aureus* reporter strains

For the generation of double fluorescence-labeled *S. aureus* reporter strains, Φ11-lysates obtained from the single reporter strains were used to transduce single reporter recipient strains. The lysate of strain CYL316 with integrated plasmid pCG317 was used to transduce strain Newman, pJL54, producing a double reporter construct with a Cerulean-linked cap promoter in the *geh* site and

a Venus-linked agr promoter in the SaPI1 site. This resulted in *S. aureus* double-reporter strains Newman concurrently expressing two different derivatives of GFP, Venus and Cerulean, under the control of two different promoters, agr and cap.

3.1.3 Verification of vector integration

The constructed strains were verified using PCR amplifying with one primer reading outward from the plasmids and a second recognizing a region adjacent to the chromosomal attachment site reading inward. To verify the integration of the vector into the lipase site, we used the primer pair pCG295links (on the integration vector reading outwards) and scv1 (on *S. aureus* chromosome reading inwards). The PCR product is expected to be 1007bp. Figure 11 shows a simplified version of the verification PCR.

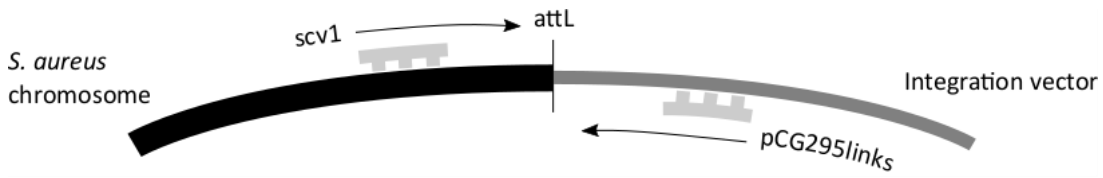

Figure 11. Location of primer pair (1) pCG295links and (2) scv1

As can be seen in Figure 12, PCR products have been amplified for strains for which integration into *geh* was expected. For strains Newman, pCG317, Newman, pCG318 and Newman, pJL54, pCG317, the product was of the expected size. For strain Newman, pCG302 (Figure 12, lane (B)), the product was slightly smaller. Therefore, another integration verification PCR with two different primers was used.

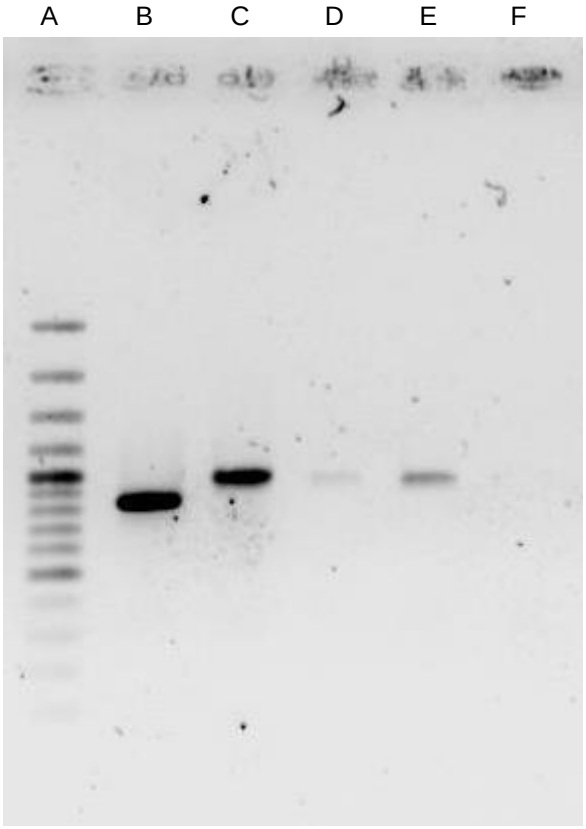

Figure 12. PCR with primers (1) pCG295links and (2) scv1
(A) 100bp Plus Gene ruler, (B) Newman, pCG302, (C) Newman, pCG317,
(D) Newman, pCG318, (E) Newman, pJL54, pCG317, (F) H_2O

The second pair of primers we used to verify the integration of the vector into the lipase site were (1) pCG295rechts and (2) scv2.1 (Figure 13). The PCR product is expected to be 536 bp. This PCR was used for strain Newman, pCG302, where the first primer pair yielded a product smaller than expected. The electrophoresis (Figure 14) of the PCR product for strain Newman, pCG302 shows bands appearing just above the 500bp mark, suggesting correct PCR product size. This was used as an indicator for successful integration.

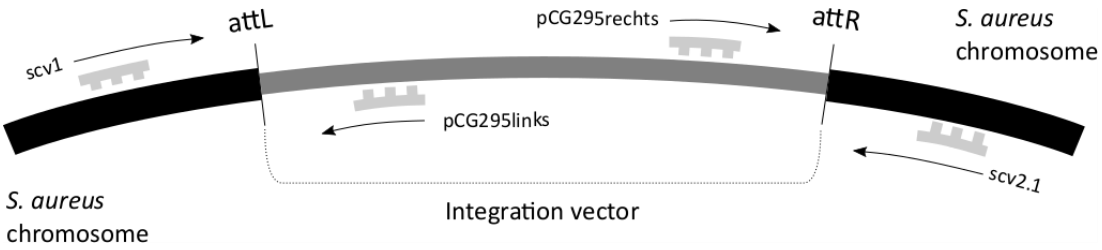

Figure 13. Location of primer pair (1) pCG295links and (2) scv1 and primer pair (1) pCG295rechts and (2) scv2.1.

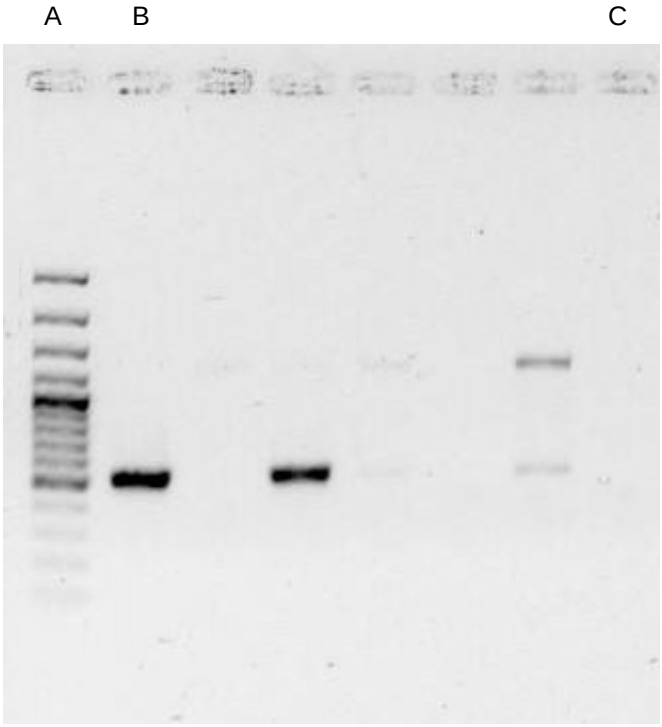

Figure 14. PCR with primers (1) pCG295rechts and (2) scv2.1
(A) 100bp Plus Gene ruler, (B) Newman, pCG302, (C) H_2O

The integration into the SaPI1 site was verified using primers (1) SaPI_int_for and (2) SaPI_int_rev. The expected products were 500bp in size. Figure 15 shows the gel electrophoresis with PCR products. In this Figure, PCR products are the correct size, suggesting successful integration into the SaPI1 site.

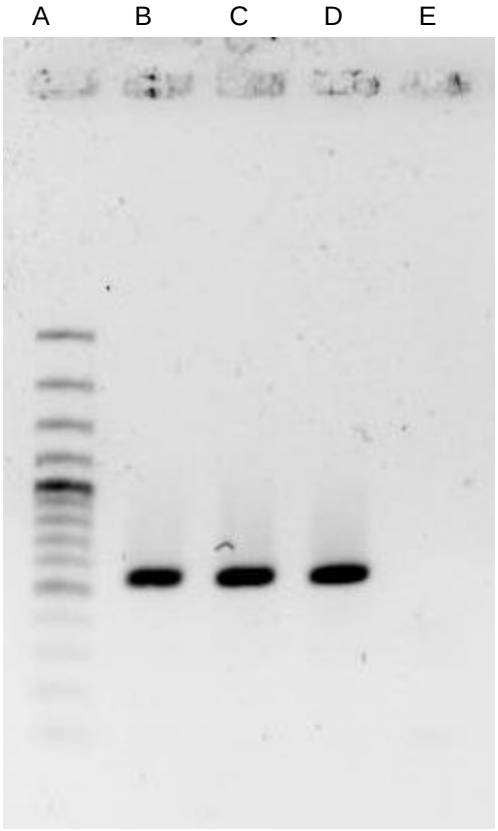

Figure 15. PCR with primers (1) SaPI_int_for and (2) SaPI_int_rev
(A) 100bp Plus Gene ruler, (B) Newman, pJL53, (C) Newman, pJL54, (D) Newman, pJL54, pCG317, (E) H_2O

To ensure the presence of the fluorophore, an additional PCR was performed using primers that flanked the fluorophore region itself. Both primers (1) GFP control for and (2) GFP control rev hybridise on the integration vector. Their product reads over the *gfp* gene itself as well as the promoter. The agr promoter is larger in size compared to the cap promoter. Hence, the PCR products for agr promoter are larger in size than those for cap promoter strains. Figure 16 shows primer sites on plasmid pCG318. PCR products were separated in gel electrophoresis (Figure 17), showing bands at the expected sizes, 1600bp for the agr P_3 promoter and 1380bp for the cap promoter.

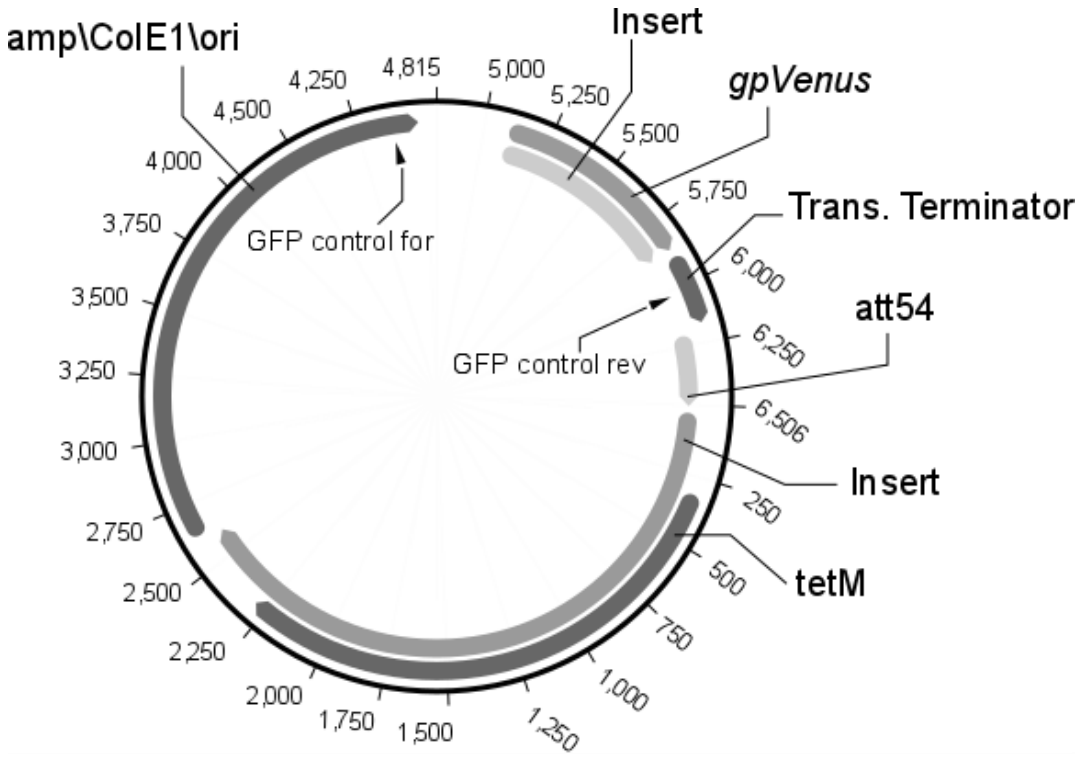

Figure 16. Plasmid pCG318 showing primer sites for GFP control for and GFP control rev.

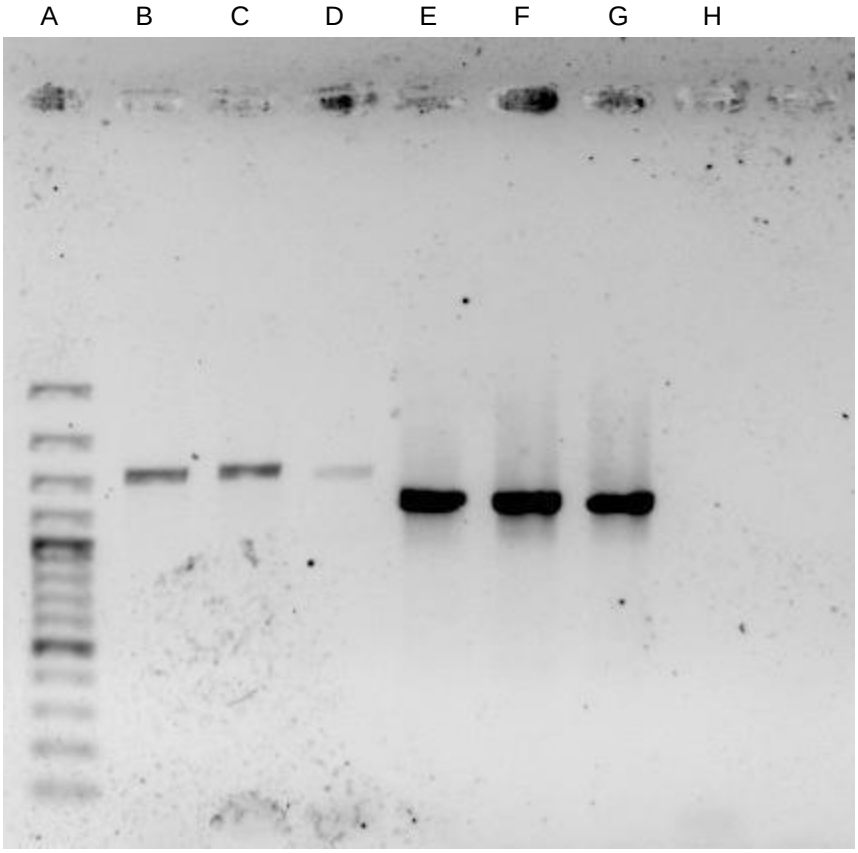

Figure 17. PCR with primers (1) GFP control for and (2) GFP control rev
(A) 100bp Plus Gene ruler, (B) Newman, pJL53, (C) Newman, pJL54, (D) Newman, pCG302, (E) Newman, pCG317, (F) Newman, pCG318, (G) Newman, pJL54, pCG317, (H) H_2O

3.2 Assessment and comparison of single reporter promoter-linked fluorescence activity

We observed single construct strains under the microscope, to verify that fluorescence genes are expressed and to assess fluorescence distribution pattern. This was performed for all constructed strains at three time points to represent different growth phases. Bacteria were harvested at an OD_{600} of 0.3 (T_0), representing the log-phase, 6 hours after T_0, representing the stationary phase and bacteria from the overnight culture were harvested, to represent a stress condition.

For all bacterial strains, the brightfield image shows that not all bacteria are in focus, suggesting bacteria are in different focal planes (Figure 18, (A)). Therefore,

z-stacking was used for image acquisition and a maximum intensity projection was performed with the fluorescence channel to merge all planes into a single picture (Figure 18, (B)). We then used a single-plane image of the brightfield z-stack and merged it with the maximum intensity projection of the fluorescence channel. This resulted in an image which showed all bacteria visible in the brightfield channel as well as the fluorescence across all z-planes. Using this merged image, we analysed fluorescence distribution (Figure 18, (C)).

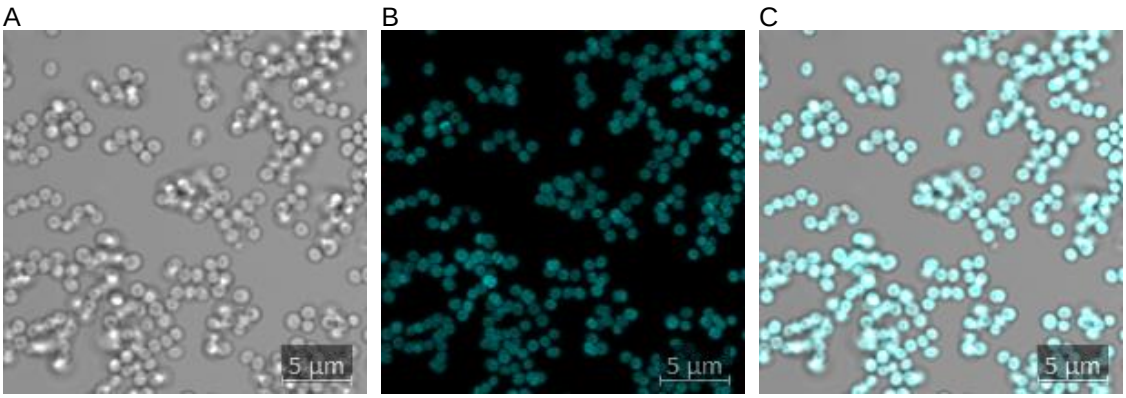

Figure 18. Overnight culture of strain Newman, pCG302 (A) Brightfield image shows that not all bacterial cells are in focus, suggesting they are not in a single plane, therefore a maximum intensity projection of the fluorescence channel was performed. (B) Maximum intensity projection of the cerulean channel (C) Merge picture between the brightfield channel of a single z-plane and the maximum intensity projection of the fluorescence channel shows all bacterial cells express the *gpcer* gene

For all promoters, fluorescence signal was strongest after overnight growth. Almost no signal was detected in the log phase (T_0, Figure 19) and an intermediate level of fluorescence was expressed during the stationary phase (T_0 + 6h, Figure 20).

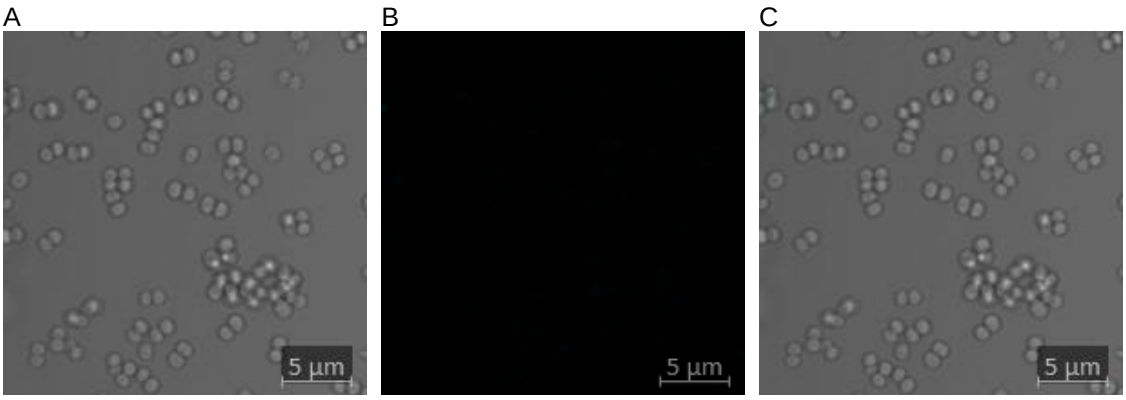

Figure 19. Strain Newman, pCG302 at T_0 (A) brightfield image of a single z-plane (B) Maximum intensity projection of the cerulean channel (C) Merge picture between the brightfield channel of a single z-plane and the maximum intensity projection of the fluorescence channel shows no bacterial cells express the *gpcer* gene.

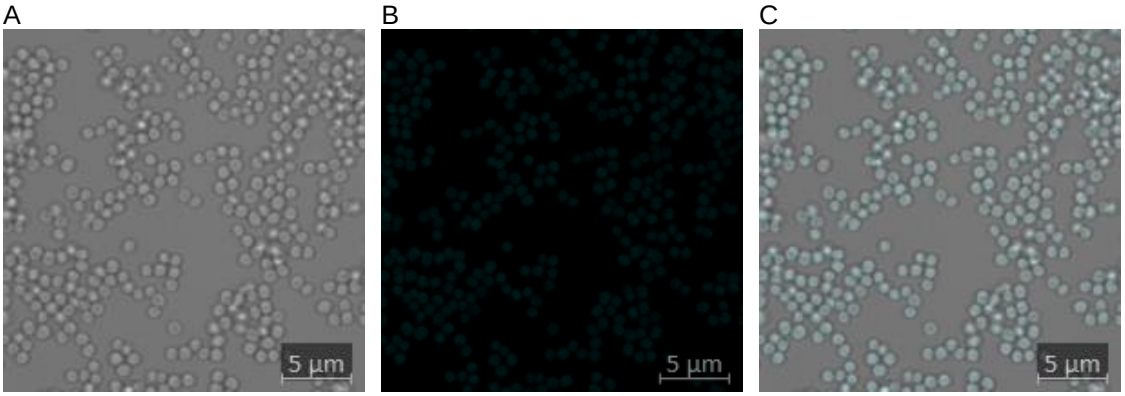

Figure 20. Strain Newman, pCG302 at T_0 + 6h (A) brightfield image of a single z-plane (B) Maximum intensity projection of the cerulean channel (C) Merge picture between the brightfield channel of a single z-plane and the maximum intensity projection of the fluorescence channel shows that *gpcer* expression is present in all bacterial cells, albeit not to the same extent as in the overnight culture.

For the following comparisons, we always show the merge image of the brightfield image and the maximum intensity projection of the fluorescence channel, as well as the image showing just the fluorescence channel.

3.2.1 Comparison between cloning sites SaPI and *geh*

We compared fluorescence activity of the same fluorophore in two different attachment sites for time points T_0 and T_0 + 6h and for the overnight culture. For

this comparison, strains Newman, pCG302 and Newman, pJL53 were used. Both have *gpcer* under the control of the agr P_3 promoter, for Newman, pJL 53, the attachment site is SaPI1 and for Newman, pCG317, the attachment site is the *geh* gene. As previously stated, fluorescence was strongest in the overnight culture and was present homogenously for both strains (Figure 21 and 22, A and B). At T_0, no fluorescence signal was detected (Figure 21 and 22, C and D). At T_0 + 6h, fluorescence signal was detectable again, showing a homogenous distribution pattern in both strains (Figure 21 and 22, E and F).

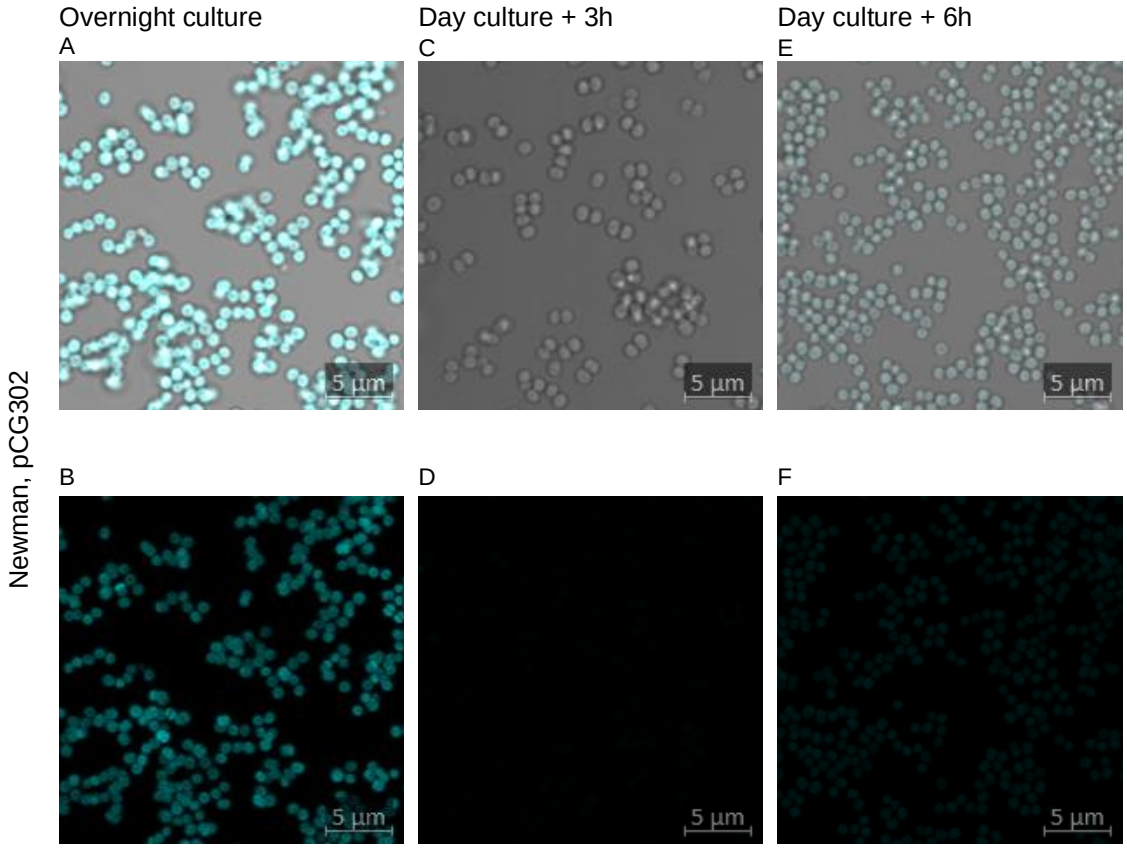

Figure 21. Newman, pCG302. (A) and (B) show the overnight culture, where (A) is a merge image of the brightfield channel and the maximum intensity projection of the fluorescence channel and (B) shows the fluorescence channel. The images show that all bacterial cells express *gpcer*. (C) and (D) show staphylococci at T_0, where (C) is a merge image of the brightfield and the maximum intensity projection of the fluorescence channel and (D) shows the fluorescence channel. The images show that there is no fluorescence activity detected at this time point. (E) and (F) show staphylococci at T_0 + 6h, where (E) is a merge image of the brightfield and the maximum intensity projection of the fluorescence channel and (F) shows the fluorescence channel. The images show that there is homogenous expression of the fluorophore gene at this time point and that is lower in intensity than the overnight culture.

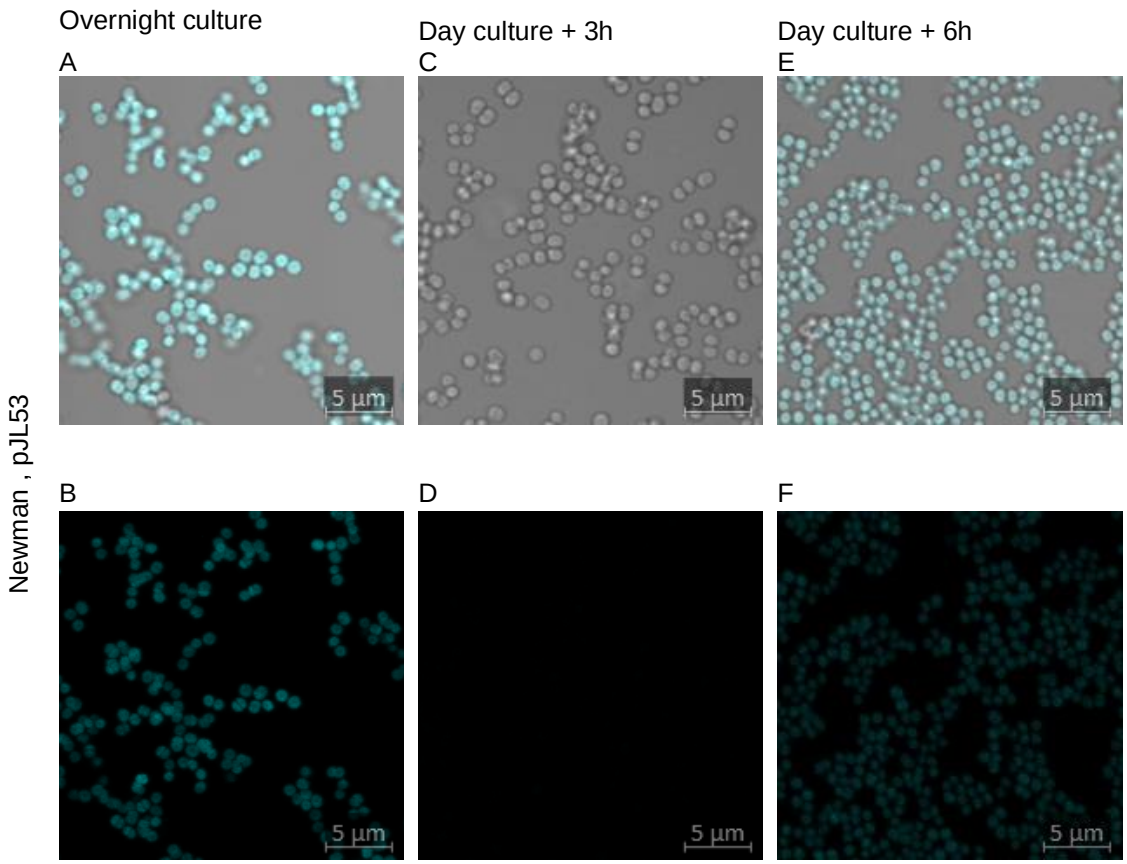

Figure 22. Newman, pJL53. (A) and (B) show the overnight culture, where (A) is a merge image of the brightfield channel and the maximum intensity projection of the fluorescence channel and (B) shows the fluorescence channel. The images show that all bacterial cells express gpcer. (C) and (E) show staphylococci at T_0, where (C) is a merge image of the brightfield and the maximum intensity projection of the fluorescence channel and (E) shows the fluorescence channel. The images show that there is no fluorescence activity detected at this time point. (E) and (F) show staphylococci at T_0 + 6h, where (E) is a merge image of the brightfield and the maximum intensity projection of the fluorescence channel and (F) shows the fluorescence channel. The images show that there is homogenous expression of the fluorophore gene at this time point and that is less in intensity compared to the overnight culture.

These findings correlate to comparable expression patterns for the agr P_3 promoter between the two attachment sites SaPI-1 and *geh*. Both show high and homogenously distributed levels of Agr activity in the overnight culture. This activity is lost upon dilution into the day culture and regained after 6h of growth.

3.2.2 Comparisons between fluorophores Cerulean and Venus under the control of the agr P_3 promoter

Next, we compared expression pattern depending on the derivative of GFP used. Newman strain with two different fluorophores in the same attachment site was observed. The following Figures depict fluorescence activity of staphylococci with *gpcer* in the SaPI1 attachment site and staphylococci with *gpven* in the SaPI1 attachment site, both under control of the agr P_3 promoter. The observations showed a difference between fluorophores both in terms of brightness and in terms of expression pattern. Fluorescence signal in Newman, pJL53 showed homogeneous distribution as stated above (Figure 23). Fluorescence signal in Newman, pJL54, which is fluorophore *gpven* under the control of the same promoter, was weaker and inhomogeneously distributed, most evident at T_0 + 6h, where only single bacterial cells expressed Venus (Figure 24).

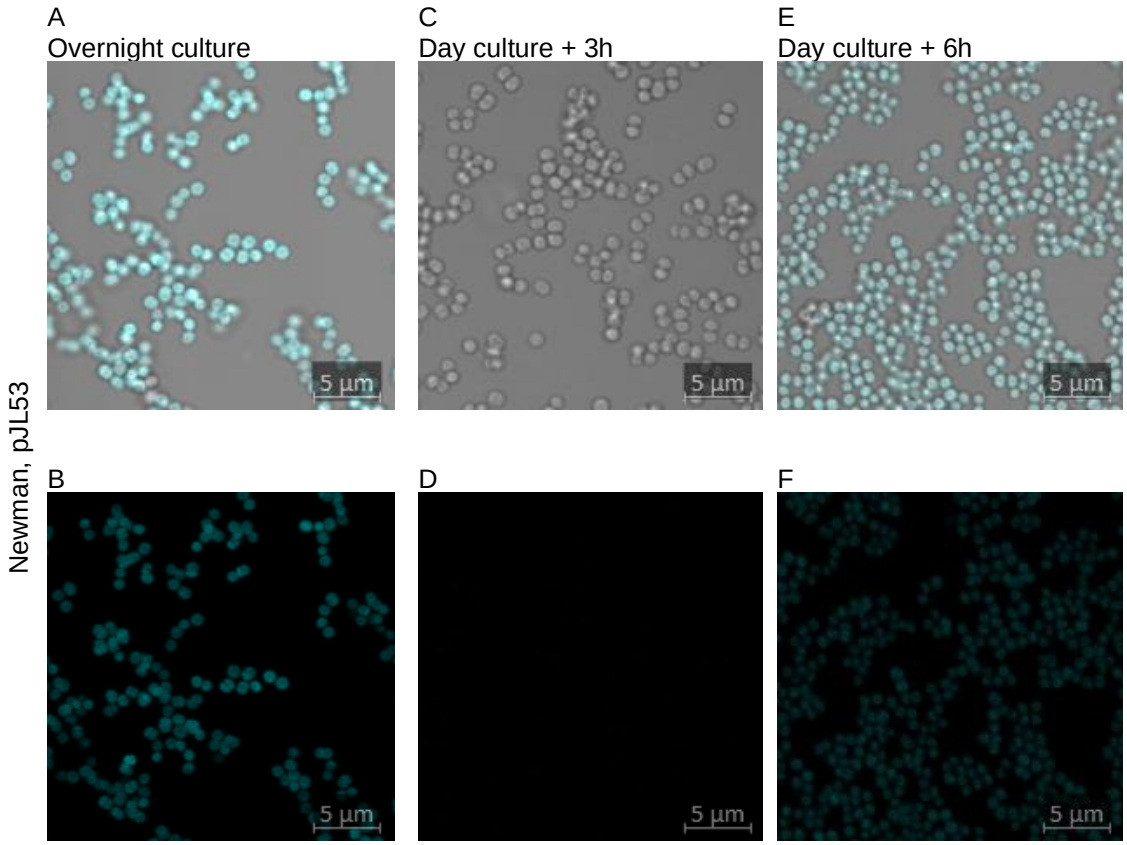

Figure 23. Newman, pJL53. (A) and (B) show the overnight culture. (C) and (D) show staphylococci at T_0. (E) and (F) show staphylococci at T_0 + 6h. Description as above.

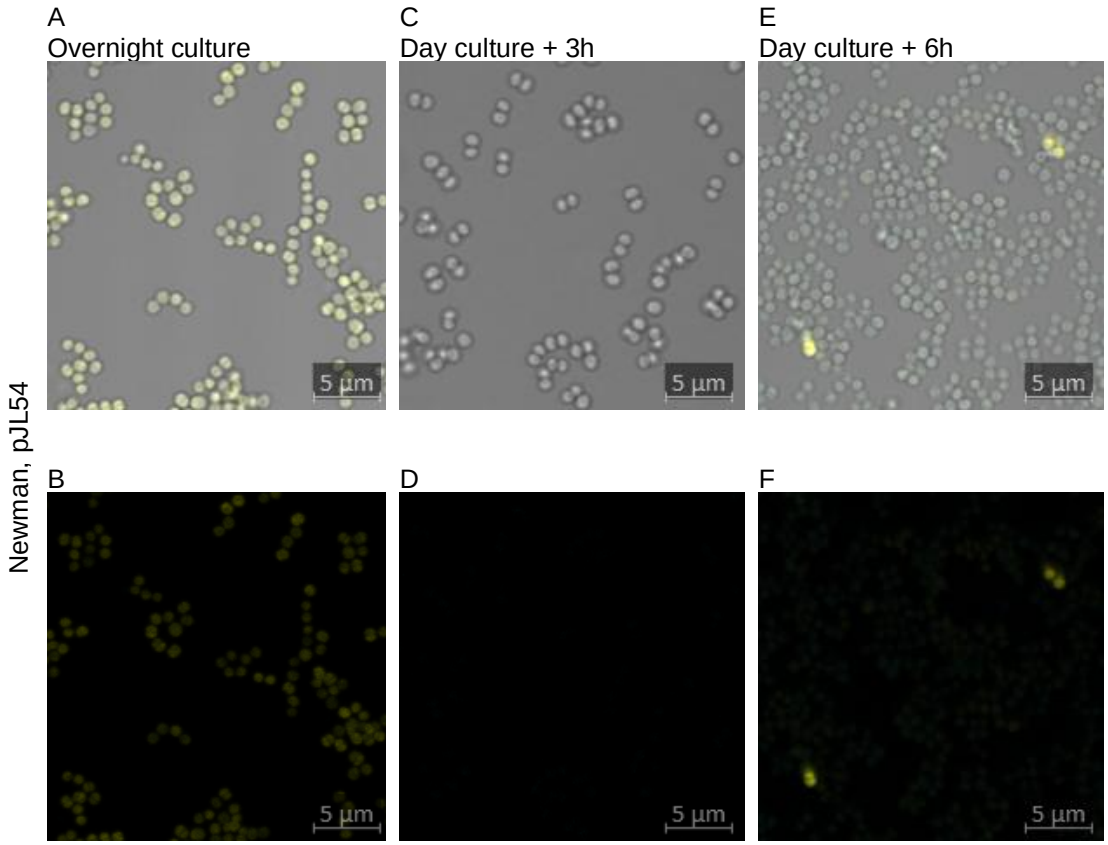

Figure 24. Newman, pJL54. (A) and (B) show the overnight culture, where (A) is a merge image of the brightfield channel and the maximum intensity projection of the fluorescence channel and (B) shows the fluorescence channel. The images show that all bacterial cells express *gpven*, albeit at various intensities. (C) and (D) show staphylococci at T_0, where (C) is a merge image of the brightfield and the maximum intensity projection of the fluorescence channel and (D) shows the fluorescence channel. The images show that there is no fluorescence activity detected at this time point. (E) and (F) show staphylococci at T_0 + 6h, where (E) is a merge image of the brightfield and the maximum intensity projection of the fluorescence channel and (F) shows the fluorescence channel. The images show that only single bacterial cells express the *gpven* gene.

These findings indicate that expression pattern varies for different fluorophores. Expression of Venus appeared to be more inhomogeneous within one culture than the expression of Cerulean, even though both are under the control of the same promoter.

3.2.3 Comparisons between fluorophores Cerulean and Venus under the control of the cap promoter

We also compared fluorescence expression pattern between fluorophores under the control of the cap promoter. The following images show the fluorescence at time points T_0, T_0 + 6h and the fluorescence of the overnight culture. Fluorescence signal is inhomogeneous for both fluorophores. While in Newman, pCG317, all bacterial cells showed fluorescence, single bacteria displayed a much stronger signal (Figure 25). For Newman, pCG318, the distribution was also heterogeneous, with some bacteria not displaying fluorescence at all, and others emitting a very strong signal (Figure 26).

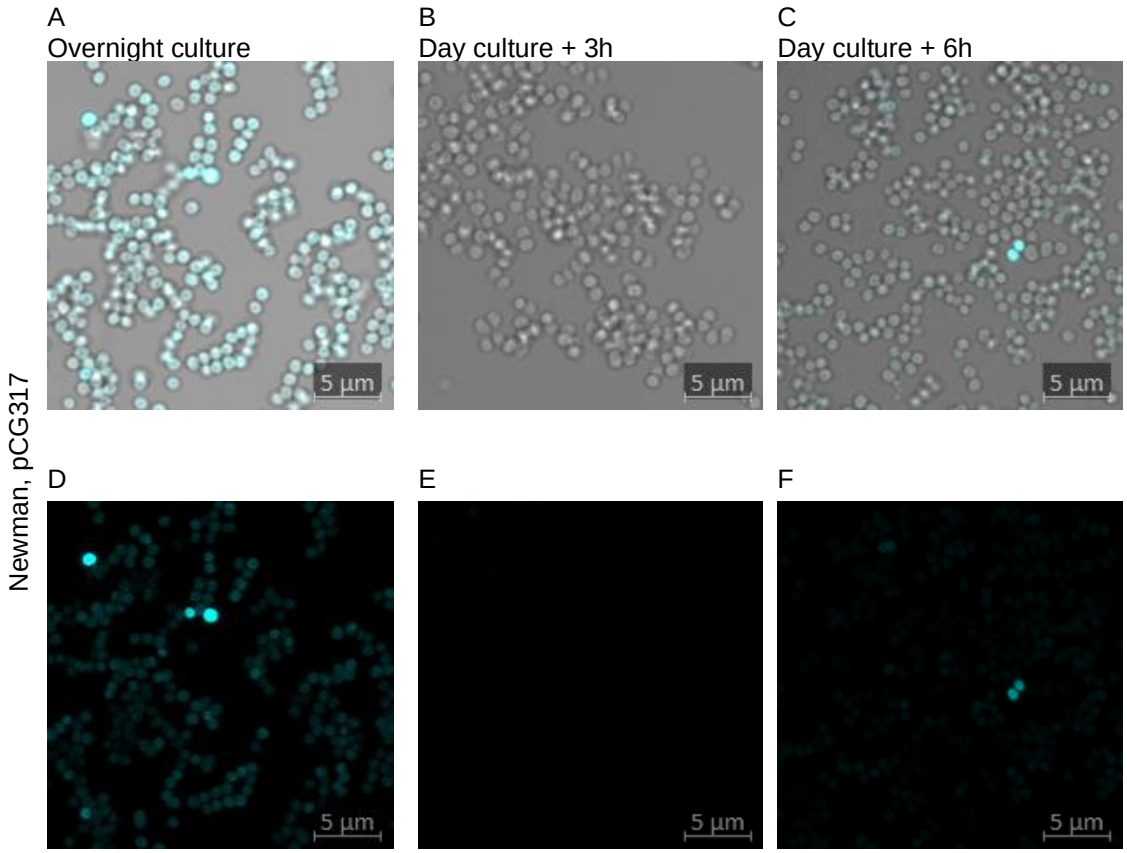

Figure 25. Newman, pCG317. (A) and (D) show the overnight culture, where (A) is a merge image of the brightfield channel and the maximum intensity projection of the fluorescence channel and (D) shows the fluorescence channel. The images show that all bacterial cells express *gpcer*, albeit at various intensities. Single bacterial cells display a very high level of cap-promoter activity. (B) and (E) show staphylococci at T_0, where (B) is a merge image of the brightfield and the maximum intensity projection of the fluorescence channel and (E) shows the fluorescence channel. The images show that there is no fluorescence activity detected at this time point. (C) and (F) show staphylococci at T_0 + 6h, where (C) is a merge image of the brightfield and the maximum intensity projection of the fluorescence channel and (F) shows the fluorescence channel. The images show that only single bacterial cells express the *gpcer* gene.

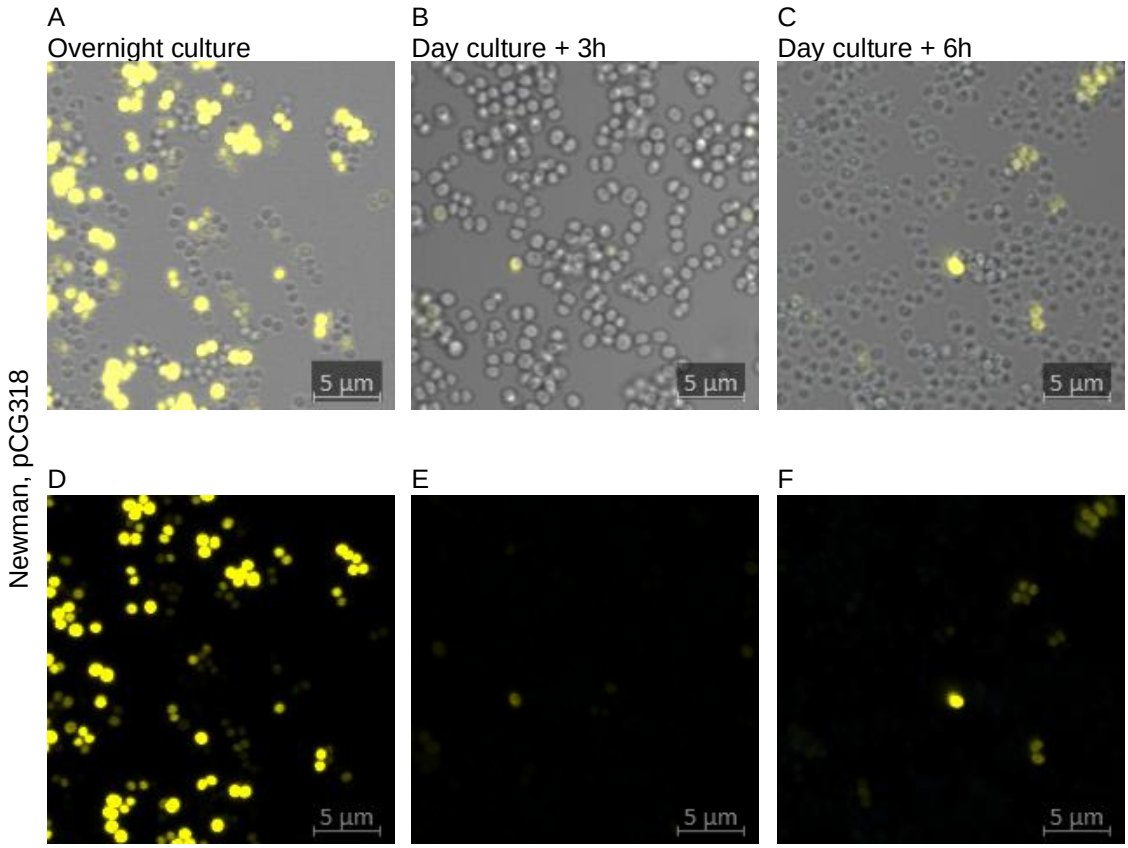

Figure 26. Newman, pCG318. (A) and (D) show the overnight culture, where (A) is a merge image of the brightfield channel and the maximum intensity projection of the fluorescence channel and (D) shows the fluorescence channel. The images show that expression of *gpven* is very inhomogeneous. Some bacterial cells display a very high level of expression, there is also a population of bacterial cells showing a weak fluorescence signal and there is a population showing no activity at all. (B) and (E) show staphylococci at T_0, where (B) is a merge image of the brightfield and the maximum intensity projection of the fluorescence channel and (E) shows the fluorescence channel. The images show that single bacterial cells display weak fluorescence at this time point. (C) and (F) show staphylococci at T_0 + 6h, where (C) is a merge image of the brightfield and the maximum intensity projection of the fluorescence channel and (F) shows the fluorescence channel. The images show a heterogeneous picture with single bacterial cells expressing the *gpcer* gene at a high level and single bacterial cells expressing the gene at a low level. There is a large proportion that does not display any fluorescence at all.

These findings suggest that cap-promoter activity level is inhomogeneously distributed within one bacterial colony. While activity level varied within one culture, it was also noted that there was a difference between expression pattern between Cerulean and Venus. This corresponds to the noted difference between the two fluorophores under the control of the agr P_3 promoter, described in the previous section.

3.3 Assessment of double reporter cap- and agr-linked fluorescence activity

The same assay used for single-reporter strains was used for the assessment of the double reporter strain Newman, pJL54, pCG317. This double reporter strain had *gpven* under the control of the agr P_3 promoter and *gpcer* under the control of the cap promoter. Observation of its growth over time showed that the highest level of fluorescence was visible after overnight growth. Very few bacteria express any of the two fluorophores when diluted into the day culture and fluorescence signal increases again over time. In the overnight culture, all bacteria display Venus fluorescence in various intensities and weak Cerulean fluorescence. Of that, single bacteria showed a very high level of Cerulean expression. In the day culture, single bacteria displayed Venus expression, with no detectable signal for Cerulean at all. The day culture + 6h showed a very different picture to the overnight culture. Most bacteria in the day culture + 6h showed a weak Cerulean signal and single bacteria emitted a strong Cerulean signal, single bacteria emitted a weak Venus signal (Figure 27).

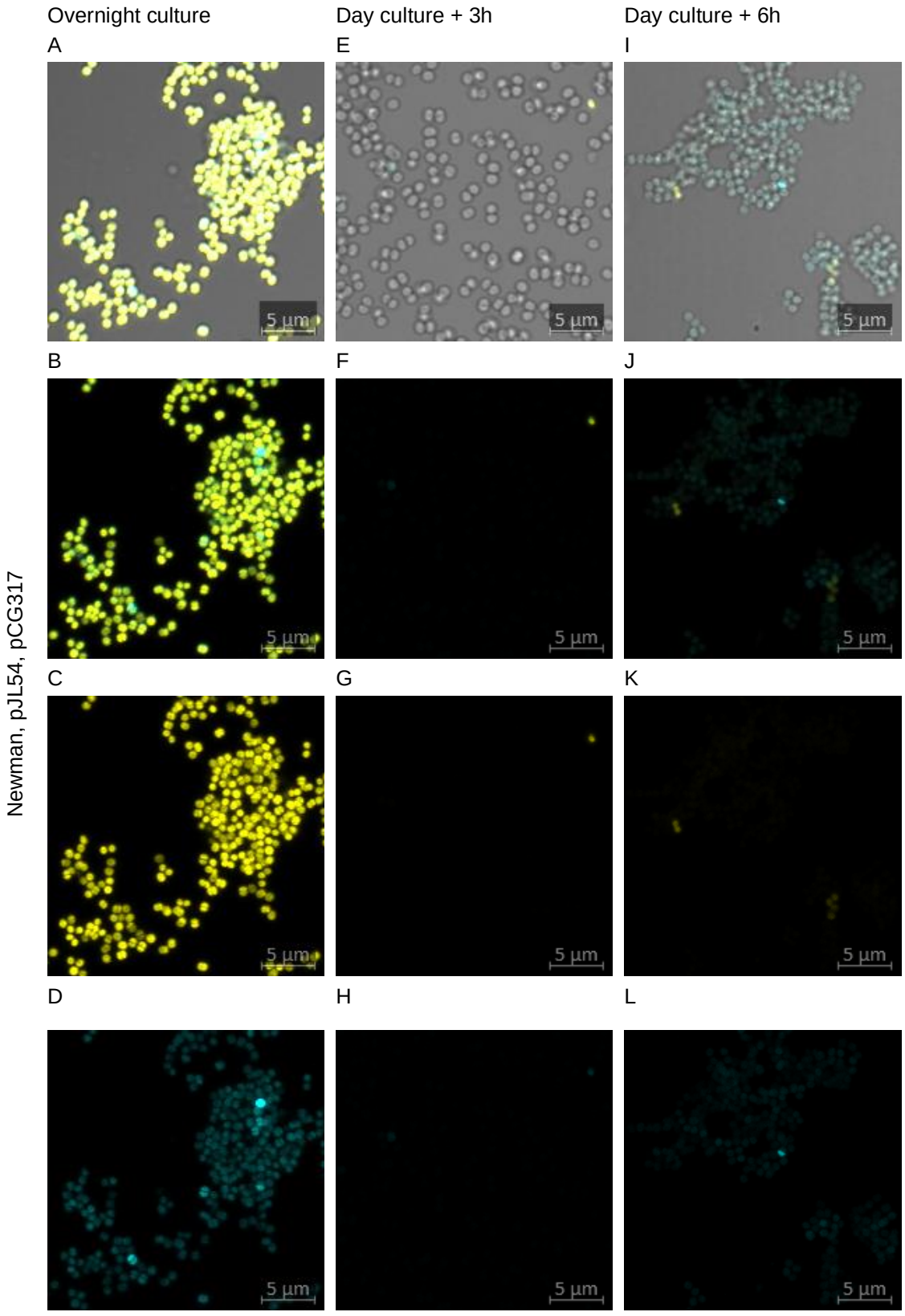

(description see next page)

Figure 27. Newman, pJL54, pCG317. (A) - (D) show the overnight culture, where (A) is a merge image of the brightfield channel and the maximum intensity projection of the fluorescence channels, (B) shows both the Venus and Cerulean fluorescence channel image, (C) shows the Venus fluorescence channel image and (D) shows the Cerulean fluorescence channel image. They show that all bacterial cells express gpven and gpcer at various intensities. In addition to that, single bacterial cells display a very high level of cerulean fluorescence. (E) - (H) show staphylococci at T_0, where (E) is a merge image of the brightfield and the maximum intensity projection of the fluorescence channels, (F) shows both the Venus and Cerulean fluorescence channel image, (G) shows the Venus fluorescence channel image and (H) shows the Cerulean fluorescence channel image. The images show that there is practically no fluorescence expressed in at this time point. In this frame, there is one single bacterial cell displaying Venus fluorescence. (I) – (L) show staphylococci at T_0 + 6h, where (I) is a merge image of the brightfield and the maximum intensity projection of the fluorescence channel, (J) shows both the Venus and Cerulean fluorescence channel image, (K) shows the Venus fluorescence channel image and (L) shows the Cerulean fluorescence channel image. The images show that at T_0 + 6h, bacterial cells predominantly display weak cerulean fluorescence and only single bacterial cells do not display cerulean fluorescence, but Venus instead.

These findings correlate to high activity of the agr P_3 promotor during the overnight growth phase with single bacteria simultaneously displaying cap-promoter activity. Upon dilution, the agr promoter activity is nearly completely suspended and with day culture growth, cap promoter activity increases. This differed from what was observed in single constructs, when the day culture expression pattern was similar to that of the overnight culture.

3.4 Bacterial colony growth in a 3D cell culture model with bovine collagen type I

3.4.1 Fabrication of collagen gel matrices

For a closer *in vitro* simulation of bacterial tissue infection, reporter strains were grown in a 3D cell culture model using bovine collagen type I gel to form an extracellular matrix. It has been shown in a series of experiments performed by Guggenberger *et al.* (Guggenberger *et al.*, 2012) that a 3D collagen gel matrix acts as a an inert fibrillary collagen meshwork in which distinct 3D colony growth can be observed using confocal microscopy. Bacteria embedded in the collagen gel matrix were less likely to drift out of focus. The chamber slide was kept inert, but during time series acquisition over a period of several days, growing bacteria were found to drift out of the focal plane. This is most likely due to heat expansion of instruments or microcirculation in growth medium. Therefore, embedding reporter strains in a rigid collagen gel matrix allowed focused acquisition of distinct bacteria over an extended period.

The experiment was conducted with double reporter strain Newman, pJL54, pCG317. The chamber slides were overlaid with growth medium that was supplemented with human plasma or growth medium with no added plasma.

3.4.2 Comparison between colony morphology in medium with plasma and without plasma supplementation

We observed formation of microcolonies 13 hours after incubation across all chambers (Figures 28 and 29). No capsule, pseudocapsule or meshwork formation was noted. Bacterial grown in medium without plasma supplementation showed more distinct colony edges and the colonies were larger in diameter (Figure 28). Chambers that were not supplemented with plasma also showed scattered growth of staphylococci in the lower parts of the chamber, without colony formation in addition to distinct colonies. Bacteria grown in medium with

plasma supplementation showed indistinct colony borders, but no scattered growth in lower parts of the chamber (Figure 28, B and C).

After a second overnight incubation period, the colonies growing in plasma were larger in diameter and displayed a more defined colony border in comparison to the colony grown in medium without plasma, suggesting a capsule structure surrounding the colonies. For staphylococci that grew without plasma supplementation, scattered bacteria in the lower part of the chamber grew into a dense layer (Figure 29, B).

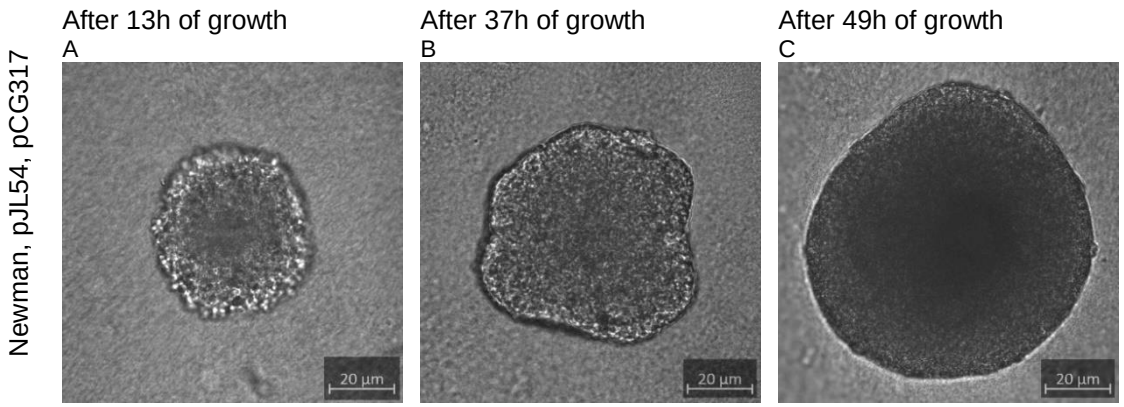

Figure 28. Newman, pJL54, pCG317. Growth in 5µg/ml collagen, supplemented with 5µl human plasma in RPMI 1640. A shows an aggregate after 13h of growth, B shows a microcolony with a well distinct border after 37h of growth and C shows a larger colony with a distinct border surrounding the microcolony after 49h of growth.

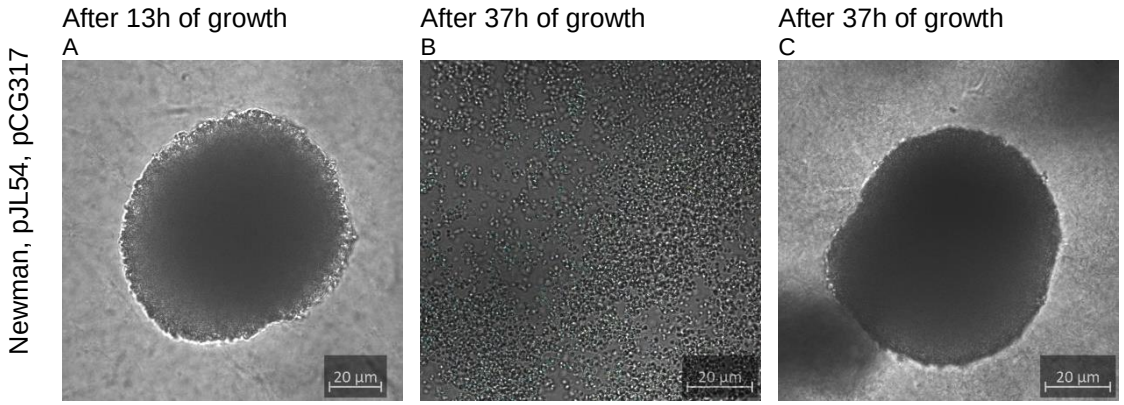

Figure 29. Newman, pJL54, pCG317. Growth in 5µg/ml collagen, RPMI 1640, no plasma supplementation. A shows an aggregate after 13h of growth, B and C show images acquired after 37h of growth, where B is an image of the scattered growth in the lower part of the gel matrix and C is an image of a microcolony with a distinct border.

These findings indicated that embedding staphylococci in a collagen matrix slows their growth significantly. Supplementing growth medium with plasma showed to contribute to formation of colonies and bacteria did not show scattered growth. In both cases, colony formation could be observed. In addition to forming an aggregate, bacteria grown in medium with plasma, showed hemispherical colony shape and a more distinct colony border.

3.4.3 Comparison between growth and fluorescence in medium with and without plasma supplementation

We observed the fluorescence expression of bacteria over time in the 3D-collagen model. After overnight growth, a weak Cerulean fluorescence signal was detected in chambers that were supplemented with plasma, correlating to cap promoter activity. This signal was primarily detected around the edges of the colonies and distributed inhomogeneously. Staphylococci in the centre of the colony displayed little to no fluorescence. Figure 30 shows slices of a z-stack across a colony. We also noted that the shape of the colonies was hemispherical (Figure 31). Cerulean signal intensity and distribution was found to decrease over time. After a second overnight growth period, only very little signal was detected in single bacteria across one colony. No fluorescence was detected after a further incubation of 12 hours. No *gpven* expression was noted throughout the observation period (Figure 32).

Newman, pJL54, pCG317

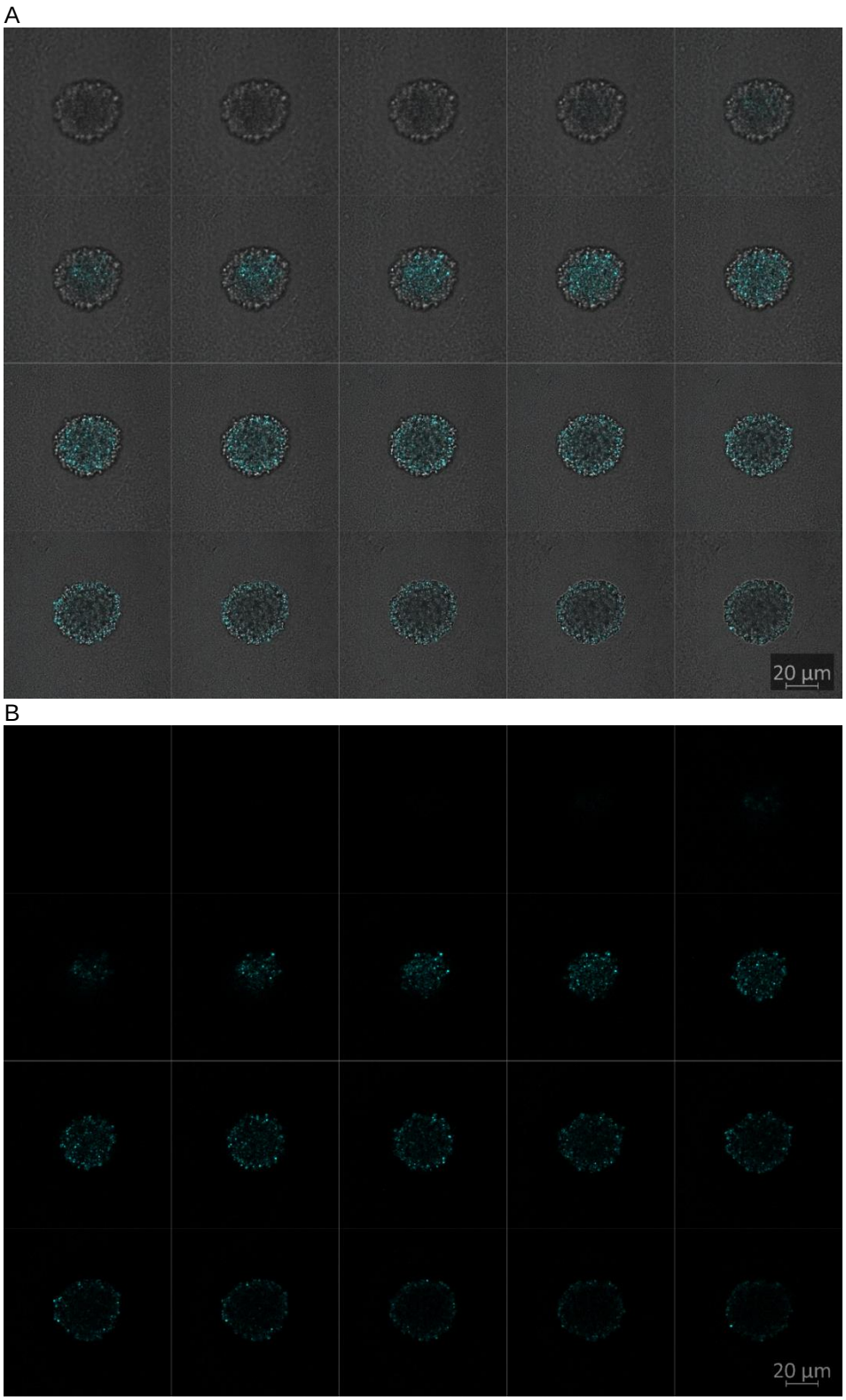

Figure 30. Newman, pJL54, pCG317 after 37h of incubation. (A) shows the z-stack of a colony grown in collagen with growth medium that contained human plasma in both the brightfield and the fluorescence channels Venus and Cerulean. (B) shows the z-stack of the colony only in fluorescence channels. The images show that the fluorescence signal is distributed inhomogeneously and limited to bacteria on the outer edge of the colony.

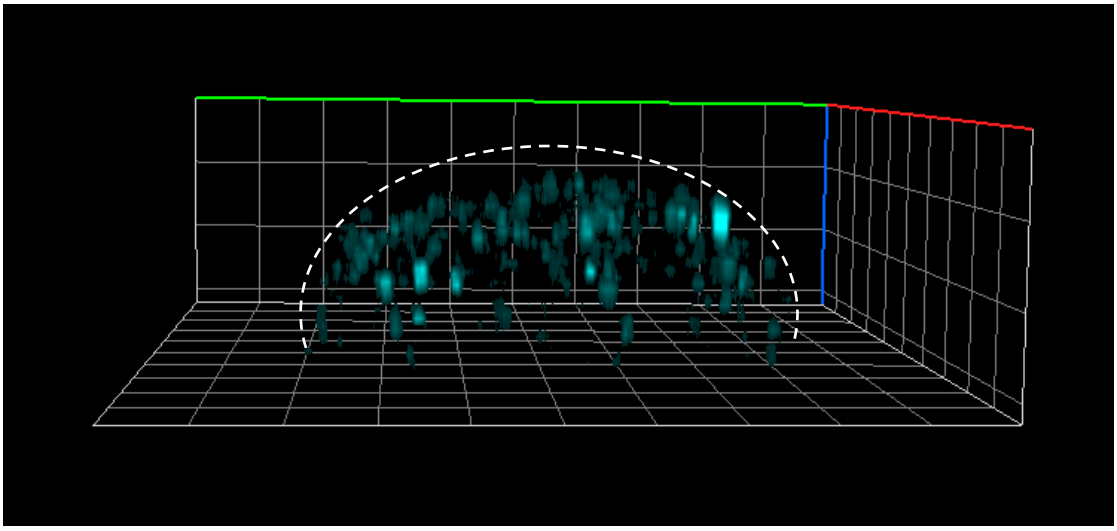

Figure 31. Newman, pJL54, pCG317 after 37h of incubation. The three-dimensional reconstruction of fluorescent bacterial cells on the outer border of the colony shows that the morphology of a staphylococcus colony is hemispherical. The radius of the colony was measured to be ~21µm.

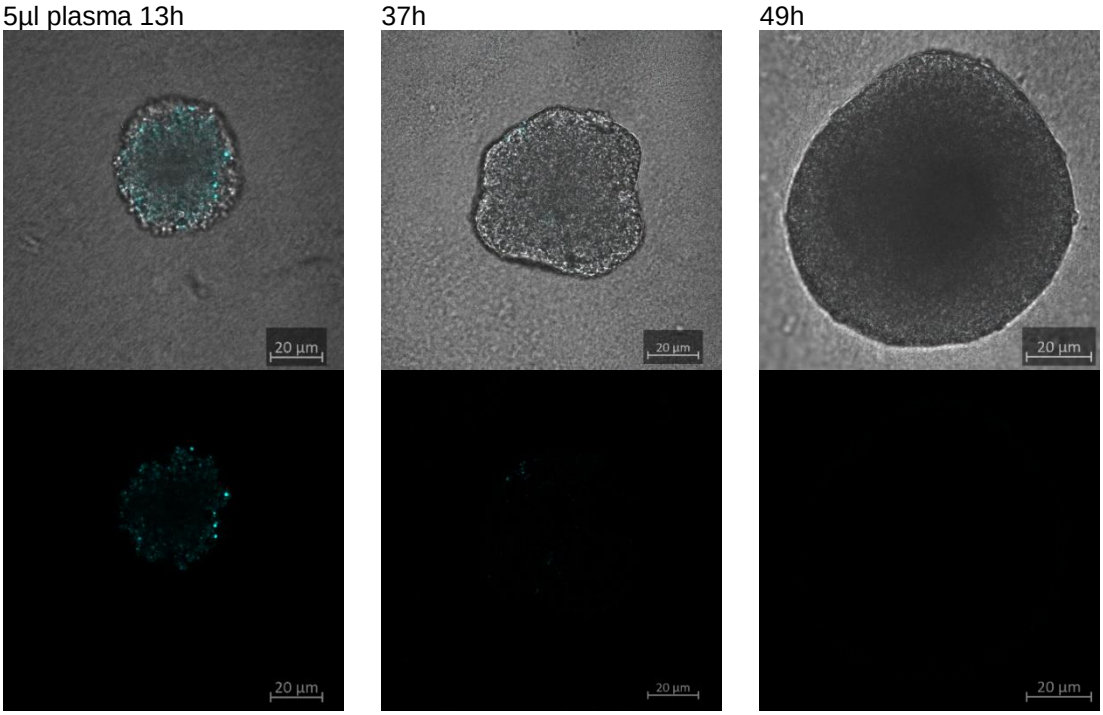

Figure 32. Newman, pJL54, pCG317. (A) shows fluorescence after 13h of incubation. Cerulean signal could be detected around the edges of the colonies (B) fluorescence after 37h. Only single bacteria displayed fluorescence. (C) fluorescence after 49h. No fluorescence signal was detected,

There was no fluorescence expression in colonies that grew in plasma-depleted medium, however inhomogeneous Cerulean and Venus fluorescence was detected in scattered bacteria at the lower part of the chamber after 37 hours of growth (Figure 33).

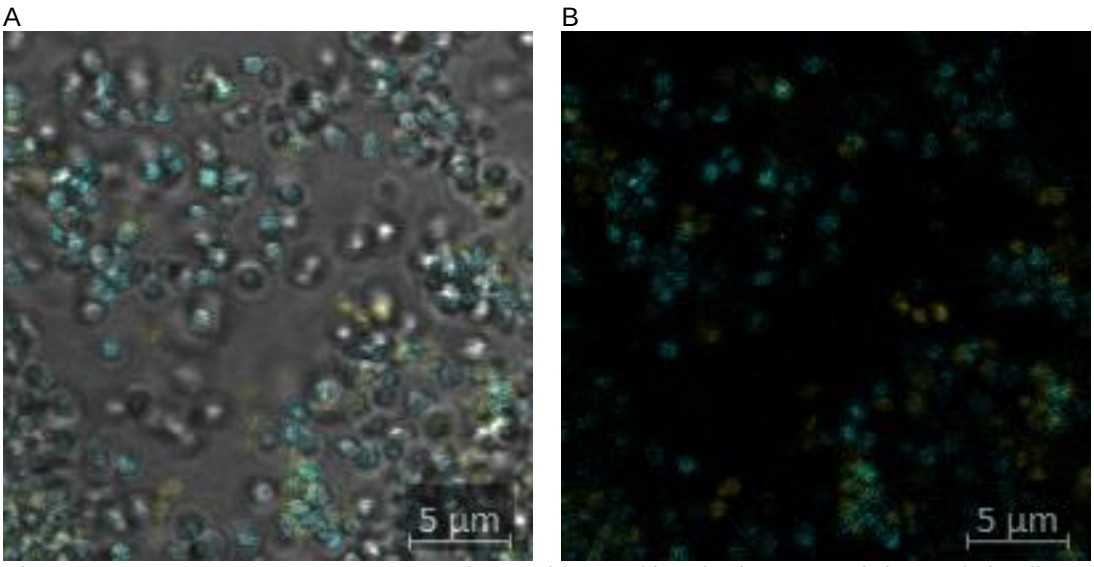

Figure 33. Newman, pJL54, pCG317 after 37 hours of incubation. Growth in 5µg/ml collagen, RPMI 1640, no plasma supplementation. (A) shows the merge between the brightfield image and the fluorescence channels Venus and Cerulean. (B) shows the fluorescence channels image. They show that there was inhomogenous expression of *gpven* and *gpcer* in bacteria grown scattered in the lower part of the chamber without plasma supplementation.

These findings suggested that embedding staphylococci in collagen created an environment in which they were able to grow into a shaped colony. Expression of the Cerulean fluorophore was initially present in bacteria on the outer edge of the colony, correlating to activity of the cap promoter. This activity decreased over time. For staphylococci growing in medium supplemented with plasma, capsule structure formation was visible.

4 Discussion

4.1 Construction of chromosomally integrated reporter strains: loss of genetic material and multiple integration of vector plasmids

We verified the integration of plasmids by several PCR-based strategies. The chosen oligonucleotides hybridized with both flanking integration sites and within the *gfp* gene itself. All control PCRs were able to detect the expected integration of the plasmids, gaining the expected size in most of the transductants. Thus, correct integration of vector plasmids into the SaPI-site could be verified for strains Newman, pJL53 and Newman, pJL54 and correct integration into the lipase site could be verified for strains Newman, pCG302, Newman, pCG317 and Newman, pCG318. Correct integration was also verified for the double reporter construct Newman, pJL54, pCG317.

However, in some strains, the results were partially inconsistent. In single reporter strain Newman, pCG302, the PCR revealed that the fragment flanking the integration site was slightly smaller in size than expected. This suggested a loss of genetic material during integration. PCR using primers spanning the promoter-*gfp* construct showed that the promoter-*gfp* construction was not affected. This was also verified as the strain phenotypically displayed the expected fluorescence. Thus, although the cause for the partial truncation remains unclear, the constructed strain is nonetheless valuable for analysis of promoter activity.

The phenotypical analysis revealed that the level of Venus fluorescence in strain Newman, pJL318 and Newman, pJL54, pCG317 was higher than that of all other assessed strains. This might be due to multiple integration of the vector into the chromosome or by additional second site mutation in these strains. For further analysis, we performed a pulsed field gel electrophoresis (PGFE) on reporter strains, to investigate the integration of the vector plasmid. Results are discussed in the section below.

It was also not possible to obtain a working reporter strain, Newman, pCG303 (vector with the agr P_3 promoter and *gpven*, integrating into the lipase site). Though the verification PCR had been positive, there was no fluorescence observed for the transductants. For further verification, the integrated *agr-gpven* site should be amplified from the transductants and sequenced to analyse whether sequence errors are present which might have been introduced by the electroporation and transduction procedure.

4.1.1 Pulsed field gel electrophoresis of reporter strains

To further analyse whether plasmids were integrated at the expected site, whether other genome rearrangement of the strains occurred during transduction or whether multiple plasmid integrations can occur, various transductants were analysed by PFGE. Generally, PGFE is used for the separation of large DNA molecules and its main application is for genotyping. The advantage of a PGFE compared to a single PCR is, that the whole genome is analysed, resulting in a unique fingerprint for each strain. In the PGFE, we separated *Sma*I digested chromosomal fragments and hybridized them with a GFP-DIG-probe to verify the presence of the *gfp* gene.

We analysed strains Newman, pCG318, Newman, pJL53 and the double reporter Newman, pCG318, pJL53 using PGFE. In the same PGFE, we also analysed other strains including the vector pCG318 cloned into various backgrounds (Newman 383, USA300, HG 001, Cyl 316 and RN 9011). The gel is depicted in Figure 34 A below, the result after hybridization and detection is shown in Figure 34 B. We expected the digestion of the single reporters to yield a single fragment that hybridizes with the GFP-DIG-probe. This was true for reporter strain Newman, pJL53 (Figure 34, B, lane 5). For Newman, pCG318 however, multiple fragments were detected. This suggests multiple integration of the vector plasmid pCG318 (Figure 34, B, lane 4). Interestingly, multiple integration was also noted for the pCG318 vector when cloned into different backgrounds (Figure 34, B, lanes 7, 11, 15, 18 and 20).

The PGFE of the double reporter strain Newman, pCG318, pJL53, which was not shown in this study, but the work of George et al. (George et al. 2015, the publication arising from this work) showed a similar picture to single reporter strain Newman, pCG318. (Figure 34, B, lane 6). We expected two fragments, indicating the presence of the integration of two vector plasmids. However, multiple bands were detected, indicating that the gene was present in multiple copies within the genome.

Given that single reporter strain Newman, pCG318 displayed a much higher level of fluorescence than the single reporter strain Newman, pCG317 in spite of both having the same promoter, multiple integration of pCG318 seems a likely explanation for this observation. The mechanism of multiple integration remains to be elucidated.

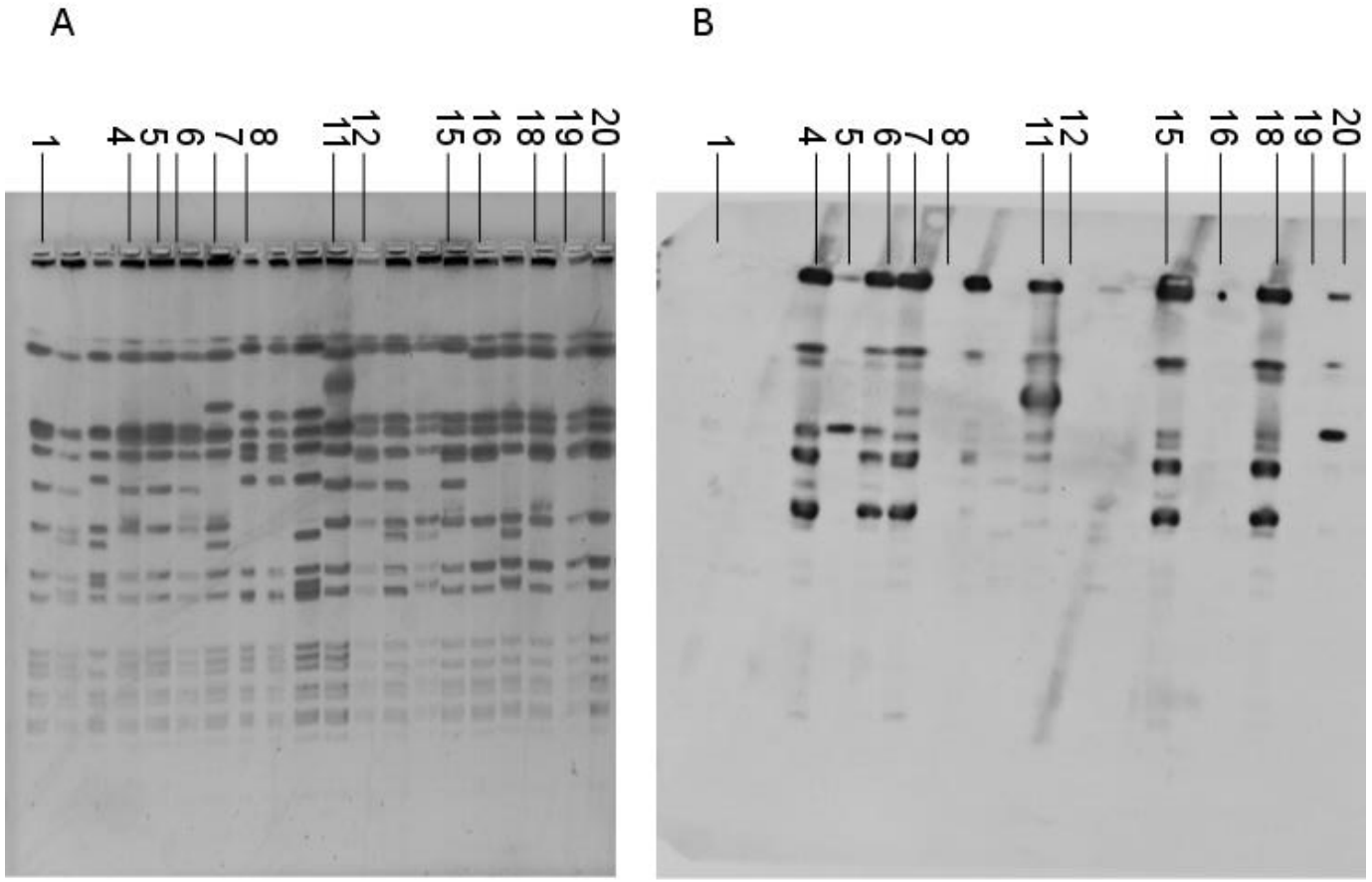

Figure 34. PFGE of various strains. Various strains of *S. aureus* were digested with *Sma*I and blotted on a membrane. Lane 1: Newman WT, 4: Newman, pCG318, 5: Newman, pJL53, 6: Newman.pCG318, pJL53, 7: Newman 383, pCG318, 8: USA 300 JE 2, 11: USA 300, pCG318, 12: HG 001WT, 15: HG 001, pCG318, 16: Cyl 316, 18: Cyl 316, pCG318, 19: RN 9011, 20: RN 9011, pJL53. PGFE after hybridisation with GFP-DIG-probe and detection. Lanes 4, 6, 7, 15 and 18 show multiple bars of the same fragment size hybridizing with the GFP-probe. Probes from those lanes have got the vector pCG318 in common. Lanes 5 and 20 show one distinct bar at the same fragment size.

Surprisingly, the *agr-ven* of pJL54 appeared much brighter in the double construct compared to the single construct. The reason for this discrepancy is unknown. One possible explanation is that during transduction, a duplication of the vector may have occurred, similar to that shown for pCG318.

4.2 Factors influencing fluorescence levels

In our experiments assessing reporter strain fluorescence, we found that Agr activity is largely homogeneous for our promoter constructs and that the attachment site does not influence the fluorescence expression. We have also found that cap activity is inhomogeneous within a single culture.

However, we noted some discrepancies when comparing strains Newman, pJL53 and Newman, pJL54. In both strains, the agr promoter controlled the fluorescence gene. Fluorescence of the vector construct containing *gpven* showed a lower level of fluorescence as well as an inhomogeneous distribution.

We concluded that there are differences in fluorophore expression. However, it remains to be analysed whether these differences reflect differences in Agr promoter activity, or whether they resulted from some variation between fluorophores. If the differences arose from fluorophore variation, the mechanism remains to be elucidated. One explanation could be a second site mutation in one of the constructs. Multiple integration of the vector plasmid pJL53 could be excluded in the PGFE (see previous section).

Other factors influencing the level of fluorophores could be the process of fluorophore maturation itself. Fluorophore formation requires proper protein folding, cyclisation, oxidation and dehydration (Kremers *et al.* 2006). Misfolded protein can lead to aggregation and can contribute to overall lower levels of fluorescence independent of promoter activity. One possible explanation could be that Venus is more prone to misfolding or aggregation. However, there is no evidence of this in the literature of which we are aware.

4.2.1 Heterogeneity of the cap promoter activity within a single culture

In reporter strains with integrated vectors containing the cap promoter, the fluorescence distribution was found to be highly inhomogeneous. This was particularly evident in strain Newman, pCG318, where *gpven* was downstream of the cap promoter. Within the culture of this strain, there were bacterial cells showing very high levels of fluorescence, cells giving off a weaker fluorescence signal, and cells which did not display any fluorescence at all. This suggested different levels of cap promoter activity in individual bacterial cells within one colony.

The heterogeneous expression pattern we observed is in agreement with previous observations that expression of CP is highly variable within a given culture, which has previously been shown by flow cytometry by Poutrel *et al.* (Bernard Poutrel, Rainard, & Sarradin, 1997) . Pöhlmann-Dietze *et al.* found, in immunofluorescence assays in staphylococci taken from the stationary phase, CP could be detected in only 39% of bacteria, indicating heterogeneous expression (Pöhlmann-Dietze *et al.* 2000). The *in vitro* observations were supported by our *in vivo* findings in nasal swabs of persistently colonised carriers, where fluorescence in-situ hybridisation identified that only a subpopulation of staphylococci were CP positive (George et al., 2015). Here we could show that heterogeneity of CP synthesis is reflected by the promoter activity of the CP biosynthesis gene cluster. We deducted from this result, that the heterogeneity is a purposely adaptive measure of the culture, to improve overall survival in changing conditions.

Heterogeneity within one culture can arise on a genetic level or on the level of gene expression. Genetic mutations within a population giving rise to a heterogeneous culture has been described for example in small colony variants, where single staphylococci acquire mutations in housekeeping genes, resulting in increased fitness to resist host defenses (Besier et al., 2008; Proctor, van Langevelde, Kristjansson, Maslow, & Arbeit, 1995). On the level of gene

expression, heterogeneity could be due to stochastic fluctuations directed by multiple different systems and factors, resulting in “noise” in gene expression.

The concept of genetic noise has previously been described in staphylococci in the context of persistence. It was found that after treating a culture with penicillin, a small fraction of staphylococci would always survive (Bigger, 1944). These findings suggested that, within a single clonal population, mechanisms were in place to ensure phenotypic heterogeneity in order to survive exposure to antibiotics. This variability has been termed the “adaptomics” of a population (Ryall, Eydallin, and Ferenci 2012), describing single-cell variations within a culture rendering the culture as a whole more adaptable. Phenotypic heterogeneity has also been observed for other bacterial species, such as *E. coli* (Moyed & Bertrand, 1983). Possible explanations for the gene expression noise could be the influence of nucleoid-associated proteins that are analogous to eukaryotic histones, fluctuations of chromosome supercoiling states and RNA polymerase availability (Gene-Wei Li, 2011).

As demonstrated in previous work, expression of CP can be advantageous, as it acts as an anti-phagocytic agent (Riordan & Lee, 2004). However, it also masks adherence proteins on the bacterial cell surface, therefore hindering colonization. In a study that investigating bacterial endocarditis, CP mutants were found to be more virulent, likely secondary to more efficient adherence to endocardial membranes (Baddour et al., 1992). It is likely that the heterogeneity which we observed was orchestrated via complex gene regulation mechanisms, with Agr being one of the influencing factors.

However, the degree of heterogeneity was not as high for strain Newman, pCG317 compared to Newman, pCG318. In Newman, pCG317 almost all bacterial cells displayed a low level of fluorescence and only single bacteria displayed a very high level. This corresponds to cap promoter activity in all cells within the culture and a high level of cap activity in single cells within the culture.

Thus, the differences between strains Newman, pCG318 and Newman, pCG317 (both utilize the cap promoter, but different fluorophores) suggest, that the heterogeneity that we observed is at least in part also due to the fluorophore differences.

4.3 Double reporter strains fluorescence

For double reporter Newman, pJL54(*agr-gpven*), pCG317(*cap-gpcer*), we have found that after overnight growth, all bacterial cells displayed simultaneous agr and cap promoter activity, and of those, single cells displayed high cap promoter activity. From this result, we surmise that agr activity may in part be driving cap activity, but that it is not the only driver of *cap* expression in the stationary phase. This result was also observed for our double reporter strain Newman, pJL53(*agr-gpcer*), pCG318(*cap-gpven*) (George et al., 2015).

However, after dilution and a second growth phase, this picture changed fundamentally. The day culture of Newman, pJL54, pCG317 showed, that only single bacteria displayed agr promoter activity and for most bacteria expressed *cap*, with single cells displaying a high cap promoter activity. This result contradicted previous observations during our study, where all bacterial strains showed similar expression patterns when comparing the overnight culture and day culture +6h. Further analysis is required to verify that this result is reproducible and reflects promoter activity.

In previous work, it has been thought that quorum sensing systems are a significant driver of heterogeneity within a culture in Gram-negative organisms such as *Vibrio spp*. (Anetzberger, Schell, & Jung, 2012; Delfino Pé Rez & Hagen, 2010). With our double reporter strain, we sought to elucidate this principle by simultaneously observing the activity of both the cap and the agr P_3 promoter.

The results obtained suggest that the observations are not purely representative of promoter activity, but also at least in part due to the vectors we used and due to differences in fluorophores.

4.4 Infection model

4.4.1 Microcolony formation

When staphylococci were embedded into a collagen matrix, we found that supplementation of the growth medium with human plasma diminished scattered growth. Instead, we observed the formation of hemispherical microcolonies and over time, and we found microcolonies to form distinct borders to the surrounding matrix, suggesting the formation of a pseudocapsule. The size of microcolonies varied, with diameters between 15 and 40µm.

However, we also observed that even after extensive observation periods, colony growth ceased and bacteria did not break out of the microcolony aggregate. We also could not detect the formation of a microcolony-associated meshwork.

One possible factor for the discrepancies between our result and previous work could be the use of different collagen gel concentrations. For our experiments, a higher concentration of bovine collagen type I was used. This could contribute to creating a more rigid matrix, and thereby slow diffusion rates and reduce cell mobility.

The impact of growth in serum has been assessed by Oogai *et al.* (Oogai et al., 2011). In their study, they have shown that many virulence factors (e.g. hemolysins, leukocidins and adhesins) were expressed at a higher level when staphylococci were grown in calf, rabbit and human sera.

In the light of this result, we interpreted that the supplemented human plasma influenced cap and agr promoter activity and contributed to the different picture

of the colony growth versus the growth in liquid medium. In addition to this, the human plasma that was used in our experiments was obtained from our university blood bank. It is a non-standardised supplement, and as such has the potential to show large variability in composition. As minimal changes in environmental factors can impact on growth dynamics of staphylococci, the plasma itself is likely to also act as an influencing factor on the expression of *cap* and *agr*. Future work to improve the model could therefore be to formulate a more standardised solution, e.g. supplementing growth medium with fibrinogen and other clotting factors. This would emulate plasma, but allows for more control of the medium's composition.

4.4.2 Fluorophore expression in a microcolony: Influence of growth medium, human plasma and oxygen depletion

We observed that fluorescence in microcolonies was weaker than when grown in liquid medium, and almost exclusively displayed by bacteria on the outer edge of the colony. It was also noted that, unlike when grown in liquid medium, only cap promoter activity was detected.

This suggests that, in addition to the impact of the upstream promoter, factors in the environment surrounding a bacterial colony and the micro-environment within a colony can influence the overall level of a fluorophore. These factors can influence the activity on the level of the promoter, on the level of gene expression and in post-translational processes.

For example, it is known, that maturation of GFP requires molecular oxygen and is most efficient at a pH of 7. Therefore, it is important to consider oxygen levels within a microcolony when assessing fluorescence in colonies grown in a 3D-collagen matrix. In this context, we also need to consider how readily nutrients can diffuse to the inner parts of a microcolony. The medium surrounding the gel matrix can also have an influence on growth and fluorophore expression.

As we did not replace the medium during the experiment, it is likely that the availability of nutrients, as well as pH shifted during the growth period. This could have had an impact on the overall metabolism of bacteria, in particular on the expression of virulence genes and gene regulators. A step towards improvement of the model would be to frequently replace the growth medium during the extensive periods of observation.

Oxygen depletion in bacterial aggregates could contribute to lower fluorophore expression levels. This has been investigated by Wessel *et al.* (Wessel *et al.* 2014) in a 3D-growth model embedding *Pseudomonas aeruginosa (P. aeruginosa)* in a 3D-printed matrix. In their study, GFP was used as a biosensor detecting oxygen levels below 2%. It was found that oxygen depletion could be observed starting from a colony radius of ~27µm. The colonies from our model were found to have a similar radius, and it is therefore likely that oxygen levels were depleted at the centre of the colonies. Whilst oxygen depletion can therefore influence the expression of *cap*, it is unlikely to affect the maturation of GFP as it can be used as a biosensor for low oxygen levels <2% as shown in Wessel *et al.*'s study. *S. aureus* is known to be able to survive under both aerobic and anaerobic conditions, and it has been found that growth is slower under anaerobic conditions (Fuchs, Pané-Farré, Kohler, Hecker, & Engelmann, 2007). Oxygen levels also have been shown to influence virulence gene regulation (Pragman, Yarwood, Tripp, & Schlievert, 2004). It is therefore likely, that low oxygen levels have played a role in our experiment in suppressing cap promoter activity, resulting in little to no expression at the centre of a colony. It remains unclear why no Agr activity could be observed.

To improve this in future work, various factors impacting on growth have to be considered and optimized. One aspect that has been studied by Stewart *et al.* is the diffusion of nutrients across a matrix. In their study, a mathematical model was created to model diffusion in biofilms (Stewart, 2003). With the use of newer technology to create matrices, e.g. 3D-printing techniques, bacterial clusters can be created in a more precise manner, allowing mathematical models to predict

the various influencing factors in bacterial growth. This would create a more controlled environment in which reporter constructs could be observed.

4.5 Conclusions

Results from promoter-linked fluorescence activity suggest that, within a population, *S. aureus* bacteria tend to behave differently from one another. The fact that *S. aureus* is a very adaptable pathogen is likely to be at least partly due to the observed expression heterogeneity. We concluded from the obtained results that this heterogeneity is an evolutionary strategy for *S. aureus* to persist in a changing, challenging environment. Depending on the selection pressure, single better-adapted staphylococci within a clonal culture may survive and thereby ensure the survival of the culture as a whole.

This genetic noise and expression heterogeneity can have large impacts on colony composition. As mentioned in the introduction, cell wall proteins such as MSCRAMMs, Protein A and the fibrinogen-, fibronectin- and collagen-binding proteins are expressed during the stationary phase, whereas secreted enzymes such as proteases and toxins are preferably translated during the exponential growth phase. A number of changes that take place at the transition from the log to the stationary phase can be attributed to the Agr system. This growth phase-dependent gene expression and the expression heterogeneity ultimately complicates the selection of potential targets for applications in immunization strategies. Hence, characterizing the exact mechanisms behind this phenomenon can drive research in this area towards a more targeted drug administration scheme according to bacterial growth phase and expression patterns.

However, the vector cassette system has proved to give inconsistent results at several steps. For instance, integration could result in partial loss of the plasmid or to multiple integration into the chromosome. Furthermore, sequence-based error could not be excluded. Experiments to determine fluorescence for vectors with the same promoter but different fluorophore did not yield comparable results. Thus, this genetic tool requires extensive controls to yield reliable and reproducible results. However, after further optimization, it is feasible to use such

constructs to assess promoter activity on the single-cell level under different conditions.

To circumvent the extensive cloning and control procedure, strains with low-copy plasmids with dual promoter constructs could be analysed. This approach would be more straightforward as integration is not required. Cloning two genes on one plasmid would also accelerate the cloning procedure considerably.

The collagen model has shown that staphylococci surround themselves with a pseudocapsule during growth in a rigid matrix, similar to the structures in an *in vivo* abscess. As the process of establishing this model is ongoing, our results were still inconclusive; however, it has previously been shown by Guggenberger *et al.* (Guggenberger *et al.*, 2012) that the collagen model yields reproducible results in terms of formation of a pseudocapsule and a MAM. As the collagen solution used by Guggenberger *et al.* was not commercially available, we used a solution from a different manufacturer, which differed in concentration. It is therefore likely that this has contributed to the differences that were observed in our experiments and that further experiments to optimize the collagen gel constitution will improve the model.

5 Summary

Staphylococcus aureus (*S. aureus*) is a gram-positive bacterium with a “split personality”. Staphylococci are part of the normal skin flora, but can also cause skin and wound infections as well as fatal septicaemia. The mechanism of transition from apathogenic colonisation to invasive infections is modulated by several gene regulators.

An important gene regulator is the Accessory Gene Regulator (Agr) system, which is responsible for the modulation of hundreds of genes. The *agr locus* consists of two transcriptional units expressed from two divergent promoters P_2 and P_3. The Agr system is a typical two-component system and is regulated by a quorum sensing mechanism, whereby staphylococci produce an extracellular autoinducing peptide (AIP). AIP binds to its receptor, the histidine kinase AgrA and causes the autoinduction of the Agr operon itself through the agr P_2 promoter, as well as the activation of various target genes through the agr P_3 promoter. Gene expression is activated by a regulatory RNAIII molecule (originating from the agr P_3 promoter) and, among other regulatory functions, leads to the expression of the capA-P biosynthesis cluster, which leads to the synthesis of capsular polysaccharide (CP). The capA-P operon is controlled by the capP promoter upstream of capA. CPs protect staphylococci from opsono-phagocytosis, but also mask surface molecules and therefore reduce the ability of staphylococci to adhere to tissue surfaces. Analysis using fluorescence-activated cell sorting and immunofluorescence staining have revealed that not all staphylococci within a single culture produce CP in the post-exponential phase, but rather present phenotypically heterogeneous.

The aim of this study was to establish reporter strains to simultaneously analyse the activity of both the agr-P3 and the cap-P promoter on a single cell level. For this, promoters with fluorescence proteins were cloned into integration vectors and integrated into the *S. aureus* chromosome. We used integration vectors that either used the *S. aureus* pathogenicity island I (SaPI-I) as an attachment site, or

integrated with a phage (attachment site *geh*). Plasmids with various combinations of fluorescence genes Venus (*ven)* or Cerulean (*cer*) and different selection markers were tested. The generated strains were verified using PCR to confirm correct integration, and phenotypically analysed using confocal fluorescence microscopy. We were able to show that all reporter strains had successfully integrated the vector plasmid at the correct attachment site. In one case, partial deletion of the integration plasmid was observed. In another case, we were able to detect multiple integration of the vector. Fluorescence microscopy revealed that 1. Agr-activity is largely homogeneous and is highest in the post-exponential phase. 2. cap-A activity is also at highest levels in the post-exponential phase. 3. cap-P activity is highly heterogeneous within a single culture. 4. Promoter fusion constructs with Venus displayed a stronger fluorescence signal than fusion constructs with Cerulean. 5. The analysis of the double reporter strain gave inconclusive results and needs to be analysed further.

In the second part of this work, we aimed to establish a 3D collagen model, in which reporter strains could be observed over an extended period. Guggenberger *et al.* have shown that embedding staphylococci in collagen with fibrinogen led to the formation of a pseudocapsule from fibrinogen deposits, as well as a surrounding microcolony-associated meshwork (Guggenberger C, Wolz C, Morrissey JA, Heesemann J (2012) Two Distinct Coagulase-Dependent Barriers Protect *Staphylococcus aureus* from Neutrophils in a Three Dimensional *in vitro* Infection Model. PLoS Pathogens). These structures are similar to those found in an abscess, therefore we aimed to simulate an *in vitro* abscess with our model. Pseudocapsule and a microcolony-associated meshwork formation was observed partially. Analysis of promoter activity within the collagen/fibrinogen-structure revealed preliminary results: 1. The intensity of fluorescence signal was weaker for both promoter fusion genes compared to growth in liquid medium. 2. cap-Promoter activity seems significantly higher than agr activity. 3. Bacteria in the periphery of a microcolony displayed higher levels of fluorescence. These results represent first steps towards the establishment of a system to analyse promoter activity within an *in vitro* abscess model.

6 References

Abtin, A., Jain, R., Mitchell, A. J., Roediger, B., Brzoska, A. J., Tikoo, S., … Weninger, W. (2014). Perivascular macrophages mediate neutrophil recruitment during bacterial skin infection. *Nature Immunology*, *15*(1), 45–53. http://doi.org/10.1038/ni.2769

Alonzo III, F., Benson, M. A., Chen, J., Novick, R. P., Shopsin, B., & Torres, V. J. (2012). Staphylococcus aureus leucocidin ED contributes to systemic infection by targeting neutrophils and promoting bacterial growth in vivo. *Molecular Microbiology*, *83*(2), 423–435. http://doi.org/10.1111/j.1365-2958.2011.07942.x

Anetzberger, C., Schell, U., & Jung, K. (2012). Single cell analysis of Vibrio harveyi uncovers functional heterogeneity in response to quorum sensing signals. *BMC Microbiology*, *12*, 1. http://doi.org/10.1186/1471-2180-12-209

Arbeit, R. D., Karakawa, W. W., Vann, W. F., & Robbins, J. B. (1984). Predominance of two newly described capsular polysaccharide types among clinical isolates of Staphylococcus aureus. *Diagnostic Microbiology and Infectious Disease*, *2*(2), 85–91. http://doi.org/10.1016/0732-8893(84)90002-6

Baba, T., Bae, T., Schneewind, O., Takeuchi, F., & Hiramatsu, K. (2008). Genome sequence of Staphylococcus aureus strain Newman and comparative analysis of staphylococcal genomes: polymorphism and evolution of two major pathogenicity islands. *Journal of Bacteriology*, *190*(1), 300–10. http://doi.org/10.1128/JB.01000-07

Baddour, L. M., Lowrance, C., Albus, A., Lowrance, J. H., Anderson, S. K., & Lee, J. C. (1992). Staphylococcus aureus Microcapsule Expression Attenuates Bacterial Virulence in a Rat Model of Experimental Endocarditis. *Journal of Infectious Diseases*, *165*(4), 749–753.

http://doi.org/10.1093/infdis/165.4.749

Berube, B. J., & Wardenburg, J. B. (2013). Staphylococcus aureus α-Toxin: Nearly a Century of Intrigue. *Toxins*, *5*, 1140–1166. http://doi.org/10.3390/toxins5061140

Besier, S., Zander, J., Siegel, E., Saum, S. H., Hunfeld, K.-P., Ehrhart, A., … Wichelhaus, T. A. (2008). Thymidine-Dependent Staphylococcus aureus Small-Colony Variants: Human Pathogens That Are Relevant Not Only in Cases of Cystic Fibrosis Lung Disease. *JOURNAL OF CLINICAL MICROBIOLOGY*, *46*(11), 3829–3832. http://doi.org/10.1128/JCM.01440-08

Bestebroer, J., Poppelier, M. J. J. G., Ulfman, L. H., Lenting, P. J., Denis, C. V, Van Kessel, K. P. M., … De Haas, C. J. C. (2007). Staphylococcal superantigen-like 5 binds PSGL-1 and inhibits P-selectin–mediated neutrophil rolling, *109*, 2936–2943. http://doi.org/10.1182/blood-2006

Bigger, J. W. (1944). Treatment of staphylococcal infections with penicillin by intermittent sterilisation. *Lancet*, (244), 497–500.

Boisset, S., Geissmann, T., Huntzinger, E., Fechter, P., Bendridi, N., Possedko, M., … Romby, P. (2007). Staphylococcus aureus RNAIII coordinately represses the synthesis of virulence factors and the transcription regulator Rot by an antisense mechanism. *Genes & Development*, *21*(11), 1353–66. http://doi.org/10.1101/gad.423507

Borregaard, N., Sørensen, O. E., & Theilgaard-Mönch, K. (2007). Neutrophil granules: a library of innate immunity proteins. *Trends in Immunology*, *28*(8), 340–345. http://doi.org/10.1016/j.it.2007.06.002

Botelho-Nevers, E., Gagnaire, J., Verhoeven, P. O., Cazorla, C., Grattard, F., Pozzetto, B., … Lucht, F. (2016). Decolonization of Staphylococcus aureus carriage in 2016. *Médecine et Maladies Infectieuses*. http://doi.org/10.1016/j.medmal.2016.10.005

Campbell, R. E., Tour, O., Palmer, A. E., Steinbach, P. A., Baird, G. S., Zacharias, D. A., & Tsien, R. Y. (2002). A monomeric red fluorescent protein. *Proceedings of the National Academy of Sciences of the United States of America*, *99*(12), 7877–82. http://doi.org/10.1073/pnas.082243699

Charpentier, E., Anton, A. I., Barry, P., Alfonso, B., Fang, Y., & Novick, R. P. (2004). Novel Cassette-Based Shuttle Vector System for Gram-Positive Bacteria, *70*(10), 6076–6085. http://doi.org/10.1128/AEM.70.10.6076

Cheng, A. G., Kim, H. K., Burts, M. L., Krausz, T., Schneewind, O., & Missiakas, D. M. (2009). Genetic requirements for Staphylococcus aureus abscess formation and persistence in host tissues. *FASEB Journal : Official Publication of the Federation of American Societies for Experimental Biology*, *23*(10), 3393–404. http://doi.org/10.1096/fj.09-135467

Cheung, A. L., Bayer, M. G., & Heinrichs, J. H. (1997). sar Genetic determinants necessary for transcription of RNAII and RNAIII in the agr locus of Staphylococcus aureus. *Journal of Bacteriology*, *179*(12), 3963–71. http://doi.org/10.1128/JB.179.12.3963-3971.1997

Chien, Y., & Cheung, A. L. (1998). Molecular interactions between two global regulators, sar and agr, in Staphylococcus aureus. *The Journal of Biological Chemistry*, *273*(5), 2645–52. http://doi.org/10.1074/JBC.273.5.2645

Cho, J. S., Guo, Y., Ramos, R. I., Hebroni, F., Plaisier, S. B., Xuan, C., … Miller, L. S. (2012). Neutrophil-derived IL-1b Is Sufficient for Abscess Formation in Immunity against Staphylococcus aureus in Mice. http://doi.org/10.1371/journal.ppat.1003047

Cho, J. S., Pietras, E. M., Garcia, N. C., Ramos, R. I., Farzam, D. M., Monroe, H. R., … Miller, L. S. (2010). IL-17 is essential for host defense against cutaneous Staphylococcus aureus infection in mice. *The Journal of Clinical Investigation*, *120*(5), 1762–73. http://doi.org/10.1172/JCI40891

Claes, J., Vanassche, T., Peetermans, M., Liesenborghs, L., Vandenbriele, C., Vanhoorelbeke, K., … Verhamme, P. (2014). Adhesion of Staphylococcus aureus to the vessel wall under flow is mediated by von Willebrand factor-binding protein. *Blood*, *124*(10), 1669–1676. http://doi.org/10.1182/blood-2014-02-558890

Clarke, S. R., Andre, G., Walsh, E. J., Dufrêne, Y. F., Foster, T. J., & Foster, S. J. (2009). Iron-regulated surface determinant protein A mediates adhesion of Staphylococcus aureus to human corneocyte envelope proteins. *Infection and Immunity*, *77*(6), 2408–16. http://doi.org/10.1128/IAI.01304-08

Cooney, J., Kienle, Z., Foster, T. J., & O 'toole2t, P. W. (1993). The Gamma-Hemolysin Locus of Staphylococcus aureus Comprises Three Linked Genes, Two of Which Are Identical to the Genes for the F and S Components of Leukocidin. *INFECTION AND IMMUNITY*, *61*(2), 768–771. Retrieved from https://www.ncbi.nlm.nih.gov/pmc/articles/PMC302792/pdf/iai00014-0408.pdf

Cubitt, A. B., Heim, R., Adams, S. R., Boyd, A. E., Gross, L. A., & Tsien, R. Y. (1995). Understanding, improving and using green fluorescent proteins. *Trends in Biochemical Sciences*, *20*(11), 448–55. Retrieved from http://www.ncbi.nlm.nih.gov/pubmed/8578587

Cunnion, K. M., Lee, J. C., & Frank, M. M. (2001). Capsule production and growth phase influence binding of complement to Staphylococcus aureus. *Infection and Immunity*, *69*(11), 6796–803. http://doi.org/10.1128/IAI.69.11.6796-6803.2001

Dassy, B., & Fournier, J.-M. (1996). Respiratory Activity Is Essential for Post-Exponential-Phase Production of Type 5 Capsular Polysaccharide by Staphylococcus aureus. *INFECTION AND IMMUNITY*, *64*(7), 2408–2414. Retrieved from https://www.ncbi.nlm.nih.gov/pmc/articles/PMC174090/pdf/642408.pdf

Dassy, B., Stringfellow, W. T., Lieb, M., & Fournier, J. M. (1991). Production of type 5 capsular polysaccharide by Staphylococcus aureus grown in a semi-synthetic medium. *Journal of General Microbiology*, *137*(5), 1155–1162. http://doi.org/10.1099/00221287-137-5-1155

de Haas, C. J. C., Veldkamp, K. E., Peschel, A., Weerkamp, F., Van Wamel, W. J. B., Heezius, E. C. J. M., … van Strijp, J. A. G. (2004). Chemotaxis Inhibitory Protein of Staphylococcus aureus, a Bacterial Antiinflammatory Agent. *Journal of Experimental Medicine*, *199*(5). Retrieved from http://jem.rupress.org/content/199/5/687

DeLeo, F. R., Otto, M., Kreiswirth, B. N., & Chambers, H. F. (2010). Community-associated meticillin-resistant Staphylococcus aureus. *Lancet (London, England)*, *375*(9725), 1557–68. http://doi.org/10.1016/S0140-6736(09)61999-1

Delfino Pé Rez, P., & Hagen, S. J. (2010). Heterogeneous Response to a Quorum-Sensing Signal in the Luminescence of Individual Vibrio fischeri. http://doi.org/10.1371/journal.pone.0015473

Dryden, M. S. (2010). Complicated skin and soft tissue infection. *Journal of Antimicrobial Chemotherapy*, *65*(Supplement 3), iii35-iii44. http://doi.org/10.1093/jac/dkq302

Durr, M. C., Kristian, S. A., Otto, M., Matteoli, G., Margolis, P. S., Trias, J., … Peschel, A. (2006). Neutrophil chemotaxis by pathogen-associated molecular patterns - formylated peptides are crucial but not the sole neutrophil attractants produced by Staphylococcus aureus. *Cellular Microbiology*, *8*(2), 207–217. http://doi.org/10.1111/j.1462-5822.2005.00610.x

Emonts, M., Uitterlinden, A. G., Nouwen, J. L., Kardys, I., Maat, M. P. M. de, Melles, D. C., … Belkum, A. van. (2008). Host Polymorphisms in Interleukin 4, Complement Factor H, and C-Reactive Protein Associated with Nasal Carriage of *Staphylococcus aureus* and Occurrence of Boils. *The Journal of Infectious Diseases*, *197*(9), 1244–1253. http://doi.org/10.1086/533501

Fischer, J., Lee, J. C., Peters, G., & Kahl, B. C. (2014). Acapsular clinical Staphylococcus aureus isolates lack agr function. *Clinical Microbiology and Infection*, *20*(7), O414–O417. http://doi.org/10.1111/1469-0691.12429

Foster, T. J. (2009). Colonization and infection of the human host by staphylococci: adhesion, survival and immune evasion. *Veterinary Dermatology*, *20*(5–6), 456–470. http://doi.org/10.1111/j.1365-3164.2009.00825.x

Foster, T. J., Geoghegan, J. A., Ganesh, V. K., & Höök, M. (2014). Adhesion, invasion and evasion: the many functions of the surface proteins of Staphylococcus aureus. *Nature Publishing Group*, *12*. http://doi.org/10.1038/nrmicro3161

Fridkin, S. K., Hageman, J. C. S., Morrison, M., Thomson Sanza, L., Como-Sabetti, K., Jernigan, J. A., … Farley, M. M. (2005). Methicillin-Resistant Staphylococcus aureus Disease in Three Communities for the Active Bacterial Core Surveillance Program of the Emerging Infections Program Network. *N Engl J Med*, *35214*. Retrieved from http://www.nejm.org/doi/pdf/10.1056/NEJMoa043252

Fuchs, S., Pané-Farré, J., Kohler, C., Hecker, M., & Engelmann, S. (2007). Anaerobic gene expression in Staphylococcus aureus. *Journal of Bacteriology*, *189*(11), 4275–89. http://doi.org/10.1128/JB.00081-07

Gene-Wei Li, S. X. (2011). Central dogma at the single-molecule level in living cells. *Nature*, *457*(7356), 308–15. http://doi.org/10.1038/nature10315

George, S. E., Nguyen, T., Geiger, T., Weidenmaier, C., Lee, J. C., Liese, J., & Wolz, C. (2015). Phenotypic Heterogeneity and Temporal Expression of the Capsular Polysaccharide in Staphylococcus aureus. *Molecular Microbiology*, n/a-n/a. http://doi.org/10.1111/mmi.13174

Gómez, M. I., Lee, A., Reddy, B., Muir, A., Soong, G., Pitt, A., … Prince, A. (2004). Staphylococcus aureus protein A induces airway epithelial inflammatory responses by activating TNFR1. *Nature Medicine*, *10*(8), 842–848. http://doi.org/10.1038/nm1079

Graves, S. F., Kobayashi, S. D., Braughton, K. R., Diep, B. A., Chambers, H. F., Otto, M., & DeLeo, F. R. (2010). Relative contribution of Panton-Valentine leukocidin to PMN plasma membrane permeability and lysis caused by USA300 and USA400 culture supernatants. *Microbes and Infection*, *12*(6), 446–456. http://doi.org/10.1016/j.micinf.2010.02.005

Gravet, A., Colin, D. A., Keller, D., Giradot, R., Monteil, H., & Prévost, G. (1998). Characterization of a novel structural member, LukE-LukD, of the bi-component staphylococcal leucotoxins family. *FEBS Letters*, *436*(2), 202–208. http://doi.org/10.1016/S0014-5793(98)01130-2

Greenberg, E. P. (1994). Quorum sensing in bacteria : the LuxR-LuxI MINIREVIEW Quorum Sensing in Bacteria : the LuxR-LuxI Family of Cell Density-Responsive Transcriptional Regulatorst, *176*(2).

Greenlee-Wacker, M. C., Rigby, K. M., Kobayashi, S. D., Porter, A. R., DeLeo, F. R., & Nauseef, W. M. (2014). Phagocytosis of Staphylococcus aureus by Human Neutrophils Prevents Macrophage Efferocytosis and Induces Programmed Necrosis. *The Journal of Immunology*, *192*(10). Retrieved from http://www.jimmunol.org/content/192/10/4709

Gresham, H. D., Lowrance, J. H., Caver, T. E., Wilson, B. S., Cheung, A. L., & Lindberg, F. P. (2000). Survival of Staphylococcus aureus inside neutrophils contributes to infection. *Journal of Immunology (Baltimore, Md. : 1950)*, *164*(7), 3713–22. Retrieved from http://www.ncbi.nlm.nih.gov/pubmed/10725730

Grunert, T., Wenning, M., Barbagelata, M. S., Fricker, M., Sordelli, D. O., Buzzola, F. R., & Ehling-Schulz, M. (2013). Rapid and reliable identification of Staphylococcus aureus capsular serotypes by means of artificial neural network-assisted Fourier transform infrared spectroscopy. *Journal of Clinical Microbiology*, *51*(7), 2261–6. http://doi.org/10.1128/JCM.00581-13

Guggenberger, C., Wolz, C., Morrissey, J. a, & Heesemann, J. (2012a). Two distinct coagulase-dependent barriers protect Staphylococcus aureus from neutrophils in a three dimensional in vitro infection model. *PLoS Pathogens*, *8*(1), e1002434. http://doi.org/10.1371/journal.ppat.1002434

Guggenberger, C., Wolz, C., Morrissey, J. a, & Heesemann, J. (2012b). Two distinct coagulase-dependent barriers protect Staphylococcus aureus from neutrophils in a three dimensional in vitro infection model. *PLoS Pathogens*, *8*(1), e1002434. http://doi.org/10.1371/journal.ppat.1002434

Heinrichs, J. H., Bayer, M. G., & Cheung, A. L. (1996). Characterization of the sar locus and its interaction with agr in Staphylococcus aureus. *Journal of Bacteriology*, *178*(2), 418–23. http://doi.org/10.1128/JB.178.2.418-423.1996

Herbert, S., Newell, S. W., Lee, C., Wieland, K.-P., Dassy, B., Fournier, J.-M., … Ring, G. D. (2001). Capsular Polysaccharides by CO 2. *JOURNAL OF BACTERIOLOGY*, *183*(15), 4609–4613. http://doi.org/10.1128/JB.183.15.4609–4613.2001

Herbert, S., Worlitzsch, D., Dassy, B., Boutonnier, A., Fournier, J. M., Bellon, G., … Döring, G. (1997). Regulation of Staphylococcus aureus capsular polysaccharide type 5: CO2 inhibition in vitro and in vivo. *The Journal of Infectious Diseases*, *176*(2), 431–8. Retrieved from http://www.ncbi.nlm.nih.gov/pubmed/9237709

Hochkeppel, H. K., Braun, D. G., Vischer, W., Imm, A., Sutter, S., Staeubli, U., … Fournier, J. M. (1987). Serotyping and electron microscopy studies of Staphylococcus aureus clinical isolates with monoclonal antibodies to capsular polysaccharide types 5 and 8. *Journal of Clinical Microbiology*, *25*(3), 526–30. Retrieved from http://www.ncbi.nlm.nih.gov/pubmed/2437148

Kluytmans, J. (1998). Reduction of surgical site infections in major surgery by elimination of nasal carriage of Staphylococcus aureus. *The Journal of Hospital Infection*, *40 Suppl B*, S25-9. Retrieved from http://www.ncbi.nlm.nih.gov/pubmed/9777530

Kluytmans, J. A. N. (1997). Nasal carriage of Staphylococcus aureus : epidemiology , underlying mechanisms , and associated risks . Nasal Carriage of Staphylococcus aureus : Epidemiology , Underlying Mechanisms , and Associated Risks, *10*(3).

Kobayashi, S. D., Malachowa, N., & DeLeo, F. R. (2015). Pathogenesis of Staphylococcus aureus Abscesses. *The American Journal of Pathology*, *185*(6), 1518–1527. http://doi.org/10.1016/j.ajpath.2014.11.030

König, B., Prévost, G., Piémont, Y., & König, W. (1995). Effects of Staphylococcus aureus leukocidins on inflammatory mediator release from human granulocytes. *The Journal of Infectious Diseases*, *171*(3), 607–13. Retrieved from http://www.ncbi.nlm.nih.gov/pubmed/7533198

Kreger, A. S., Kim, K.-S., Zaboretzky, F., & Bernheimer, A. W. (1971). Purification and Properties of Staphylococcal Delta Hemolysin. *INFECTION AND IMMUNITY*, *3*(3), 449–465.

Kreiswirth, B. N., Löfdahl, S., Betley, M. J., O'Reilly, M., Schlievert, P. M., Bergdoll, M. S., & Novick, R. P. (1983). The toxic shock syndrome exotoxin structural gene is not detectably transmitted by a prophage. *Nature*, *305*(5936), 709–12. Retrieved from http://www.ncbi.nlm.nih.gov/pubmed/6226876

Kremers, G.-J., Goedhart, J., Van Munster, E. B., & Gadella, T. W. J. (n.d.). Cyan and Yellow Super Fluorescent Proteins with Improved Brightness, Protein Folding, and FRET Förster Radius. http://doi.org/10.1021/bi0516273

Labas, Y. A., Gurskaya, N. G., Yanushevich, Y. G., Fradkov, A. F., Lukyanov, K. A., Lukyanov, S. A., & Matz, M. V. (2002). Diversity and evolution of the green fluorescent protein family. *Proceedings of the National Academy of Sciences of the United States of America*, *99*(7), 4256–61.

http://doi.org/10.1073/pnas.062552299

Lee, C. Y., Buranen, S. L., & Ye, Z. H. (1991). Construction of single-copy integration vectors for Staphylococcus aureus. *Gene*, *103*(1), 101–5. Retrieved from http://www.ncbi.nlm.nih.gov/pubmed/1652539

Lee, J. C., Liu, M.-J., Parsonnet, J., & Arbeit2, R. D. (1990). Expression of Type 8 Capsular Polysaccharide and Production of Toxic Shock Syndrome Toxin 1 Are Associated among Vaginal Isolates of Staphylococcus aureus. *JOURNAL OF CLINICAL MICROBIOLOGY*, *28*(12), 2612–2615. Retrieved from https://www.ncbi.nlm.nih.gov/pmc/articles/PMC268243/pdf/jcm00060-0038.pdf

Lee, J. C., Takeda, S., Livolsi, P. J., & Paoletti, L. C. (1993). Effects of In Vitro and In Vivo Growth Conditions on Expression of Type 8 Capsular Polysaccharide by Staphylococcus aureus. *INFECrION AND IMMUNITY*, *61*(5), 1853–1858. Retrieved from https://www.ncbi.nlm.nih.gov/pmc/articles/PMC280775/pdf/iai00017-0269.pdf

Lorenz, L. L., & Duthie, E. S. (1952). Staphylococcal Coagulase: Mode of Action and Antigenicity. *Microbiology*, *6*(1–2), 95–107. http://doi.org/10.1099/00221287-6-1-2-95

Lowy, F. D. (1998). *Staphylococcus aureus* Infections. *New England Journal of Medicine*, *339*(8), 520–532. http://doi.org/10.1056/NEJM199808203390806

Luong, T. (2002). Regulation of Staphylococcus aureus Capsular Polysaccharide Expression by agr and sarA. *Infection and Immunity*, *70*(2), 444–450. http://doi.org/10.1128/IAI.70.2.444-450.2002

Luong, T. T., & Lee, C. Y. (2007). Improved single-copy integration vectors for Staphylococcus aureus. *Journal of Microbiological Methods*. http://doi.org/10.1016/j.mimet.2007.04.007

Lyon, G. J., Mayville, P., Muir, T. W., & Novick, R. P. (2000). Rational design of a global inhibitor of the virulence response in Staphylococcus aureus, based in part on localization of the site of inhibition to the receptor-histidine kinase, AgrC. *Proceedings of the National Academy of Sciences of the United States of America*, *97*(24), 13330–5. http://doi.org/10.1073/pnas.97.24.13330

Malachowa, N., Kobayashi, S. D., Braughton, K. R., Whitney, A. R., Parnell, M. J., Gardner, D. J., & Deleo, F. R. (n.d.). Staphylococcus aureus Leukotoxin GH Promotes Inflammation. http://doi.org/10.1093/infdis/jis495

M Rooijakkers, S. H., Ruyken, M., Roos, A., Daha, M. R., Presanis, J. S., Sim, R. B., … G van Strijp, J. A. (n.d.). Immune evasion by a staphylococcal complement inhibitor that acts on C3 convertases. http://doi.org/10.1038/ni1235

Mayville, P., Ji, G., Beavis, R., Yang, H., Goger, M., Novick, R. P., & Muir, T. W. (1999). Structure-activity analysis of synthetic autoinducing thiolactone peptides from Staphylococcus aureus responsible for virulence. *Biochemistry*, *96*, 1218–1223. Retrieved from https://www.ncbi.nlm.nih.gov/pmc/articles/PMC15443/pdf/pq001218.pdf

McLoughlin, R. M., Solinga, R. M., Rich, J., Zaleski, K. J., Cocchiaro, J. L., Risley, A., … Lee, J. C. (2006). CD4+ T cells and CXC chemokines modulate the pathogenesis of Staphylococcus aureus wound infections. *Proceedings of the National Academy of Sciences*, *103*(27), 10408–10413. http://doi.org/10.1073/pnas.0508961103

MDowell, P., Affas, Z., Reynolds, C., Holden, M. T. G., Wood, S. J., Saint, S., … Williams, P. (2001). Structure, activity and evolution of the group I thiolactone peptide quorum-sensing system of Staphylococcus aureus. *Molecular Microbiology*, *41*(2), 503–512. http://doi.org/10.1046/j.1365-2958.2001.02539.x

Merzlyak, E. M., Goedhart, J., Shcherbo, D., Bulina, M. E., Shcheglov, A. S., Fradkov, A. F., … Chudakov, D. M. (2007). Bright monomeric red fluorescent protein with an extended fluorescence lifetime. *Nature Methods*, *4*(7), 555–557. http://doi.org/10.1038/nmeth1062

Minegishi, Y., Saito, M., Nagasawa, M., Takada, H., Hara, T., Tsuchiya, S., … Karasuyama, H. (2009). Molecular explanation for the contradiction between systemic Th17 defect and localized bacterial infection in hyper-IgE syndrome. *The Journal of Experimental Medicine*, *206*(6), 1291–301. http://doi.org/10.1084/jem.20082767

Morfeldt, E., Taylor1, D., Von Gabain2, A., & Arvidson3, S. (1995). Activation of alpha-toxin translation in Staphylococcus aureus by the trans-encoded antisense RNA, RNAIII The synthesis of virulence factors in Staphylococcus. *The EMBO Journal*, *14*(18), 4569–4577. Retrieved from https://www.ncbi.nlm.nih.gov/pmc/articles/PMC394549/pdf/emboj00042-0193.pdf

Moyed, H. S., & Bertrand, K. P. (1983). hipA, a Newly Recognized Gene of Escherichia coli K-12 That Affects Frequency of Persistence After Inhibition of Murein Synthesis. *JOURNAL OF BACTERIOLOGY*, *155*(2), 768–775. Retrieved from https://www.ncbi.nlm.nih.gov/pmc/articles/PMC217749/pdf/jbacter00243-0332.pdf

Nagai, T., Ibata, K., Park, E. S., Kubota, M., Mikoshiba, K., & Miyawaki, A. (2002). A variant of yellow fluorescent protein with fast and efficient maturation for cell-biological applications. *Nature Biotechnology*, *20*(1), 87–90. http://doi.org/10.1038/nbt0102-87

Nemeth, J., & Lee, J. C. (1995). Antibodies to Capsular Polysaccharides Are Not Protective against Experimental Staphylococcus aureus Endocarditis. *INFECTION AND IMMUNITY*, *63*(2), 375–380. Retrieved from https://www.ncbi.nlm.nih.gov/pmc/articles/PMC173005/pdf/630375.pdf

Nilsson, I.-M., Lee, J. C., Bremell, T., Rydé N, C., & Tarkowski, A. (1997). The Role of Staphylococcal Polysaccharide Microcapsule Expression in Septicemia and Septic Arthritis. *INFECTION AND IMMUNITY*, *65*(10), 4216–4221. Retrieved from https://www.ncbi.nlm.nih.gov/pmc/articles/PMC175605/pdf/654216.pdf

Novick, R. P., & Geisinger, E. (2008). Quorum sensing in staphylococci. *Annual Review of Genetics*, *42*, 541–64. http://doi.org/10.1146/annurev.genet.42.110807.091640

Novick, R. P., Ross, H. F., Projan, S. J., Kornblum, J., Kreiswirth, B., & Moghazeh, S. (1993). Synthesis of staphylococcal virulence factors is controlled by a regulatory RNA molecule. *The EMBO Journal*, *12*(10), 3967–3975. Retrieved from https://www.ncbi.nlm.nih.gov/pmc/articles/PMC413679/pdf/emboj00082-0256.pdf

O'Brien, L. M., Walsh, E. J., Massey, R. C., Peacock, S. J., & Foster, T. J. (2002). *Staphylococcus aureus* clumping factor B (ClfB) promotes adherence to human type I cytokeratin 10: implications for nasal colonization. *Cellular Microbiology*, *4*(11), 759–770. http://doi.org/10.1046/j.1462-5822.2002.00231.x

Olaru, F., & Jensen, L. E. (2010). Staphylococcus aureus Stimulates Neutrophil Targeting Chemokine Expression in Keratinocytes through an Autocrine IL-1α Signaling Loop. *Journal of Investigative Dermatology*, *130*(7), 1866–1876. http://doi.org/10.1038/jid.2010.37

Onderdonk, A. B., Shapiro, M. E., Finberg, R. W., Zaleznik, D. F., & Kasper, D. L. (n.d.). Use of a model of intraabdominal sepsis for studies of the pathogenicity of Bacteroides fragilis. *Reviews of Infectious Diseases*, *6 Suppl 1*, S91-5. Retrieved from http://www.ncbi.nlm.nih.gov/pubmed/6372042

Oogai, Y., Matsuo, M., Hashimoto, M., Kato, F., Sugai, M., & Komatsuzawa, H. (2011). Expression of virulence factors by Staphylococcus aureus grown in serum. *Applied and Environmental Microbiology*, *77*(22), 8097–105. http://doi.org/10.1128/AEM.05316-11

Panton, P. N., & Valentine, F. C. O. (1932). STAPHYLOCOCCAL TOXIN. *The Lancet*, *219*(5662), 506–508. http://doi.org/10.1016/S0140-6736(01)24468-7

Plata, K., Rosato, A. E., & Węgrzyn, G. (2009). Staphylococcus aureus as an infectious agent: overview of biochemistry and molecular genetics of its pathogenicity. Retrieved from http://www.actabp.pl/pdf/4_2009/597.pdf

Pöhlmann-dietze, P., Ulrich, M., Kiser, K. B., Lee, J. C., Fournier, J., Wolz, C., & Do, G. (2000). Adherence of Staphylococcus aureus to Endothelial Cells : Influence of Capsular Polysaccharide , Global Regulator agr , and Bacterial Growth Phase Adherence of Staphylococcus aureus to Endothelial Cells : Influence of Capsular Polysaccharide , Global Regu. http://doi.org/10.1128/IAI.68.9.4865-4871.2000.Updated

Portolé, M., Kiser, K. B., Bhasin, N., Chan, K. H. N., & Lee, J. C. (2001). Staphylococcus aureus Cap5O Has UDP-ManNAc Dehydrogenase Activity and Is Essential for Capsule Expression. *INFECTION AND IMMUNITY*, *69*(2), 917–923. http://doi.org/10.1128/IAI.69.2.917–923.2001

Poutrel, B., Gilbert, F. B., & Lebrun, M. (1995). Effects of Culture Conditions on Production of Type 5 Capsular Polysaccharide by Human and Bovine Staphylococcus aureus Strains, *2*(2), 166–171. Retrieved from https://www.ncbi.nlm.nih.gov/pmc/articles/PMC170121/pdf/020166.pdf

Poutrel, B., Rainard, P., & Sarradin, P. (1997). Heterogeneity of Cell-Associated CP5 Expression on Staphylococcus aureus Strains Demonstrated by Flow Cytometry, *4*(3), 275–278. Retrieved from https://www.ncbi.nlm.nih.gov/pmc/articles/PMC170518/pdf/040275.pdf

Poutrel, B., Rainard, P., & Sarradin, P. (1997). Heterogeneity of cell-associated CP5 expression on Staphylococcus aureus strains demonstrated by flow cytometry. *Clinical and Diagnostic Laboratory Immunology*, *4*(3), 275–8. Retrieved from http://www.ncbi.nlm.nih.gov/pubmed/9144363

Powers, M. E., Kim, H. K., Wang, Y., & Bubeck Wardenburg, J. (2012). ADAM10 mediates vascular injury induced by Staphylococcus aureus α-hemolysin. *The Journal of Infectious Diseases*, *206*(3), 352–6. http://doi.org/10.1093/infdis/jis192

Prabhakara, R., Foreman, O., De Pascalis, R., Lee, G. M., Plaut, R. D., Kim, S. Y., … Merkel, T. J. (2013). Epicutaneous model of community-acquired Staphylococcus aureus skin infections. *Infection and Immunity*, *81*(4), 1306–15. http://doi.org/10.1128/IAI.01304-12

Pragman, A. A., Yarwood, J. M., Tripp, T. J., & Schlievert, P. M. (2004). Characterization of Virulence Factor Regulation by SrrAB, a Two-Component System in Staphylococcus aureus. *JOURNAL OF BACTERIOLOGY*, *186*(8), 2430–2438. http://doi.org/10.1128/JB.186.8.2430–2438.2004

Prat, C., Bestebroer, J., de Haas, C. J. C., van Strijp, J. A. G., & van Kessel, K. P. M. (2006). A New Staphylococcal Anti-Inflammatory Protein That Antagonizes the Formyl Peptide Receptor-Like 1. *The Journal of Immunology*, *177*(11). Retrieved from http://www.jimmunol.org/content/177/11/8017

Prévost, G., Cribier, B., Couppié, P., Petiau, P., Supersac, G., Finck-Barbançon, V., … Piemont, Y. (1995). Panton-Valentine leucocidin and gamma-hemolysin from Staphylococcus aureus ATCC 49775 are encoded by distinct genetic loci and have different biological activities. *Infection and Immunity*, *63*(10), 4121–9. Retrieved from http://www.ncbi.nlm.nih.gov/pubmed/7558328

Proctor, R. A., van Langevelde, P., Kristjansson, M., Maslow, J. N., & Arbeit, R. D. (1995). Persistent and relapsing infections associated with small-colony variants of Staphylococcus aureus. *Clinical Infectious Diseases : An Official Publication of the Infectious Diseases Society of America*, *20*(1), 95–102. Retrieved from http://www.ncbi.nlm.nih.gov/pubmed/7727677

Puel, A., Picard, C., Lorrot, M., Pons, C., Chrabieh, M., Lorenzo, L., … Casanova, J.-L. (2008). Recurrent staphylococcal cellulitis and subcutaneous abscesses in a child with autoantibodies against IL-6. *Journal of Immunology (Baltimore, Md. : 1950)*, *180*(1), 647–54. Retrieved from http://www.ncbi.nlm.nih.gov/pubmed/18097067

Ray, G. T., Suaya, J. A., & Baxter, R. (2013). Microbiology of skin and soft tissue infections in the age of community-acquired methicillin-resistant Staphylococcus aureus. *Diagnostic Microbiology and Infectious Disease*, *76*(1), 24–30. http://doi.org/10.1016/j.diagmicrobio.2013.02.020

Rechtin, T. M., Gillaspy, A. F., Schumacher, M. A., Brennan, R. G., Smeltzer, M. S., & Hurlburt, B. K. (1999). Characterization of the SarA virulence gene regulator of Staphylococcus aureus. *Molecular Microbiology*, *33*(2), 307–16. Retrieved from http://www.ncbi.nlm.nih.gov/pubmed/10411747

Rg Hartleib, J., Kö, N., Dickinson, R. B., Chhatwal, G. S., Sixma, J. J., Hartford, O. M., … Herrmann, M. (n.d.). Protein A is the von Willebrand factor binding protein on Staphylococcus aureus. Retrieved from http://www.bloodjournal.org/content/bloodjournal/96/6/2149.full.pdf

Riordan, K. O., & Lee, J. C. (2004). Staphylococcus aureus Capsular Polysaccharides Staphylococcus aureus Capsular Polysaccharides, *17*(1). http://doi.org/10.1128/CMR.17.1.218

Rizzo, M. A., Springer, G. H., Granada, B., & Piston, D. W. (2004). An improved cyan fluorescent protein variant useful for FRET. *Nature Biotechnology*, *22*(4), 445–449. http://doi.org/10.1038/nbt945

Roben, P. W., Salem, A. N., Silverman, G. J., Roben, P. W., Salem, A. N., & Silverman, C. J. (2017). staphylococcal protein A. VH3 family antibodies bind domain D of V,3 Family Protein A' Antibodies Bind Domain D of Staphylococcal. *J Immunol*, *154*, 6437–6445. Retrieved from http://www.jimmunol.org/content/154/12/6437

Rooijakkers, S. H. M., Ruyken, M., van Roon, J., van Kessel, K. P. M., van Strijp, J. A. G., & van Wamel, W. J. B. (2006). Early expression of SCIN and CHIPS drives instant immune evasion by Staphylococcus aureus. *Cellular*

Microbiology, *8*(8), 1282–1293. http://doi.org/10.1111/j.1462-5822.2006.00709.x

Ruimy, R., Angebault, C., Djossou, F., Dupont, C., Epelboin, L., Jarraud, S., … Andremont, A. (2010). Are Host Genetics the Predominant Determinant of Persistent Nasal *Staphylococcus aureus* Carriage in Humans? *The Journal of Infectious Diseases*, *202*(6), 924–934. http://doi.org/10.1086/655901

Ryall, B., Eydallin, G., & Ferenci, T. (n.d.). Culture History and Population Heterogeneity as Determinants of Bacterial Adaptation: the Adaptomics of a Single Environmental Transition. http://doi.org/10.1128/MMBR.05028-11

Sadler, J. E. (1998). BIOCHEMISTRY AND GENETICS OF VON WILLEBRAND FACTOR. *Annu. Rev. Biochem*, *67*, 395–424. Retrieved from http://www.annualreviews.org/doi/pdf/10.1146/annurev.biochem.67.1.395

Saïd-Salim, B., Dunman, P. M., McAleese, F. M., Macapagal, D., Murphy, E., McNamara, P. J., … Kreiswirth, B. N. (2003). Global regulation of Staphylococcus aureus genes by Rot. *Journal of Bacteriology*, *185*(2), 610–9. Retrieved from http://www.ncbi.nlm.nih.gov/pubmed/12511508

Sarkar, P., Koushik, S. V, Vogel, S. S., Gryczynski, I., & Gryczynski, Z. (2009). Photophysical Properties of Cerulean and Venus Fluorescent Proteins. http://doi.org/10.1117/1.3156842

Shcherbo, D., Merzlyak, E. M., Chepurnykh, T. V, Fradkov, A. F., Ermakova, G. V, Solovieva, E. A., … Chudakov, D. M. (2007). Bright far-red fluorescent protein for whole-body imaging. *Nature Methods*, *4*(9), 741–746. http://doi.org/10.1038/nmeth1083

Sinha, B., François, P. P., Nüsse, O., Foti, M., Hartford, O. M., Vaudaux, P., … Krause, K. H. (1999). Fibronectin-binding protein acts as Staphylococcus

aureus invasin via fibronectin bridging to integrin alpha5beta1. *Cellular Microbiology*, *1*(2), 101–17. Retrieved from http://www.ncbi.nlm.nih.gov/pubmed/11207545

Sompolinsky, D., Samra, Z., Karakawa, W. W., Vann, W. F., Schneerson, R., & Zvi, A. (1985). Encapsulation and Capsular Types in Isolates of Staphylococcus aureus from Different Sources and Relationship to Phage Types. *JOURNAL OF CLINICAL MICROBIOLOGY*, *22*(5), 828–834. Retrieved from https://www.ncbi.nlm.nih.gov/pmc/articles/PMC268536/pdf/jcm00112-0164.pdf

Speziale, P., Pietrocola, G., Rindi, S., Provenzano, M., Provenza, G., Di Poto, A., … Arciola, C. R. (2009). Structural and functional role of *Staphylococcus aureus* surface components recognizing adhesive matrix molecules of the host. *Future Microbiology*, *4*(10), 1337–1352. http://doi.org/10.2217/fmb.09.102

Steven, A. C., & Steinert, P. M. (1994). Protein composition of cornified cell envelopes of epidermal keratinocytes. *Journal of Cell Science*, *107*(2).

Stewart, P. S. (2003). Diffusion in biofilms. *Journal of Bacteriology*, *185*(5), 1485–91. http://doi.org/10.1128/JB.185.5.1485-1491.2003

Sutra, L., Rainard, P., & Poutrel, A. B. (1990). Phagocytosis of Mastitis Isolates of Staphylococcus aureus and Expression of Type 5 Capsular Polysaccharide Are Influenced by Growth in the Presence of Milk. *JOURNAL OF CLINICAL MICROBIOLOGY*, *28*(10), 2253–2258. Retrieved from https://www.ncbi.nlm.nih.gov/pmc/articles/PMC268157/pdf/jcm00058-0105.pdf

Talan, D. A., Krishnadasan, A., Gorwitz, R. J., Fosheim, G. E., Limbago, B., Albrecht, V., & Moran, G. J. (2011). Comparison of Staphylococcus aureus From Skin and Soft-Tissue Infections in US Emergency Department Patients, 2004 and 2008. *Clinical Infectious Diseases*, *53*(2), 144–149. http://doi.org/10.1093/cid/cir308

Thakker, M., Park, J. S., Carey, V., & Lee, J. C. (1998). Staphylococcus aureus serotype 5 capsular polysaccharide is antiphagocytic and enhances bacterial virulence in a murine bacteremia model. *Infection and Immunity*, *66*(11), 5183–9. Retrieved from http://www.ncbi.nlm.nih.gov/pubmed/9784520

Thammavongsa, V., Missiakas, D. M., & Schneewind, O. (2013). Staphylococcus aureus degrades neutrophil extracellular traps to promote immune cell death. *Science (New York, N.Y.)*, *342*(6160), 863–6. http://doi.org/10.1126/science.1242255

Tuchscherr, L., Bischoff, M., Lattar, S. M., Noto Llana, M., Pförtner, H., Niemann, S., … Löffler, B. (2015). Sigma Factor SigB Is Crucial to Mediate Staphylococcus aureus Adaptation during Chronic Infections. *PLOS Pathogens*, *11*(4), e1004870. http://doi.org/10.1371/journal.ppat.1004870

Tzianabos, A. O., Kasper, D. L., Cisneros, R. L., Smith, R. S., & Onderdonk, A. B. (1995). Polysaccharide-mediated protection against abscess formation in experimental intra-abdominal sepsis. *Journal of Clinical Investigation*, *96*(6), 2727–2731. http://doi.org/10.1172/JCI118340

Uhlén, M., Guss, B., Nilsson, B., Gatenbeck, S., Philipson, L., & Lindberg, M. (1984). Complete sequence of the staphylococcal gene encoding protein A. A gene evolved through multiple duplications. *The Journal of Biological Chemistry*, *259*(3), 1695–702. Retrieved from http://www.ncbi.nlm.nih.gov/pubmed/6319407

van den Akker, E. L. T., Nouwen, J. L., Melles, D. C., Rossum, E. F. C. van, Koper, J. W., Uitterlinden, A. G., … van Belkum, A. (2006). *Staphylococcus aureus* Nasal Carriage Is Associated with Glucocorticoid Receptor Gene Polymorphisms. *The Journal of Infectious Diseases*, *194*(6), 814–818. http://doi.org/10.1086/506367

Ventura, C. L., Malachowa, N., Hammer, C. H., Nardone, G. A., Robinson, M. A., Kobayashi, S. D., … Horsburgh, M. J. (2010). Identification of a Novel Staphylococcus aureus Two- Component Leukotoxin Using Cell Surface Proteomics. *PLoS ONE*, *5*(7). http://doi.org/10.1371/journal.pone.0011634

Wang, R., Braughton, K. R., Kretschmer, D., Bach, T.-H. L., Queck, S. Y., Li, M., … Otto, M. (2007). Identification of novel cytolytic peptides as key virulence determinants for community-associated MRSA. *Nature Medicine*, *13*(12), 1510–4. http://doi.org/10.1038/nm1656

Weidenmaier, C., Goerke, C., & Wolz, C. (2012). Staphylococcus aureus determinants for nasal colonization. *Trends in Microbiology*, *20*(5), 243–50. http://doi.org/10.1016/j.tim.2012.03.004

Weidenmaier, C., & Lee, J. C. (2015). Structure and Function of Surface Polysaccharides of Staphylococcus aureus (pp. 1–37). Springer Berlin Heidelberg. http://doi.org/10.1007/82_2015_5018

Weidenmaier, C., Peschel, A., Kempf, V. A. J., Lucindo, N., Yeaman, M. R., & Bayer, A. S. (2005). DltABCD-and MprF-Mediated Cell Envelope Modifications of Staphylococcus aureus Confer Resistance to Platelet Microbicidal Proteins and Contribute to Virulence in a Rabbit Endocarditis Model. *INFECTION AND IMMUNITY*, *73*(12), 8033–8038. http://doi.org/10.1128/IAI.73.12.8033–8038.2005

Wessel, A. K., Arshad, T. A., Fitzpatrick, M., Connell, J. L., Bonnecaze, R. T., Shear, J. B., & Whiteley, M. (n.d.). Oxygen Limitation within a Bacterial Aggregate. http://doi.org/10.1128/mBio.00992-14

Zacharias, D. A., Baird, G. S., & Tsien, R. Y. (2000). Recent advances in technology for measuring and manipulating cell signals. *Current Opinion in Neurobiology*, *10*(3), 416–21. Retrieved from http://www.ncbi.nlm.nih.gov/pubmed/10851181

Ziebandt, A.-K., Becher, D., Ohlsen, K., Hacker, J., Hecker, M., & Engelmann, S. (2004). The influence of agr and sigmaB in growth phase dependent regulation of virulence factors in Staphylococcus aureus. *Proteomics*, *4*(10), 3034–47. http://doi.org/10.1002/pmic.200400937

7 Deutsche Zusammenfassung

Staphylococcus aureus (S. aureus) ist ein grampositives Bakterium mit „gespaltener Persönlichkeit“. Staphylokokken kommen als Teil der natürlichen Hautflora vor, können aber auch als pathogenes Bakterium Haut- und Wundinfektionen bis hin zu tödlich verlaufenden Blutstrominfektionen verursachen. Der Übergang von apathogener Kolonisation zu invasiver Infektion wird durch eine Vielzahl von Genregulatoren moduliert.

Ein wichtiger Genregulator bildet das Accessory Gene Regulator (Agr) System, das für die Modulation von über hundert Genen verantwortlich ist. Der *agr locus* besteht aus zwei Transkriptionseinheiten, die von zwei divergenten Promotoren, agr P2 und agr P3 kontrolliert werden. Das Agr System ist ein klassisches Zwei-Komponentensystem und wird über einen Quorum Sensing Mechanismus gesteuert, wobei das autoinduzierende Protein autoinducing peptide (AIP) von Staphylokokken in den Extrazellulärraum sezerniert wird. Durch Rückbindung an seinen Rezeptor, der Histidinkinase AgrA, kommt es zur Selbstaktivierung des Agr Operons über den agr P2 Promotor, sowie zur Aktivierung von verschiedenen Zielgenen über den agr P3 Promotor: Die aktivierte Genexpression der regulatorischen RNAIII (ausgehend von dem Promoter agr P3) führt u.a. zur Expression des capA-P Biosynthesegencluster welches für Enzyme zur Synthese Kapselpolysaccharide (CP) führt. Das capA-P Operon wird durch einen Promoter upstream von capA (cap-P) gesteuert. CPs schützen Staphylokokken vor der Opsonophagozytose durch Immunzellen, führen aber gleichzeitig zur Maskierung von Oberflächenmolekülen und mindern somit die Fähigkeit zur Adhärenz an Gewebeoberflächen. Analysen mittels fluoreszenzaktivierter Durchflusszytometrie, sowie Immunfluoreszenzmethoden haben gezeigt, dass nicht alle Staphylokokken in der postexponentiellen Phase innerhalb einer Kultur CP produzieren, sondern sich phänotypisch heterogen präsentieren.

Das Ziel der Studie war, Reporterstämme herzustellen, mit denen die Aktivitäten der Promotoren agr-P3 und cap-P auf der Ebene einzelner Zellen simultan

analysiert werden können. Hierzu wurden Promotern mit Fluoreszenzproteingenen in Integrationsvektoren kloniert und chromosomal in das Staphylokokkenchromosom integriert. Dabei wurden Plasmide verwendet die entweder in die „attachment site“ für die Pathogenitätsinsel I (SaPI) oder die mittels eines Phagen (attachment site in geh) integrieren. Es konnten Plasmide mit verschiedenen Kombinationen von den Fluoreszenzgenen Venus (ven) oder Verulean (cer) und verschiedenen Selektionsmarkern getestet werden. Dadurch sollte es möglich sein, Doppel-Integranten mit agr-P3-cer, agr-P3 ven, capA-cer, capA-ven herzustellen. Die generierten Stämme wurden mittels PCR auf korrekte Integration überprüft und die Fluoreszenz mikroskopisch detektiert. dienen. Es konnte gezeigt werden, dass alle Reporterstämme das Vektorplasmid an den zu erwartenden Stellen chromosomal integriert hatten. In einem Fall kam es zur partiellen Deletion des Integrationsplasmids und in mindestens einem Fall konnte gezeigt werden, dass es zur Mehrfachintegration des Vektors kam. Die Fluoreszenzuntersuchungen zeigten, dass 1. die agr-P3 Aktivität größtenteils homogen ist und maximal in der post-exponentiellen Wachstumsphase ist. 2. die cap-P Aktivität ist ebenfalls maximal in der post-exponentiellen Wachstumsphase. 3. cap-P Aktivität ist sehr heterogen innerhalb einer Kultur. 4. Promoterfusionen mit ven zeigten ein stärkeres Signal als Fusionen mit cer. 5. Die Analyse der Doppel-Integrante lieferte inkonsistente Ergebnisse und bedarf der weiteren Überprüfung

Im zweiten Teil dieser Arbeit sollte einer 3D-Kollagenmodells, in dem die Reporterstämme über einen längeren Zeitraum beobachtet werden können, etabliert werden. Guggenberger et al. konnten zeigen, dass Staphylokokken, die in Kollagen mit Fibrinogen eingebettet werden, eine Pseudokapsel aus Fibrinablagerungen und eine Mikrokolonie-assoziiertes Netzwerk ausbildeten (Guggenberger C, Wolz C, Morrissey JA, Heesemann J (2012) Two Distinct Coagulase-Dependent Barriers Protect Staphylococcus aureus from Neutrophils in a Three Dimensional in vitro Infection Model. PLoS Pathogens). Diese Strukturen sind einem Abszess sehr ähnlich und der Versuch kann daher ein in vitro Abszess-Modell darstellen. Es gelang abszessähnliche Strukturen von S.

aureus innerhalb einer Kollagen-Matrix zu generieren. Allerdings konnte die Ausbildung der Pseudokapsel oder des Mikrokolonie-assoziierten Netzwerks nur partiell beobachtet werden. Die Analyse der Promotor-Aktivität innerhalb der Kollagen/Fibrin-Struktur zeige folgende, vorläufige Ergebnisse: 1. die Fluoreszenzintensität war für beide Promotor-Fusionen deutlich geringer als bei Wachstum der Stämme in flüssigem Kulturmedium. 2. Die cap-P Promoteraktivität scheint deutlich höher als die agr-P Aktivität zu sein. 3. Bakterien an der Peripherie der Struktur zeigten höhere Fluoreszenz. Die Ergebnisse legen einen Grundstein zur weiteren Etablierung eines Systems zur Analyse von Promoter-Aktivitäten innerhalb eines in vitro Abszess-Models.

8 Publications

Parts of this publication arose from the work presented in this study.

George, S. E., Nguyen, T., Geiger, T., Weidenmaier, C., Lee, J. C., Liese, J. and Wolz, C. (2015), Phenotypic heterogeneity and temporal expression of the capsular polysaccharide in *Staphylococcus aureus*. Molecular Microbiology, 98: 1073–1088. doi:10.1111/mmi.13174

9 Erklärung zum Eigenanteil der Dissertationsschrift

Die Arbeit wurde am Institut für Medizinische Mikrobiologie und Hygiene unter Betreuung von Professor Dr. I.B. Autenrieth durchgeführt.

Die Konzeption der Studie erfolgte durch Dr. Jan Liese (Leiter Krankenhaushygiene) und Prof. Dr. Christiane Wolz (Arbeitsgruppenleiterin AG Wolz).

Sämtliche Versuche wurden (nach Einarbeitung durch Prof. Dr. Christiane Wolz, Dr. Tobias Geiger, Dr. Jan Liese, Kathleen Strauss-Oppitz, Natalya Korn und Isabell Samp) von mir mit Unterstützung durch Shilpa George, Daniela Keinhörster, Natalya Korn, Nenad Katava und Isabell Samp durchgeführt. Die PFGE wurde von Isabell Samp durchgeführt.

Die in dieser Arbeit gewonnenen Erkenntnisse bildeten die Methodische Grundlage für die in der Publikation dargestellten Ergebnisse.

Ich versichere, das Manuskript selbständig (nach Anleitung durch Professor Dr. Christiane Wolz) verfasst zu haben und keine weiteren als die von mir angegebenen Quellen verwendet zu haben.

Tübingen, den 3. November 2017

10 Acknowledgements

This thesis and the experiments were performed at the Institute of Medical Microbiology and Hygiene at the University of Tuebingen under the supervision of director Prof. Dr. med I. B. Autenrieth.

This work was supported by grants from the Centre for Interdisciplinary Clinical Research (IZKF) and the German Centre for Infection Research (DZIF). I would like to express my gratitude to Prof. Dr. Marlies Knippers and Dr. Tanja Rieß from the IZFK for making this work possible and for giving me their support and supervision. I would also like to thank Dr Dirk Kraus and Gisela Bauer-Haffter from the DZIF for their support and supervision.

I would like to thank Prof. Dr. Christiane Wolz for the many ways she supported me with her excellent supervision and management skills. I would like to thank Dr Shilpa George and Daniela Keinhörster for their support and supervision and I would like to express my gratitude to Natalya Korn, Isabell Samp and Kathleen Strauss-Oppitz for the many ways they helped me during my everyday lab work. I would like to thank Dr Tobias Geiger for providing me with excellent supervision and Dr Jan Liese who taught me the basic knowledge for this project.

I would like to express my deep gratitude to my parents and I would also like to thank my brother, my aunt and my grandparents. I would also like to thank Janina, Samuel, Laura, Saiji and Mina.

I am filled with deep gratitude for Dr Andrew Steele for proofreading, correcting and formatting this work with me and for the innumerable other ways he provided me with his support and patience.

11 Curriculum vitae

Name	Thien Ngoc Tran Nguyen
Geburtsdatum	07.Juni 1991
Geburtsort	Stuttgart
Universitäre Ausbildung	
02.Juni 2017	Mündlicher Teil der Ärztlichen Prüfung M3
5/2016 – 4/2017	Praktisches Jahr 1. Tertial: Cho Ray Hospital, Ho-Chi-Minh-Stadt, Vietnam, Allgemein- und Viszeralchirurgie 2. Tertial: King's College Hospital, London, UK, Endokrinologie; Royal London Hospital, London, UK, Gastroenterologie 3. Tertial: Universitätsklinikum Tübingen, Mikrobiologie und Hygiene
04/2016	Schriftlicher Teil der 2. Ärztlichen Prüfung M2
10/2012	Promotion am Institut für Medizinische Mikrobiologie und Hygiene
09/2011	1. Ärztliche Prüfung M1
10/2009	Studium der Humanmedizin, Eberhard Karls Universität Tübingen
Schulische Ausbildung	
9/2001 – 6/2009	Friedrich Schiller Gymnasium Marbach am Neckar